NETHERLANDS GEODETIC COMMISSION
PUBLICATIONS ON GEODESY NEW SERIES
ISSN 0165 1706 NUMBER 39

SPHERICAL HARMONIC ANALYSIS OF SATELLITE GRADIOMETRY

REINER RUMMEL
MARTIN VAN GELDEREN
RADBOUD KOOP
ERNST SCHRAMA

DELFT UNIVERSITY OF TECHNOLOGY
FACULTY OF GEODETIC ENGINEERING

FERNANDO SANSÒ
MARIA BROVELLI
FREDERICA MIGGLIACCIO
FAUSTO SACERDOTE

POLITECNICO DI MILANO
DIPARTIMENTO DI INGEGNERIA IDRAULICA,
AMBIENTALE E DEL RILEVAMENTO

1993

NEDERLANDSE COMMISSIE VOOR GEODESIE, THIJSSEWEG 11, 2629 JA DELFT, THE NETHERLANDS
TEL. (31)-(0)15-782819, FAX (31)-(0)15-782348, E-MAIL SCHRODER@TUDGV1.TUDELFT.NL

CIP-DATA KONINKLIJKE BIBLIOTHEEK, DEN HAAG

Spherical

Spherical harmonic analysis of satellite gradiometry / Reiner Rummel ... [et al.]. -
Delft : Nederlandse Commissie voor Geodesie. - Ill. -
(Publications on geodesy. New series, ISSN 0165-1706 ; nr. 39)
With ref.
ISBN 90-6132-247-2
Subject headings: geodesy / gradiometry / gravity field.

PRINTED BY W.D. MEINEMA B.V., DELFT, THE NETHERLANDS

TABLE OF CONTENTS page

FOREWORD.

In 1988 the European Space Agency started with a series of studies with the goal to prepare the geodetic user community for a dedicated gravity field mission and stimulate cooperation among various groups. Thereby it was left open whether the planned mission should be based on the principle of satellite-to-satellite tracking, on satellite gradiometry or on a combination of these two methods. In the course of these studies it turned out that the group of the dipartimento di ingegneria idraulica, ambientale e del rilevamento of the politecnico di Milano and that of the faculty of geodetic engineering of the Delft University of Technology worked much along the same line. At various occasions very exciting and stimulating exchange of ideas took place between these two groups. In 1991 it was therefore decided to publish the main line of their development in gradiometry analysis, the so-called timewise and spacewise approach, in a joint report.

Compared with the benefit it would have been rather cumbersome to try to homogenize the adopted style of presentation and notation of the two groups. Thus little effort was spent on this aspect. We hope that this does not hamper reading.

The authors like to thank the European Space Agency for its support of the CIGAR-studies and the Netherlands Geodetic Commission for publishing this report.

Delft, april 1993,
Reiner Rummel.

1. INTRODUCTION.

All our current knowledge of the global gravitational field of the earth is derived from an analysis of the motion of artificial satellites. While in the pioneering days only the oblateness coefficient J_2 and thereafter J_3 could be determined, subsequently complete sets of spherical harmonic coefficients up to degree ℓ and order m 36 could be computed. Very advanced laser and radio tracking techniques, more and more satellites with a large variety in orbit characteristics, an increasing number of ground stations and last but not least more sophisticated computers and computational models made this development possible.

However there exist natural limits for further improvement. Whereas, for example, the still existing indeterminancy of individual spherical harmonic coefficients far away from the resonance bands of the satellites can probably be overcome in the near future through almost continuous space-borne tracking of low flying spacecrafts, the attenuation of the gravitational field with increasing altitude represents a natural barrier. The only way out of this dilemma is satellite gradiometry, the measurement of second derivatives of the gravitational potential V. When expressed in a spherical harmonic series, double differentiation roughly results in an amplification of the coefficients representing the gravity field by a factor ℓ^2 (with ℓ the degree of the expansion). This way the attenuation effect, which is approximately $(\frac{R}{R+h})^{\ell}$, can be compensated (R is the earth's mean radius, h the altitude of the satellite). This is illustrated in Figure 1. Figure 1 shows the signal degree-order variances of the unknown part of the gravitational potential, the disturbance potential T, at the earth's surface (altitude 0 km) and at 200 km. For the highest degree (240) the attenuation effect is three orders of magnitude. The second radial derivative of T, T_{zz}, has a much flatter spectrum at the earth's surface than T. The information about the spatial details of the field is much more pronounced. Thus, T_{zz} at 200 km altitude still contains considerable information at high spherical harmonic degrees.

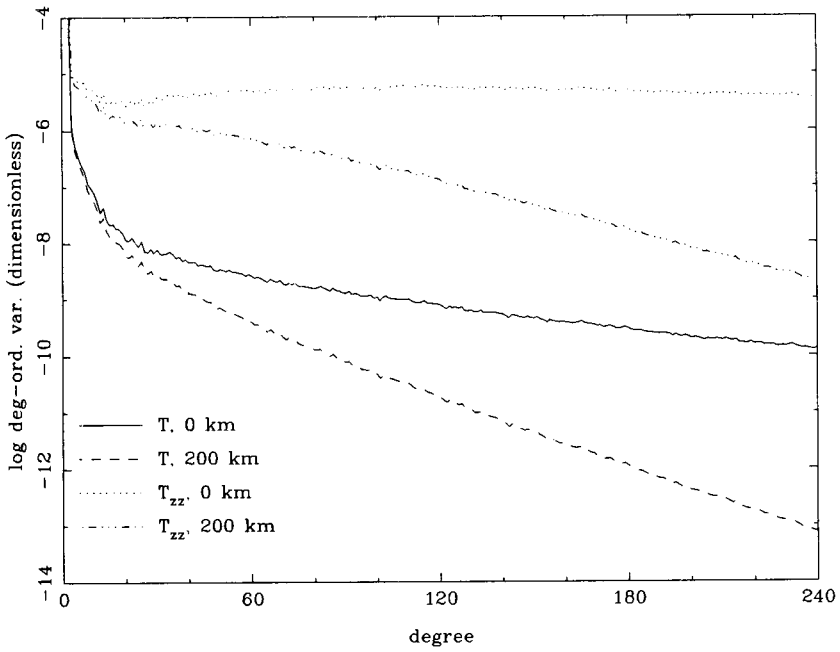

Figure 1: Altitude attenuation effect of the disturbance potential T can to a large extent be compensated by dealing with the second radial derivative T_{zz} (degree-order variances based on OSU 86F, all quantities dimensionless: $T/(GM/R)$; $T_{zz}/(2GM/R^3)$).

A satellite gradiometer measures at maximum all nine components of the gravitational tensor $\Gamma_{ij} = \frac{\partial^2 V}{\partial x^i \partial x^j}$ (with V gravitational potential) or certain linear combinations of these components. Gradiometers are either based on the principle of differential accelerometry or on that of torsion measurement. The components may be given in a space fixed coordinate triad, in case of a space-stable orientation of the instrument in the spacecraft, or in some local, e.g. rotating, triad. In the latter case the measured elements contain components of inertial motion as well. All these points and many related aspects are left aside here. For a discussion of the instrumentation refer to (Wells, 1983), (Paik & Richard, 1986), (Reinhardt et al., 1982); for a treatment of the gradiometer principles refer to (Rummel, 1986). Here we assume an ideal situation, where the gradiometer components are given in known orientation, along perfectly aligned axes and where the only signal source is the gravitational field of the earth. No disturbing acceleration exists. The

gradient components are provided in either the local orthonormal, spherical triad $\underline{e}_i$, i = 1,2,3 (with $\underline{e}_1 = \underline{e}_x$ directing north, $\underline{e}_2 = \underline{e}_y$ directing east, and $\underline{e}_3 = \underline{e}_z$ radially outwards) or the orbit triad $\underline{e}_0$, 0 = 1,2,3 (with $\underline{e}_1 = \underline{e}_a$ along track, $\underline{e}_2 = \underline{e}_c$ crosstrack, perpendicular to the orbit plane, and $\underline{e}_3 = \underline{e}_z$ radially outwards). Each component is measured independently of all others with a certain measurement error.

The purpose of this report is a discussion of alternative ways of determining an approximation of the earth's gravitational field from satellite gradiometry with the field expressed in a series of spherical harmonics. Error propagation and linear parameter estimation shall be analyzed. The subject is not new. From the days satellite gradiometry is under consideration, representation and analysis of its results in terms of spherical harmonics has been considered, see e.g. (Köhnlein, 1967), (Glaser & Sherry, 1971) or Reed's dissertation of 1973. Now, however with actual mission plans for the gradiometric satellite ARISTOTELES growing more and more concrete, a revision seems appropriate and timely.

It is remarkable to observe that dynamic satellite geodesy and physical geodesy, although strongly benefitting from each other, developed as two rather independent branches of geodesy. No serious attempt for a unified theory of gravity field determination has been undertaken. The former addresses gravitational field estimation from the solution of the equations of motion, the latter solves gravitational field and shape of the earth in the form of a boundary value problem related to the earth's surface. Gradiometer measurements are ideally suited for a study of the similarities and differences of these two approaches. Consider first the satellite as a carrier of an instrument that delivers the gravitational tensor components Γ_{ij} at regular intervals. At each time the position of the instrument is expressed by the coordinate triple $\{\varphi,\lambda,r\}$, representing the position of the satellite's center of mass, which is usually known only approximately. With each revolution of the spacecraft a new circle of densely spaced measurements is delivered. Depending on the choice of the orbit, in particular of the inclination I and precession rate of its node, $\dot{\Omega}$, an almost arbitrarily dense, global coverage of the sphere can be achieved. With $\Gamma_{ij}(\varphi,\lambda,r)$ - or by approximation $\Gamma_{ij}(\varphi,\lambda)$, if the height variation of the satellite can be

neglected or all observations are reduced to one sphere, $\sigma(0,r)$ - each tensor component represents a gravity related functional, given on a known (or unknown) boundary surface. The determination of the global gravity field in terms of spherical harmonics from such a functional is carried out by quadrature techniques or the solution of a geodetic boundary value problem (g.b.v.p.). As the measurements are considered a function of position only, this view is denoted the *spacewise approach*. It fully coincides with the techniques well established in the field of physical geodesy. This view shall be treated in chapter two.

Equally well the measured sequence of tensor components may be viewed as a discrete time series, $\Gamma_{ij}(t)$, ideally spanning the entire mission length without interruption . In this case the determination of spherical harmonics becomes possible only after connecting the spherical harmonic representation given in an earth fixed coordinate system with the time series provided along the inclined, slowly precessing orbital plane. Various ways are conceivable for this connection and for the parametrization of the time series, but the intimate relation to satellite perturbation theory is evident. We denote this the *timewise approach* to be treated in chapter 3. It is particular suited for studies of the influence of the choice of the orbit parameters on gravity field recovery and, as measurement sampling is actually a time process, for analysis of realistical instrument error models.

The close connection of the timewise approach with orbit perturbation analysis, as usually applied in dynamic satellite geodesy, becomes even more pronounced if we look at a measured tensor component from a slightly different angle. In differential accelerometry, as it has to be applied within the ARISTOTELES mission, an arbitrary tensor component is measured by prohibiting two neighboring test masses from their free motion (fall) in orbit and by constraining them to a fixed levitated position inside the instrument by means of a feedback mechanism. The feedback signal suitably differentiated is translated into the gradient measure. It permits the reconstruction - or is equivalent to the measurement - of the relative acceleration between two adjacent test masses in free fall at known distance, as discussed in (Misner, Thorne & Wheeler, 1971). Hence the signal could be modelled by means of perturbation theory of two neighbouring space trajectories. As the two

trajectories are highly similar, their absolute shape and location is of lesser importance. The gradiometric information is concealed in their relative differences (Rummel, 1978, Schneider, 1984).

2. SPACEWISE APPROACH.

In the present chapter the determination of the spherical harmonic coefficients of the gravitational potential, starting from observations assigned to well defined points on a surface or averaged over suitably chosen regions (usally rectangular blocks), is illustrated. A preliminary discussion concerning the choice of the orbit, in order to obtain a complete coverage of the earth, by data distributed in a very thin shell, is presented in section 1. The error introduced by shifting the data to a single surface is explicitly estimated, and is proved to be of the same order as the instrumental error for gravity gradient measurements. The observational model is introduced in section 2. The spatial distribution expected for measurements during the whole mission, and their block-averaging procedure are described; the use of Wiener measures for the treatment of noisy data defined in a continuum is illustrated. Section 3 deals with the least-squares approach for the estimation of a finite number of coefficients from discrete data. The particular structure of the normal matrix is analysed, in order to illustrate the numerical problems arising in the solution of the normal system. The presence of aliasing and its main features are discussed. The determination of potential coefficients by quadrature formulas is the topic of section 4; in particular, the discretization error is evaluated by suitable simulations. The general structure of boundary operators is analysed in section 5; the procedures to estimate functionals of the solution, and in particular spherical harmonic coefficients, from a boundary condition expressed as an operator acting on the unknown function, are illustrated. Such procedures are applied in section 6 to particular cases of different gravity gradient components; finally, the simultaneous use of different kinds of data (for example, different components of the gravity gradient) in an overdetermined problem approach is discussed in section 7.

2.1. Is it possible to use satellite observations in a boundary value problem approach?

Our objective is to determine the gravity field of the earth from satellite observations, to a considerable degree of resolution. To this aim, we design a reference orbit:

- as low as possible in order to decrease the exponential damping of the harmonic coefficients of the potential, the limit being imposed by the drag effects on the satellite of the upper layers of the atmosphere,
- with a polar inclination, so that all the fluctuations of the potential are explored, without neglecting polar caps,
- with a mean motion having a suitable rate to the earth's angular velocity, so that satellite subtracks, as seen from the ground, tend to distribute in longitude without repetitions, and
- with an eccentricity as small as possible, so that the satellite is sampling a potential which has always the same spectrum, as a function of φ and λ.

Among many possible solutions, in order to perform a spectral analysis of the observations along the orbit (timewise Fourier approach) a possible orbit has been identified, which is of great interest because it is frozen in inertial space; it is known as Cook's orbit and is described in detail in (Colombo, 1984). Another possible elementary choice is to have, as closely as possible, a purely circular orbit; so, by using a suitable measuring rate and a suitable rate of the satellite's to the earth's period, one realizes that the measurement points, as seen from the earth, tend to distribute in an irregular fashion, however approaching more and more the condition of a continuous distribution, i.e.

$$\lim_{N\to\infty} \operatorname{Sup}_i \operatorname{Inf}_j d(p_i, p_j) = 0 \quad , \qquad (2.1)$$

$$(i, j = 1, \ldots N)$$

over the sphere of radius r equal to the orbit's radius.

We shall come back, later on, to the limit distribution obtained in this way and to the effects it has on the estimation of the potential coefficients.

We just want to stress here that this rather simplistic choice has at least one good point from the practical point of view: the presence of a relevant drag effect tends by itself to circularize the orbit, i.e. to decrease the eccentricity e, so that it would be a waste of fuel to try to keep e constant.

This can be seen for instance from the Lagrange dynamical equations in

terms of Kepler's elements. Let's remodel the drag perturbation by a simple force-function like (cf. Kaula, 1966, § 3)

$$F = \frac{\mu}{2a} - D\ a\ M \tag{2.2}$$

a = semi major axis

$\mu = GM \cong 3.986\ 10^{14}\ m^3\ sec^{-2}$

D = drag force, assumed to be constant

M = mean anomaly,

describing essentially a satellite moving under the central field μ/r within a constant density atmosphere causing a constant tangential effect $\frac{1}{a}\frac{\partial F}{\partial M} = -D$, opposite to the direction of motion. With this force function Lagrange equations read

$$\begin{aligned}
\frac{da}{dt} &= -\frac{2D}{n} \\
\frac{de}{dt} &= -\frac{(1-e^2)}{nae}\ D \\
\frac{dM}{dt} &= \frac{2}{na}\left(\frac{\mu}{2a^2} + DM\right) = n + \frac{2D}{na}\ M \\
\frac{d\omega}{dt} &= 0 \\
\frac{di}{dt} &= 0 \\
\frac{d\Omega}{dt} &= 0
\end{aligned} \tag{2.3}$$

($n = \mu^{1/2}\ a^{-3/2}$ = mean motion).

These equations already describe the main effects of drag, which does not affect ω, i, Ω and gives rise to a decay of a, related to the law of energy, a decrease of e and an increase in the angular velocity $\dot{M}$ due to the necessity of balancing the stronger attraction implied by the decrease of a.

So the satellite will spiral down, towards the earth's surface, preserving an osculating motion of almost circular type; after a certain time, for instance a few hours, the original state is restored by firing the rockets and suitably manoeuvering the satellite.

We shall assume (see e.g. (Rummel & Colombo, 1985)) that these control operations are suitable to keep the satellite in a layer of radial distance varying ±5 km around a mean value. Already at that point, the image of the mission we are designing suggests the idea of applying some boundary value problem technique to determine the unknown anomalous potential; in general this can be pursued, on condition that the data we have are expressed in terms of point-wise functionals of the anomalous potential T. This can be very difficult if our data are derived from some type of tracking, because the orbit anomaly vector (i.e. the difference between the actual position of the satellite and that calculated from a model gravity by orbit integration) is a non-local functional of T; on the other hand gradiometric measurements are local by their very nature and so they lend themselves to be easily handled in a b.v.p. mode. To this aim it is much simpler to treat data that are ascribed to points on a very simple surface, like a sphere; if we want to have that property fulfilled we need therefore to move the observation points to a mean sphere. There might be some objection to this approach, because it is very much in the spirit of modern geodesy to avoid "reductions"; after all it has been this concept to push for Molodenskii's theory and, later on, for the foundation of collocation theory. On the other hand we should take into account that in our case the observation point will move in vacuum[1], avoiding errors due to the unknown mass density, and that we make computations within the harmonicity domain where our functions are in any way smoothed[2].

---

[1] It is easy to verify that the variations of density due to the residual atmosphere in a layer of a few kilometers, are immaterial for the computation of the 2nd order gradient.

[2] The transformation of the spectrum of a second derivative, going from the earth's surface to the level of the satellite, is governed by the approximate transfer function $(1 - \frac{h}{R})^{\ell+3}$ (h = satellite's height, R = earth's mean radius) which assumes the values 0,2 or 0,04 or 0,002 for ℓ = 50 or 100 or

To move the gravity gradient components radially we need their radial derivatives: since every component of $\Gamma = \{\frac{\partial^2 V}{\partial x_i \partial x_j}\}$ in the degree ℓ of the spherical harmonic representation is also a homogeneous function of degree $-(\ell+3)$, we can write (note that Γ, as well as $\Gamma_{\ell m}$, are 3 x 3 matrices),

$$\frac{\partial}{\partial r} \Gamma_{\ell m} = - \frac{(\ell+3)}{r} \Gamma_{\ell m} \quad . \tag{2.4}$$

Just to fix the ideas, we shall think of $\Gamma_{\ell m}$ as one of the V_{rr} harmonic components. Then it is

$$(\Gamma_{\ell m})_{rr} \sim \left(\frac{\mu}{R}\right) \frac{(\ell+1)(\ell+2)}{R^2} \left(\frac{R}{r}\right)^{\ell+3} u_{\ell m} Y_{\ell m}(\varphi, \lambda) \quad . \tag{2.5}$$

Formula (2.4) is useful in the linearized equation

$$\Gamma(r_0, \varphi, \lambda) = \Sigma_\ell \Gamma_\ell(r_0, \varphi, \lambda) = \Sigma_\ell \Sigma_m \Gamma_{\ell m}(r_0, \varphi, \lambda) =$$

$$\simeq \sum_{\ell, m} \Gamma_{0 \ell m}(r, \varphi, \lambda) - \frac{\delta r}{r} \sum_{\ell, m} (\ell+3) \Gamma_{0 \ell m}(r, \varphi, \lambda) \tag{2.6}$$

where the correction is expressed in terms of the "observed" harmonic components $\Gamma_{0\ell m}(r, \varphi, \lambda)$ and of the radial shift $\delta r = r_0 - r$. The summation in (2.6) is over m ($|m| \leq \ell$), and ℓ ($\ell = 0, 1, 2, \ldots$); we just ask ourselves what is the error we would commit, if we computed the second term in the right hand side of (2.6) by considering only the terms $\Gamma_{0,0,0}$ and $\Gamma_{0,2,0}$ as given (i.e. the point mass and the J_2-dipole terms). Referring to the (rr)-derivative and setting[3]

200 at the height of 200 km.

---

[3] Please note that with the same notation u, in slightly different contexts, we shall mean the normal potential, while δu will be replaced by the more customary T to mean the anomalous potential.

$$\begin{cases} \delta u = u - \left(\frac{\mu}{r}\right)[1 + J_2\, u_{2,0} \left(\frac{R}{r}\right)^2 \bar{P}_2(\sin\varphi)] \\ (\delta\Gamma_{\ell m})_{rr} = (\delta u_{rr})_{\ell m} \end{cases} \qquad (2.7)$$

we get

$$\sigma^2(\Gamma) = \frac{<\delta r^2>}{r^2} \Sigma_\ell (\ell+3)^2 \sigma^2(\delta\Gamma_{\ell m}) =$$

$$= \frac{<\delta r^2>}{r^2} \Sigma_\ell (\ell+3)^2(\ell+2)^2(\ell+1)^2 \left(\frac{\mu}{R^3}\right)^2 \left(\frac{R}{r}\right)^{2\ell+6} (\Sigma_m \delta u^2_{\ell m}). \qquad (2.8)$$

In (2.8) we have implicitly assumed that the "orbit discrepancy" δr is distributed independently from the geographical position (φ,λ)[4], so that

$$E\{\delta r^2 (\sum_{-\ell}^{\ell m} \delta u_{\ell m}\, Y_{\ell m})^2\} =$$

$$= <\delta r^2> \sum_{-\ell}^{\ell m} \delta u^2_{\ell m} = <\delta r^2> \sigma^2_\ell(\delta u) \quad . \qquad (2.9)$$

By assuming the simple Kaula rule, i.e.

$$\sigma^2_\ell(T) = 1.6\, \frac{10^{-10}}{\ell^3} \qquad (2.10)$$

and noting that $\mu/R^3 \cong 1.5 \cdot 10^{-6}$ sec $^{-2}$ after neglecting some minor terms, we find

$$\sigma^2(\Gamma) \cong \frac{<\delta r^2>}{r^2} (2.2) \cdot 10^{-12} \cdot (1.6) \cdot 10^{-10} \Sigma_\ell (\ell+1)(\ell+2)(\ell+3) q^{\ell+3}$$

$$(q = \left(\frac{R}{r}\right)^2 \cong 0,94) \quad . \qquad (2.11)$$

In order to use (2.11), to obtain a rough estimate of the error we must decide on $<\delta r^2>$ and we have to estimate the sum

---

4
More precisely we shall agree that δr is uniformly distributed in $r_0 \pm 5$ km and that we would find the same distribution of δr even if we rotated the underlying anomalous gravity field.

$$f(q) = \sum_{2\ell}^{+\infty} (\ell+1)(\ell+2)(\ell+3)q^{\ell+3} =$$

$$= q^3 \frac{\partial^3}{\partial q^3} \{ \sum_{0\ell}^{+\infty} q^{\ell+3} - q^3 - q^4 \}$$

$$= q^3 \{ \frac{\partial^3}{\partial q^3} (\frac{q^3}{1-q}) - 6 - 24q \} \quad . \tag{2.12}$$

As for the first problem, we stipulate that the distribution of δr in $r \pm 5$ km is uniform. This is in reasonable agreement with the law (2.3). In this case

$$\langle \delta r^2 \rangle = \frac{1}{10} \int_{-5}^{5} x^2 \, dx = 8.3 \text{ km}^2$$

and

$$\frac{\langle \delta r^2 \rangle}{r^2} \cong 1.9 \cdot 10^{-7} \quad . \tag{2.13}$$

As for (2.9) a rough computation shows that

$$f(q) \simeq 3.9 \cdot 10^5 \quad . \tag{2.14}$$

Summarizing from (2.11), (2.12), (2.13), (2.14) we obtain

$$\sigma(\Gamma) \sim 5.1 \cdot 10^{-12} \text{ sec}^{-2} = 5.1 \cdot 10^{-3} \text{ E} \quad , \tag{2.15}$$

The estimate (2.15) says that with a realistic gradiometer the measuring error will in any way dominate the error committed by moving the measure point to a fixed sphere, while using in $\frac{\partial \Gamma}{\partial r}$ only the (0,0) and (2.0) terms.

Even in case we avail ourselves of a very accurate instrument, say with an r.m.s. error of 10^{-3} E, we can easily understand that, by accepting a certain bias (say 10% of the coefficients) in a first iteration, one can exploit a much better model to compute the reduction $\frac{\partial \Gamma}{\partial r} \delta r$, so that a second iteration is certainly not needed. At this point we can already say that, after some manipulations, our data are given at points on a sphere of radius R + h (where e.g. h $\cong$ 200 km) and we can proceed almost straightforwardly to form a field

of mean block values, as customary in geodesy, after defining for instance a suitable grid of equi-angular blocks; e.g. in the sequel we shall use systematically a $1^0 \times 1^0$ geographical grid.

The last point to be discussed, before we can reason only in an earth-fixed coordinate system (e.g. in radial coordinates r, φ, λ), is how to relate the gradiometric tensor, which by its very nature is measured in a satellite-fixed frame, to the same tensor in a local frame referred to the ($\underline{e}_x$, $\underline{e}_y$, $\underline{e}_z$) unit vectors. The transformation from the instrument frame to an orbit frame where z points in the radial direction, u is tangent (along track) and v out of plane (cross-track), is a matter of identifying the attitude either by some extra device (star-tracker) or by exploiting the observations themselves; as pointed out we shall not deal with this problem here. Yet it remains to rotate from the orbit-related (u,v,z) system to the local system (x,y,z) where x points to north, y to east and z to the zenith of the satellite. The interesting point here is that there is an asymmetric behavior between the ascending and descending arcs, as illustrated in Figure 2.1.

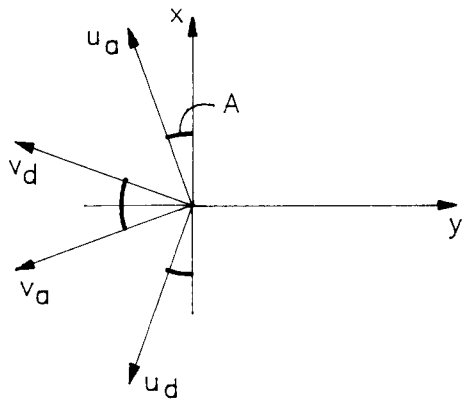

Figure 2.1: The geometry of ascending and descending orbit-related systems.

The azimuth A is given by the ratio of the earth's velocity $\dot{\theta}$ to the satellite's velocity, i.e. disregarding the sign,

$$\text{tg } A = \frac{\dot{\theta} \cos \varphi}{n} \quad , \qquad (2.15)$$

with a satellite of 1.5 hours period and considering a local equatorial frame, where it is maximal, we find $A \cong 3.5^0$.

Now the rotation can be accomplished rather easily if we take into account first of all that the z axis remains invariant so that for instance the component $\frac{\partial^2 T}{\partial z^2}$ does not need to be changed, and that

$$\begin{cases} \dfrac{\partial}{\partial v_a} = -\sin A \dfrac{\partial}{\partial x} - \cos A \dfrac{\partial}{\partial y} \\ \dfrac{\partial}{\partial v_d} = \sin A \dfrac{\partial}{\partial x} - \cos A \dfrac{\partial}{\partial y} \end{cases} \tag{2.16}$$

With these two operators we can find the two components of the tensor, that do depend on the orientation but are worth measuring, because they involve only channels orthogonal to the u-axis, which is the most disturbed by the irregular drag effects. Namely we can write

$$\begin{aligned} \frac{\partial^2 T}{\partial v_a \partial z} &= -\sin A \frac{\partial^2 T}{\partial x \partial z} - \cos A \frac{\partial^2 T}{\partial y \partial z} \\ \frac{\partial^2 T}{\partial v_d \partial z} &= \sin A \frac{\partial^2 T}{\partial x \partial z} - \cos A \frac{\partial^2 T}{\partial y \partial z} \quad , \end{aligned} \tag{2.17}$$

which, combined, give

$$\frac{1}{2}\left(\frac{\partial^2 T}{\partial v_a \partial z} + \frac{\partial^2 T}{\partial v_d \partial z}\right) = -\cos A \frac{\partial^2 T}{\partial y \partial z} \quad . \tag{2.18}$$

The orthogonal combination, with the minus sign, conveys only little information compared with (2.18), because, while $\cos A \sim 1$, $\sin A$ is rather small ($< 6 \cdot 10^{-2}$). As for the second derivatives one can write

$$\begin{aligned} \frac{\partial^2 T}{\partial v_a^2} &= \sin^2 A \frac{\partial^2 T}{\partial x^2} + \cos^2 A \frac{\partial^2 T}{\partial y^2} + 2 \sin A \cos A \frac{\partial^2 T}{\partial x \partial y} \\ \frac{\partial^2 T}{\partial v_d^2} &= \sin^2 A \frac{\partial^2 T}{\partial x^2} + \cos^2 A \frac{\partial^2 T}{\partial y^2} - 2 \sin A \cos A \frac{\partial^2 T}{\partial x \partial y} \quad , \end{aligned} \tag{2.19}$$

and again combining the two in a sum,

$$\frac{1}{2}\left(\frac{\partial^2 T}{\partial v_a^2} + \frac{\partial^2 T}{\partial v_d^2}\right) = \sin^2 A \frac{\partial^2 T}{\partial x^2} + \cos^2 A \frac{\partial^2 T}{\partial y^2} \quad . \tag{2.20}$$

Taking advantage of the harmonicity of T, we easily reduce (2.20) to the form

$$\frac{1}{2}\left(\frac{\partial^2 T}{\partial v_a^2} + \frac{\partial^2 T}{\partial v_d^2}\right) + \sin^2 A \frac{\partial^2 T}{\partial z^2} = (\cos^2 A - \sin^2 A) \frac{\partial^2 T}{\partial y^2} \quad . \tag{2.21}$$

In this relation the first member can be considered as an observable and we get in this way a functional relation to $\frac{\partial^2 T}{\partial y^2}$: naturally this creates a correlation with the observable $\frac{\partial^2 T}{\partial z^2}$, but since $\sin^2 A \leq 3.7 \cdot 10^{-3}$, this correlation is small and we shall neglect it in the further treatment of the data.

Concluding and summarizing we can say that after the radial correction, after the block averaging and after creating the combinations (2.18) and (2.21), we can assume that observation equations are given at the centers of the blocks, which expressed in terms of spherical coordinates, read

$$\begin{aligned} \Gamma_{zz} &= \frac{\partial^2 T}{\partial r^2} \\ \Gamma_{zy} &= \frac{1}{r \cos\varphi} \frac{\partial^2 T}{\partial r \partial \lambda} - \frac{1}{r^2 \cos\varphi} \frac{\partial T}{\partial \lambda} \\ \Gamma_{yy} &= \frac{1}{r^2 \cos^2\varphi} \frac{\partial^2 T}{\partial \lambda^2} - \frac{\operatorname{tg}\varphi}{r^2} \frac{\partial T}{\partial \varphi} + \frac{1}{r} \frac{\partial T}{\partial r} \end{aligned} \quad . \tag{2.22}$$

It is the task of the boundary value problem approach to analyze these as boundary relations for T, to indicate the more or less optimal methods to derive from these a suitable solution and demonstrate how the theoretical recipes can be implemented by practical numerical methods.

As a very last remark we want to stress that the information coming from satellite observations and elaborated in the form of a b.v.p. will supply us in the end with a solution which represents the anomalous potential T at the satellite's altitude; it is then an open question how this model can be backward continued, down to the earth's surface. We will not tackle this difficult problem here, but we will confine ourselves to mention that the easiest way of doing it is just to represent T in a spherical harmonic expansion and then truncate it to a maximum degree N: the truncated model then automatically gives a representation of T at the ground level. Naturally, the choice of N is a crucial point, because we would not like to amplify and propagate too much noise in our model; the criterion for the choice of N will

be discussed in the next paragraph. It is also worth mentioning that by the way our series will not really converge on the earth surface, but fortunately the degree at which adding new terms to the sum gives a worse rather than a better approximation, is so high that we will not be able to come close to such a resolution (Moritz, 1980). Henceforth we close the paragraph by saying that our aim is to solve a b.v.p. with boundary conditions (2.22), in the sense that we want to estimate the coefficients $\delta u_{\ell m}$ of the expansion of T in a spherical harmonic series on the earth's sphere (r = R), up to some maximal degree N to be specified later.

2.2. The observational model for spectral estimation from block averages.

In this paragraph we consider the problem of deriving estimates of the harmonic coefficients $u_{\ell m}$ of a function u defined on the unit sphere so that

$$u(P) = \sum_{0}^{+\infty}{}_{\ell} \sum_{-\ell}^{\ell m} u_{\ell m} Y_{\ell m}(P) \quad . \tag{2.23}$$

As input data we shall consider the values of u on a set of points $\{P_i;$ $i = 1,\ldots,\ell_{max}\}$ distributed in some way on the sphere; since this is for us the most important case, we shall mainly consider P_i as the centers of a regular geographical grid, dividing meridians in N equal intervals and parallels in 2N equal intervals, so that $\ell_{max} = 2N^2$ (for instance if N = 180, ℓ_{max} = 64800, corresponding to a grid of $1^0 \times 1^0$ blocks). Furthermore we shall assume that the available values of $u(P_i)$ come from observations including measurement errors, i.e. modelled by the equation

$$u_0(P_i) = u(P_i) + \nu_i \quad ; \tag{2.24}$$

if we assume a stochastic model for ν_i, for instance

$$E\{\nu_i\} = 0 \tag{2.25}$$

$$E\{\nu_i \nu_j\} = \sigma^2_{\nu_i} \delta_{ij} \quad , \tag{2.26}$$

we can formulate our problem as to derive estimates for $u_{\ell m}$ from (2.23), (2.24) (2.25), (2.26) when $u_0(P_i)$ are given.

Stated in this way, it is a pure problem of spectral estimation on the sphere and we use it as a preparation to treat the more complicated b.v.p.'s, which however fall in a class of problems very close to this whenever the boundary operator has diagonal representation in terms of spherical harmonics.

This problem has naturally received much attention from geodesists and we just mention some authors for reference, without any pretension of completeness: (Colombo, 1981), (Marsh et al., 1988), (Moritz, 1976), (Pavlis, 1988), (Rapp and Cruz, 1986), (Rummel, Teunissen, and Van Gelderen, 1989), (Sansò, 1990).

There are essentially two ways in which this problem can be approached: one is to reduce the solution space by truncating the series (at most) at the degree N, so that the number of unknowns, $(N+1)^2$, becomes smaller than the number of observations $2N^2$ (this happens at least if $N \geq 3$) and then a simple least squares approach can be applied, with or without prior information; the other one is to consider first the data as a continuum, apply the very definition of $u_{\ell m}$ by a quadrature formula, i.e.

$$\hat{u}_{\ell m} = \frac{1}{4\pi} \int u_0(P) Y_{\ell m}(P) d\sigma \quad , \tag{2.27}$$

and then try to approximate this in terms of the discrete available data. Also in this second case, as for the first one, there is a natural limit over which any discretization of (2.27) would loose its meaning namely $\ell \leq N$.

In fact it is just enough to consider $u(P_i)$ along parallels and observe that for each parallel one has 2N observations, so that the corresponding maximum frequency, above which the spectrum starts folding and the correspondence between values and coefficients is lost (i.e. the so-called Nyquist frequency), is exactly N. Before we come, in the next paragraph, to describe the error propagation we can expect by following one or the other approach, we must give some thought to the covariance structure (2.26) and see whether and how it is verified under the theoretical hypothesis of an instrument orbiting on a polar circular orbit and measuring at a constant rate of 1/s Hz, e.g. 1 measurement every s = 4 seconds. As a first computation, let

us start by disregarding the effect of the rotation of the earth on any single orbit; since the angular velocity of the satellite is constant and equal to n (mean motion), the satellite spends a time $\tau = \frac{\Delta\varphi}{n}$ to cross a belt of amplitude $\Delta\varphi$ in latitude, taking $\tau/s = \Delta\varphi/ns$ observations; moreover if the nodes tend to distribute uniformly along the equator, as for a mission of duration T there are $N_c = \frac{nT}{2\pi}$ cycles, i.e. $2N_c = \frac{nT}{\pi}$ crossings of the equator, we expect that $dN_c = \frac{\Delta\lambda}{\pi} N_c$ of them will fall in a sector of width $\Delta\lambda$. Therefore if we have a block of $\delta^0 \times \delta^0$ we find in it about

$$n_0 = \frac{\Delta\varphi\Delta\lambda}{2\pi^2} \frac{T}{s} = \frac{\delta^2}{64800} \frac{T}{s} \qquad (2.28)$$

observations. For a mission of a duration of 6 months and a $1^0 \times 1^0$ block, we expect 60 observations per block distributed as almost 4 observations along 16 different tracks.

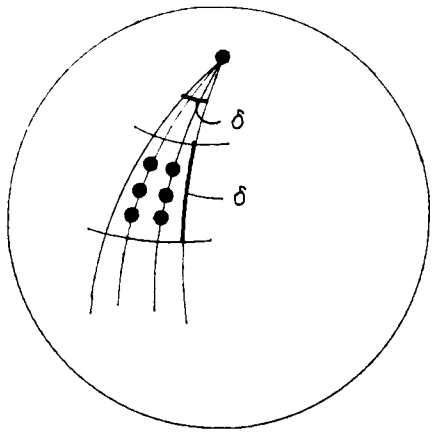

Figure 2.2: Distribution of observation points.

As we can see this distribution does not depend on λ, so that, if we allow the earth to rotate under it in the average we must expect the same number of observations per block. If we assume that each observation has an independent error ν with the same variance σ^2_ν, we can also say that by averaging the observed u_0 values over the points P_{ijk} falling into the block $B_{ij} \equiv \{i\delta \le \varphi \le (i+1)\delta;\ j\delta \le \lambda \le (j+1)\delta\}$, i.e., by forming

$$\bar{u}_0(P_{ij}) = \frac{1}{n_0} \sum_1^{n_0} u_0(P_{ijk}) \quad , \tag{2.29}$$

we should find a quantity affected by independent random noise

$$\bar{\nu}_{ij} = \frac{1}{n_0} \sum_1^{n_0} \nu_{ijk} \tag{2.30}$$

with variance $\sigma_0^2 = \frac{\sigma_\nu^2}{n_0}$. Indeed $\bar{\nu}_{ij}$ is not the only error we commit by expressing the average of u over the block B_{ij} through (2.29), because there is as well the bias, given by the formula

$$b(P_{ij}) = u(P_{ij}) - \frac{1}{n_0} \sum_1^{n_0} u(P_{ijk}) \quad . \tag{2.31}$$

This error depends on the specific shape of u and on the exact location of P_{ijk}. A big effort has been devoted to the reduction of b; the simplest solution is probably to note that the second term in the right hand side of (2.31) represents some kind of average of u over the block B_{ij}, so that we can expect more closely

$$\bar{b}(P_{ij}) = \frac{1}{B_{ij}} \int_{B_{ij}} u(P) d\sigma_P - \frac{1}{n_0} \sum_1^{n_0} u(P_{ijk}) \cong 0 \quad . \tag{2.32}$$

Formula (2.32) would not be such a good step forward, if we took it rigorously, because the action of averaging u over a square block is complicated when expressed in spectral terms; however most authors accept the approximation of considering (2.32) as an average over a circular cap C of radius ψ_0 such that the area of C equals the area of B at the equator, i.e., $2\pi(1-\cos\psi_0) = \frac{\pi^2}{N^2}$.

In this way the integral operator in (2.32) becomes a simple moving average, of which it is easy to verify the representation

$$\frac{1}{C} \int_c u(Q) d\sigma_Q = \bar{u}(P) = \sum_{\ell,m} \beta_\ell u_{\ell m} Y_{\ell m}(P) \tag{2.33}$$

where β_ℓ are the famous Pellinen coefficients

$$\beta_\ell(\psi_0) = \frac{1}{1 - \cos \psi_0} \int_0^{\psi_0} P_\ell (\cos \psi) \sin \psi \, d\psi \quad . \tag{2.34}$$

From (2.33) we see that our problem has just been changed from the estimation of u_{ℓ_m} from $u_0(P_{ij})$, to the estimation of $\bar{u}_{\ell_m} = \beta_\ell \, u_{\ell_m}$ from $\bar{u}_0(P_{ij})$. As we have clarified, the stochastic structure of the errors $\bar{\nu}_{ij}$ is that of a zero average white noise of uniform variance $\sigma_0^2 = \sigma_\nu^2/n_0$. This is verified if we are right in claiming that the residual bias implied by the various approximations is negligible as compared to the noise; a deeper discussion on the representation of block averaging in spectral terms, with more references, can be found for instance in (Rapp, 1989). Before closing this paragraph we want to discuss the stochastic model we would obtain by letting the side of our square blocks tend to zero.

We first note that by using (2.28) and (2.30), where we set $N_0 = T/s$ = total number of the observations, we can write for any pair of blocks, identified by the coordinates (φ_i, λ_j), $(\varphi_\ell, \lambda_k)$ of their centers,

$$E\{\bar{\nu}_{ij} \, \bar{\nu}_{\ell k}\} = \delta_{i\ell} \, \delta_{jk} \, \sigma_\nu^2 \, \frac{2\pi^2}{N_0 \, \Delta\varphi \, \Delta\lambda} \quad . \tag{2.35}$$

Now we observe that the area of a block is given by $\Delta\sigma_{ij} = \cos \varphi_i \, \Delta\varphi \, \Delta\lambda$, so that after introducing the field of measures

$$d\mu_{ij} = \bar{\nu}_{ij} \, \Delta\sigma_{ij} \quad ,$$

for the moment defined only on our family of blocks, we get

$$E\{d\mu_{ij} \, d\mu_{\ell k}\} = \delta_{i\ell} \, \delta_{jk} \, \frac{2\pi^2\sigma_\nu^2}{N_0} \cos \varphi_i \, \Delta\sigma_{ij} \quad . \tag{2.36}$$

Consequently for any pair of sets A,B constituted by a number of blocks, we discover that

$$E\{\mu(A)\mu(B)\} = \frac{2\pi^2\sigma_\nu^2}{N_0} \int_{A \cap B} \cos \varphi \, d\sigma \quad . \tag{2.37}$$

Now if A and B are any measurable sets over σ, by considering them as limits of multiblock sets, we see that (2.37) continues to hold; since it is also for any A

$$E\{\mu(A)\} = 0 \quad , \tag{2.38}$$

we see that our field of stochastic measures, extended in this way, is in fact a field of Wiener measures[5], with density $\frac{2\pi^2\sigma_\nu^2}{N_0}\cos\varphi$; the relevance of such measures to b.v.p.'s is illustrated in (Sansò, 1988). The most important application of such a measure is the definition, as a limit in the mean square sense, of the corresponding integral of any square integrable function f

$$I_f = \int f(P)d\mu(P) \quad , \tag{2.39}$$

which is indeed a random function belonging to the linear space spanned by $\{d\mu(P)\}$.

Notably for such integrals, the Wiener rules hold

$$E\{I_f\} = E\{ \int f(P)d\mu(P)\} = 0 \tag{2.40}$$

$$E\{I_f I_g\} = E\{ \iint f(P)g(Q)d\mu(P)d\mu(P)\} =$$

$$= \frac{2\pi^2\sigma_\nu^2}{N_0} \int f(P)g(P)\cos\varphi \, d\sigma \quad . \tag{2.41}$$

These formulas will be of fundamental importance for the computation of error models in the b.v.p. approach.

---

[5] The other characteristic of Wiener measures, i.e. the fact that they are normal random variables, is plausible in this case with the measurement noise.

2.3. The least squares approach.

From the discussion developed in the preceding paragraph we receive the following problem; by defining a function

$$\begin{cases} \bar{u}(P) = \Sigma_{\ell,m}\, \bar{u}_{\ell m}\, Y_{\ell m}(P) \\ \\ \bar{u}_{\ell m} = \beta_{\ell m} u_{\ell m} \end{cases} \tag{2.42}$$

of which we have observed values at the centers of a regular grid,

$$\bar{u}_0(P_{ij}) = \bar{u}(P_{ij}) + \bar{\nu}_{ij} \tag{2.43}$$

with a noise characterized by the stochastic behaviour

$$\begin{aligned} &E\{\bar{\nu}_{ij}\} = 0 \\ \\ &E\{\bar{\nu}_{ij}\ \bar{\nu}_{\ell k}\} = \delta_{i\ell}\ \delta_{jk}\ \sigma_0^2 \end{aligned} \qquad , \tag{2.44}$$

we want to estimate $\{\bar{u}_{\ell m}\}$. Stated in this way the problem is naturally underdeterminated ($2N^2$ observations for a set of infinite unknowns), however since we know that we cannot find any solution with a resolution higher that that implied by the maximum degree N, we just substitute (2.42) by the truncated formula

$$\bar{u}(P) \cong \sum_{0\ell}^{N} \sum_{-\ell m}^{\ell} \bar{u}_{\ell m}\, Y_{\ell m}(P) \tag{2.45}$$

with $(N+1)^2$ unknown parameters, so that the problem becomes overdetermined and we can apply to it a least squares criterion. Let us see how does it work in this case. By forming the normal system we get

$$\sum_{\substack{\ell,m \\ (\ell \le N)}} \{ \sum_{i,j}\ Y_{nk}(P_{ij}) Y_{\ell m}(P_{ij}) \} \bar{u}_{\ell m} = \sum_{i,j}\ Y_{nk}(P_{ij}) \bar{u_0}(P_{ij}) \tag{2.46}$$

that we shall divide by $2N^2$, just for convenience in further computations. So (2.46) is a classical normal system with the vector of unknowns $x = \{\bar{u}_{\ell m};\ |m| \le \ell,\ \ell \le N\}$, with normal matrix

$$N = \{\frac{1}{2N^2} \Sigma_{i,j}\ Y_{nk}(P_{ij}) Y_{\ell m}(P_{ij})\} \qquad (2.47)$$

and with known normalized term

$$L_0 = \{\frac{1}{2N^2} \Sigma_{i,j}\ Y_{nk}(P_{ij}) \bar{u}_0(P_{ij})\} \quad . \qquad (2.48)$$

Naturally since the components of our unknown vector have two indices, the same is true for L_0, while the elements of N have four indices. But it is easy to understand how to vectorize it. The computation of the solution of (2.46) would become a hard test whenever $N > 100$, was it not for the regular pattern of the grid points P_{ij}.

In fact, as pointed out by Colombo (1981), if we apply formula (2.47) by summing first along the parallels, i.e. over the index $j\{\lambda_j = j\delta,\ j = 0,1,\ldots 2N-1\}$, we can take advantage of the usual orthogonality relations holding for finite Fourier transforms, i.e.

$$\sum_{0}^{2N-1}{}_j \left\{ \begin{array}{c} \sin m\lambda_j \\ \\ \cos m\lambda_j \end{array} \right\} \{\sin k\lambda_j \ \cos k\lambda_j\} = N\delta_{mk} \left\{ \begin{array}{cc} 1 & 0 \\ \\ 0 & 1 + \delta_{0m} \end{array} \right\} . \qquad (2.49)$$

Accordingly the elements of the normal matrix N become

$$N_{nk,\ell m} = \frac{(1+\delta_{0m})}{2N} \delta_{mk} \sum_{1}^{N}{}_i \bar{P}_{n|m|}(\varphi_i) \bar{P}_{\ell|m|}(\varphi_i) \quad . \qquad (2.50)$$

Formula (2.50) implies that by reordering the unknowns as well as the normal matrix first by degrees and then by orders (see figure 2.3) we find that N has a block diagonal structure with maximum block dimension N+1.

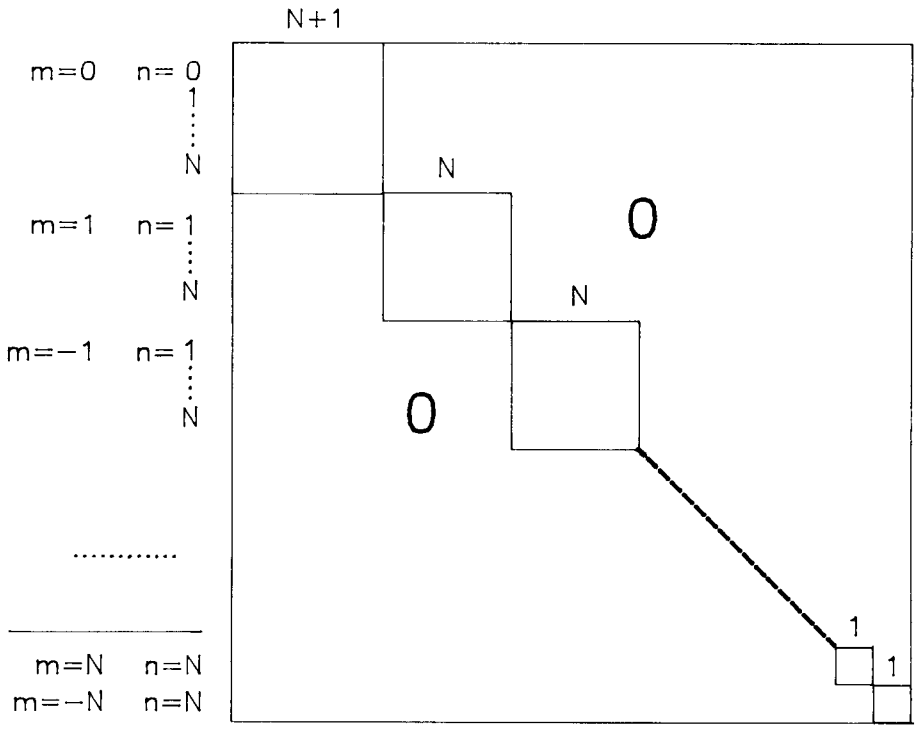

Figure 2.3: Structure of the normal matrix after suitable ordering of the unknowns.

The inversion of such a matrix poses no problem from the numerical point of view. So we can find our least squares solution and we know that it is efficient, i.e. of minimum variance in the class of linear estimators. This nice property, however, holds only if the deterministic model is correct, i.e. if there are no biases, since, as we know, the least squares approach is very sensitive to biases. The method interprets the biases as additive noise and spreads them among the residuals of all the observations in an effort of reducing their amplitude. This is indeed our case since we can write for the known normal term:

$$L_0 = \{\frac{1}{2N^2} \Sigma_{ij} Y_{nk}(P_{ij})[\bar{u}_N(P_{ij}) + \bar{\nu}_{ij} + \bar{u}^N(P_{ij})]\}$$

$$= L_N + L_\nu + L^N \quad , \qquad (2.51)$$

where we can put

$$\bar{u}(P) = \bar{u}_N(P) + \bar{u}^N(P) =$$

$$= \sum_{0}^{N}{}_{\ell,m}\ \bar{u}_{\ell m}\ Y_{\ell m}(P) + \sum_{N+1}^{+\infty}{}_{\ell,m}\ \bar{u}_{\ell m}\ Y_{\ell m}(P) \qquad . \tag{2.52}$$

Interchanging the summation in $\bar{u}_N$ with that in (2.51) we see that

$$L_N = \{\sum_{0}^{N}{}_{\ell,m}\ \frac{1}{2N^2}\ [\Sigma_{i,j}\ Y_{nk}(P_{ij})Y_{\ell m}(P_{ij})]\bar{u}_{\ell m}\} =$$

$$= N\ x \qquad . \tag{2.53}$$

Subsequently the normal system can be written as

$$N\ \hat{x} = N\ x + L_\nu + L^N \qquad , \tag{2.54}$$

showing that the l.s. estimate $\hat{x}$ would be unbiased only on condition that

$$L^N = 0 \qquad . \tag{2.55}$$

Otherwise we have a bias in $\hat{x}$ given by

$$E\{\hat{x}-x\} = N^{-1}\ L^N \qquad . \tag{2.56}$$

To understand whether (2.55) has any chance to be verified, we can imagine to study the limit of L^N if we keep fixed the truncation degree N, but we let the number of blocks N_B (which formerly was exactly $2N^2$) tend to infinity. After we observe that

$$\frac{2\pi^2}{N_B} = \Delta\varphi\ \Delta\lambda$$

and that

$$\Delta\sigma(P) = \cos\varphi\ \Delta\varphi\ \Delta\lambda \qquad ,$$

we can write

$$L^N = \{\frac{1}{2\pi^2} \Sigma_{ij} Y_{nk}(P_{ij})\bar{u}^N(P_{ij}) \frac{\Delta\sigma_{ij}}{\cos\varphi_i}\}$$

$$\rightarrow \{\frac{1}{2\pi^2} \int Y_{nk}(P) \frac{\bar{u}^N(P)}{\cos\varphi} d\sigma\} \quad . \qquad (2.57)$$

This formula shows that L^N does not vanish because of the presence of the term $(\cos\varphi)^{-1}$ describing essentially the density of data distribution which indeed tends to increase towards the poles. In fact (2.57) tells us that all frequencies (ℓ,k) with $\ell > N$ but such that

$$\int_{-\pi/2}^{\pi/2} \bar{P}_{nk}(\varphi)\bar{P}_{k}(\varphi)d\varphi \neq 0 \quad , \qquad (2.58)$$

will contribute to the bias in the (n,k) component of L^N; in other words there is an aliasing of power from the components (ℓ,k) $(\ell \geq N)$ into the lower frequency components. This aliasing is characteristic of the l.s. approach.

We can observe that formula (2.58) enforces a "selection rule" saying that odd degrees will generate aliasing in odd degrees only and similarly with the even degrees. A few simple numerical tests have been designed to give evidence to this phenomenon. At first $1^0 \times 1^0$ blocks were generated with a field[6] truncated at $N_{max} = 90$; the coefficients of this field were then estimated via least squares and compared to the original coefficients. The software used was a modified version of that written by Colombo (1981).

The comparison is displayed in Figure 2.4 in terms of the histogram of the relative differences defined as

$$d = \frac{|\text{est.coeff.}(\ell,m) - \text{true coeff.}(\ell,m)|}{|\text{true coeff.}(\ell,m)|} \quad . \qquad (2.59)$$

---

[6] In this as well as in the subsequent simulations the model OSU-81 has been used.

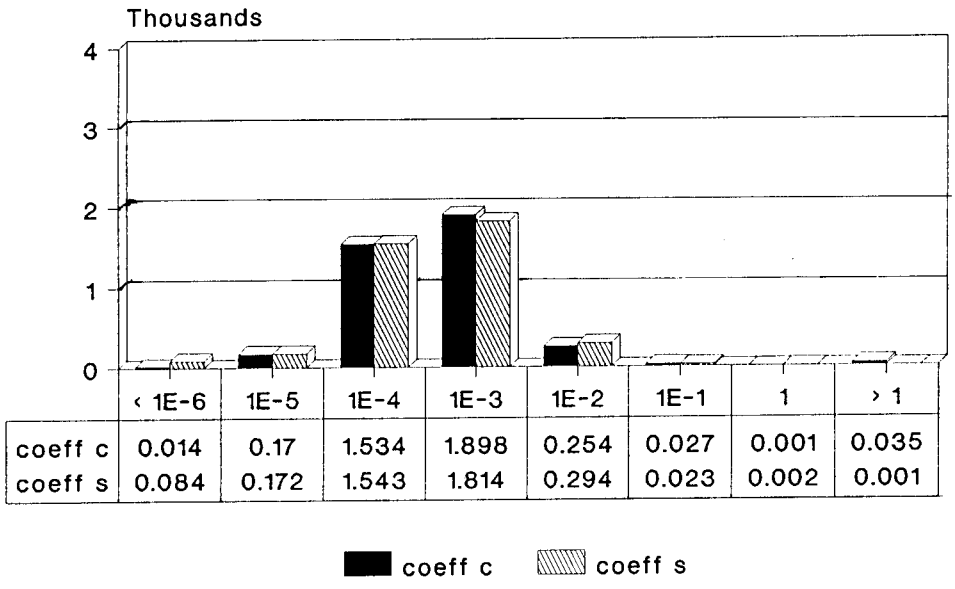

Note: Only degrees 21 - 90 were compared

Figure 2.4: Histogram of the index d (2.59).
Input degrees 0-90.
Output degrees 0-90.

As one can see the result is not fully satisfactory. This however is mostly due to numerical problems that arise in handling together unknown coefficients with magnitudes ranging over 6-7 orders. In fact if we repeat the same experiment, only eliminating the first 20 degrees, we get the result shown in Figure 2.5, which seems very good indeed.
This first experiment actually confirms the correctness of the least squares estimates when the deterministic model is also correct.

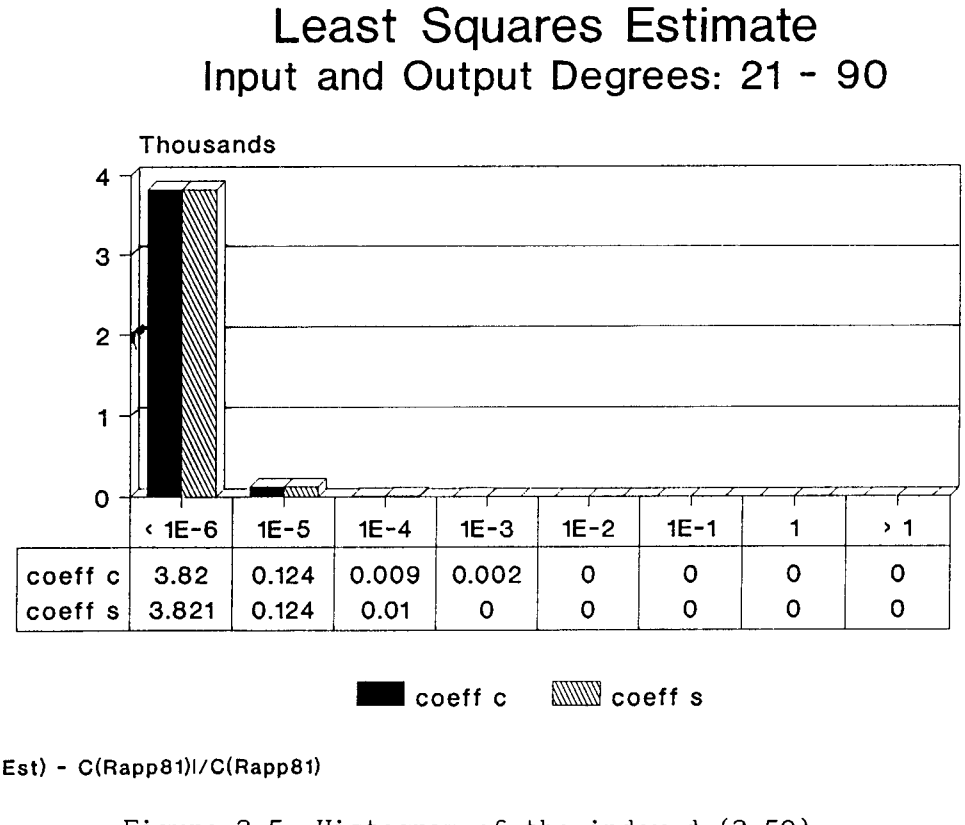

	‹ 1E-6	1E-5	1E-4	1E-3	1E-2	1E-1	1	› 1
coeff c	3.82	0.124	0.009	0.002	0	0	0	0
coeff s	3.821	0.124	0.01	0	0	0	0	0

Figure 2.5: Histogram of the index d (2.59).
Input degrees 21-90.
Output degrees 21-90.

In the next experiment we rather want to put in evidence the presence of aliasing. To this aim we have generated a $1^0 \times 1^0$ sphere by using only the odd degrees between 91 and 101 of the OSU-81 model; with this input we then estimated, by the least squares algorithm, all the odd-degree coefficients between 21 and 89. In order to weigh the amount of bias generated in this way, we have compared the estimated coefficients with the (physically meaningful) mean power of the same degree in the original model, i.e. we have computed the index

$$\text{ratio} = \frac{|\hat{u}_{\ell m}|}{\sqrt{\frac{1}{2\ell+1}\sum_{-\ell}^{\ell} u_{\ell m}^2}} \qquad (2.60)$$

$\hat{u}_{\ell,m}$ estimated coefficients

$u_{\ell,m}$ true coefficients.

In Figure 2.6 we display the behaviour of this ratio for the degrees 89 and 87.

One should believe that the only coefficients affected by a significant aliasing are those which are close to the cut frequency; in fact just observing the absolute ratio

$$\text{absolute ratio} = \left|\frac{\hat{u}_{\ell m}}{u_{\ell m}}\right| \qquad (2.61)$$

and plotting only the orders and degrees where this index is larger than 0.5 and 0.1 respectively, one gets the distribution shown in Figure 2.7. One can see that the influence of aliasing is in fact diffused also in the lower degrees, in particular at low orders.

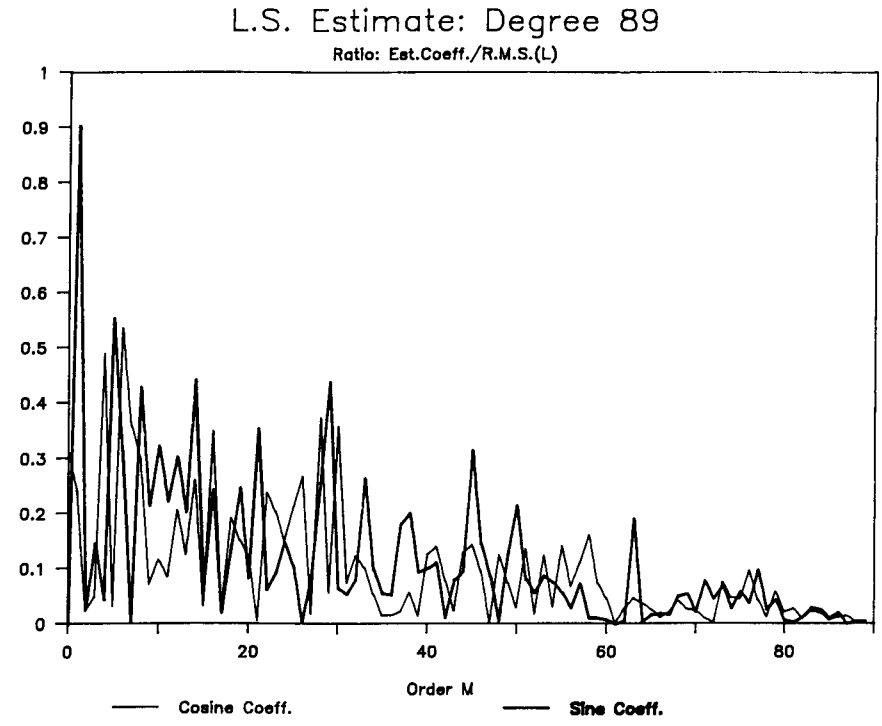

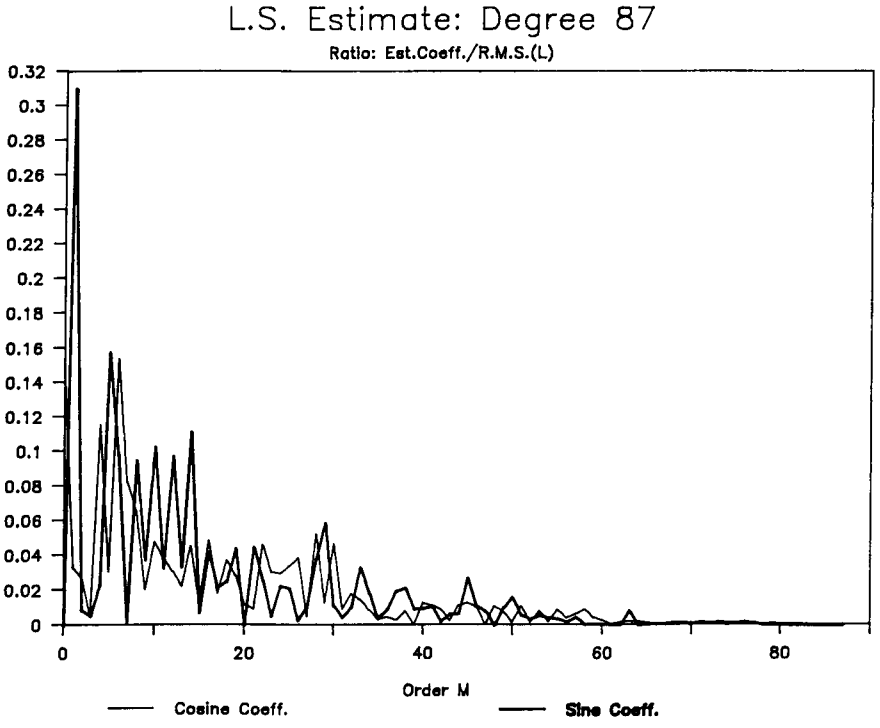

Figure 2.6: Index (2.60) for degrees 89, 87.

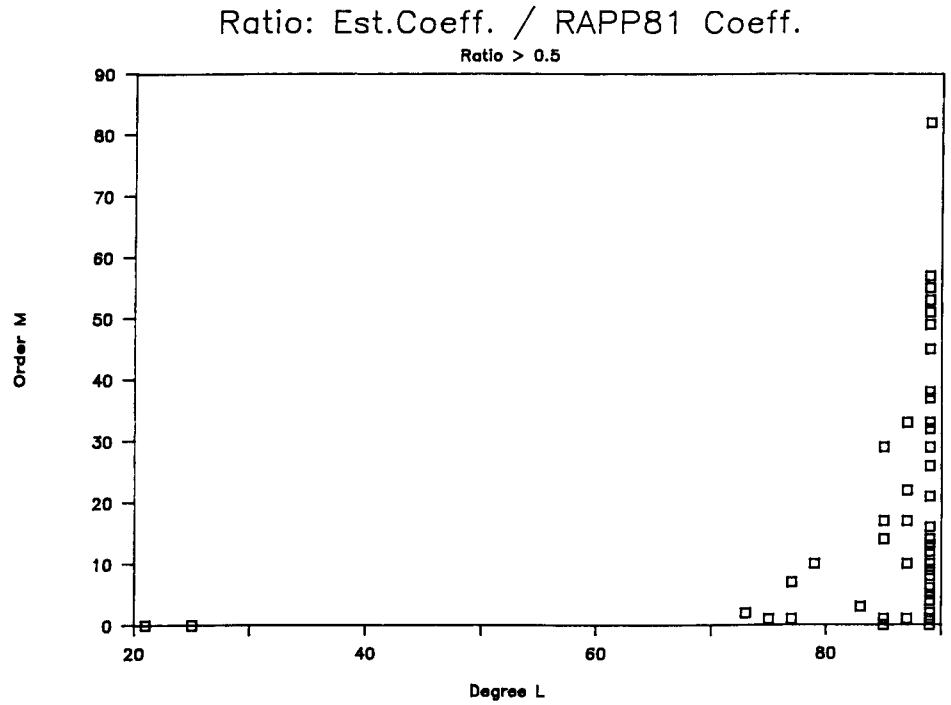

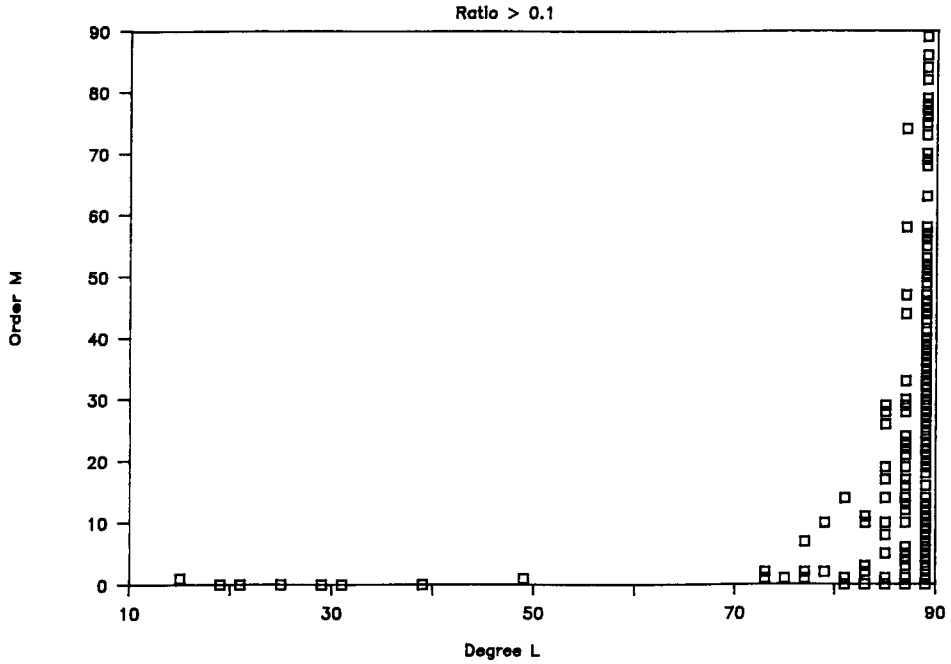

Figure 2.7: Spectral positions of the coefficients for which the index (2.61) is larger than 0.5 and 0.1 respectively.

2.4. The quadrature formulas approach.

We return to the problem stated at the beginning of paragraph 2.3, as defined by formulas (2.42), (2.43), (2.44). In this paragraph we follow a different strategy of solution, namely we first try to transform the observation equation (2.43) into its continuous counterpart; then we give the exact solution of the estimate of $\bar{u}_{\ell m}$ for the continuous case, which is nothing but a suitable quadrature formula; finally we use a discretized version of the quadrature formula to arrive at the point where we can explicitly estimate $\bar{u}_{\ell m}$ in terms of the observable quantities.

This approach is not optimal, contrary to the l.s. approach, however it avoids the aliasing implied by the truncation of the representation (2.42) at a cut-off frequency. The only bias contained in it is the unavoidable approximation of the quadrature formula by means of a summation.

Instead we need at least to compute the model of the error propagation, within this approach, first of all to be able of judging upon its performance and also to use it in further combinations.

In this paragraph we shall only analyze the case in which the orthonormality properties of the spherical harmonics at $\{Y_{\ell m}(P)\}$ are exploited; more general cases will be analyzed in the next paragraph.

So first of all we consider the limit of formula (2.43) and we notice that this cannot be performed straightforwardly as the variance of $\bar{\nu}_{ij}$ would tend to infinity for $(\Delta\varphi\Delta\lambda) \to 0$, according to formula (2.35); so in order to give a suitable meaning to this limit process, we just write the equation by multiplying it by $\Delta\sigma_{ij}$, i.e. as

$$\bar{u}_0(P_{ij})\Delta\sigma_{ij} = \bar{u}(P_{ij})\Delta\sigma_{ij} + \bar{\nu}_{ij}\Delta\sigma_{ij} \qquad (2.62)$$

and we reinterpret it in terms of fields of measures on the unit sphere. We therefore define a measurement field $d\mu_0(P)$ as

$$d\mu_0(P_{ij}) \sim \bar{u}_0(P_{ij})\Delta\sigma_{ij} \quad , \qquad (2.63)$$

its properties being defined by equating it to the second member in (2.62). Furtheron, we define the deterministic field, related to its density $\bar{u}$

$$d\mu_{\bar{u}}(P_{ij}) = \bar{u}(P_{ij})\ \Delta\sigma_{ij} \quad . \tag{2.64}$$

Finally we define a purely random Wiener measure $d\mu_w(P)$, describing the observational noise

$$d\mu_w(P_{ij}) \simeq \bar{\nu}_{ij}\Delta\sigma_{ij} \quad , \tag{2.65}$$

whose stochastic properties have been illustrated in § 2.2 ultimately in formulas (2.36), (2.38). Let us note that in this case we do not have a real density $\bar{\nu}(P)$, since there exists no regular function $\bar{\nu}(P)$ verifying the Wiener properties (2.18), (2.19). Formula (2.62) then becomes

$$d\mu_0(P) = d\mu_{\bar{u}}(P) + d\mu_w(P) \quad . \tag{2.66}$$

With such measures we can for instance compute Wiener integrals on the sphere, so that (2.66) could be written in the equivalent form

$$\int f\ d\mu_0(P) = \int f\ \bar{u}\ d\sigma(P) + \int f\ d\mu_w(P) \quad , \tag{2.67}$$

for any f square integrable over σ. If we take $f = \frac{1}{4\pi}\ Y_{\ell m}$ in (2.67) we get

$$\frac{1}{4\pi}\int Y_{\ell m}\ d\mu_0 = \bar{u}_{\ell m} + \frac{1}{4\pi}\int Y_{\ell m}\ d\mu_w \quad , \tag{2.68}$$

and since

$$E\{\frac{1}{4\pi}\int Y_{\ell m}\ d\mu_w\} = 0$$

we see that the functional

$$\hat{u}_{\ell m} = \frac{1}{4\pi}\int Y_{\ell m}(P)d\mu_0(P) \tag{2.69}$$

is a correct estimator. Naturally we cannot really compute (2.69) from the observations at hand, i.e. from $\bar{u}_0(P_{ij})$, however we can approximate (2.69) by the discretized formula

$$\hat{u}_{\ell m} = \frac{1}{4\pi} \Sigma_{ij} \bar{u}_0(P_{ij}) Y_{\ell m}(P_{ij}) \Delta\sigma_{ij} \quad . \tag{2.70}$$

In this way we introduce a bias which represents the discretization error. As we have already stated, in order that these estimates be meaningful, i.e. in order that the discretization error be reasonably small, we must limit formula (2.70) to the degrees ℓ for which $\ell \leq N$, if the sphere σ has been gridded by $2N^2$ square blocks.

As for the random noise propagated to $\hat{u}_{\ell m}$, we can get

$$\delta\hat{u}_{\ell m} = \frac{1}{4\pi} \int Y_{\ell m} \, d\mu_w \quad . \tag{2.71}$$

Therefore the error in the model that we can construct from the estimates $\hat{u}_{\ell m}$, is

$$e(P) = \hat{u}(P) - \bar{u}(P) = \sum_{0}^{N}{}_{\ell,m} \delta\hat{u}_{\ell m} Y_{\ell m}(P) - \sum_{N+1}^{+\infty}{}_{\ell,m} \bar{u}_{\ell m} Y_{\ell m}(P) \quad . \tag{2.72}$$

We define the global mean square error as

$$E^2 = E\{\frac{1}{4\pi} \int e^2(P) d\sigma\} \quad , \tag{2.73}$$

where the expectation E is taken over the population of the noise $d\mu_w$. From (2.73) we can write

$$E^2 = E_c^2 + E_0^2 \tag{2.74}$$

where we have defined the commission error as

$$E_c^2 = \sum_{0}^{N}{}_{\ell,m} E\{\delta\hat{u}_{\ell m}^2\} \quad , \tag{2.75}$$

and the omission error as

$$E_0^2 = \sum_{N+1}^{+\infty}{}_{\ell,m} u_{\ell m}^{-2} = \sum_{N+1}^{+\infty}{}_{\ell} \sigma_\ell^2 \qquad (2.76)$$

$$(\sigma_\ell^2 = \sum_{-\ell}^{n}{}_{m} u_{\ell m}^{-2}) \quad ,$$

The latter part can sometimes be analytically computed if we assume some simple law for the degree variances, e.g. like Kaula's rule. As for the computation of the commission error, from (2.36) we have

$$E\{\delta\hat{u}_{\ell m}^2\} = \frac{\sigma_\nu^2}{8N_0} \int Y_{\ell m}(P)^2 \cos\varphi \, d\sigma \quad . \qquad (2.77)$$

On the other hand by recalling the summation rule

$$\sum_{-\ell}^{n}{}_{m} Y_{\ell m}(P) Y_{\ell m}(Q) = (2n+1) P_\ell(\cos\psi_{PQ})$$

and the fact that $P_\ell(1) = 1$, from (2.77) we find

$$\sum_{-\ell}^{\ell}{}_{m} E\{\delta\hat{u}_{\ell m}^2\} = \frac{\sigma_\nu^2(2\ell+1)}{8N_0} \int \cos\varphi \, d\sigma =$$

$$= \frac{\sigma_\nu^2(2\ell+1)\pi^2}{8N_0} \quad . \qquad (2.78)$$

It is not desirable to push further this computation because the direct observation of $\bar{u}_0(P_{ij})$ is not a case of real interest here; whence, after having explained the principle of the computation of E^2, we close the paragraph only reporting a small numerical experiment designed to control the bias introduced by the discretized formula (2.70) (and by the numerical noise). To this aim we have produced a $1^0 \times 1^0$ grid of values of a potential u truncated at degree 160; more precisely we have used the OSU-81 model from degree 21 to degree 160.

We have then used formula (2.70), discretized with $\Delta\sigma_{ij} \sim 1^0 \times 1^0$ and computed the corresponding coefficients $\hat{u}_{\ell m}$, with no other noise but the intrinsic numerical one.

The result, in terms of relative differences

$$d = \frac{|\hat{u}_{\ell m} - u_{\ell m}|}{|u_{\ell m}|}$$

is displayed in Figure 2.8, showing that the estimation procedure is quite satisfactory.

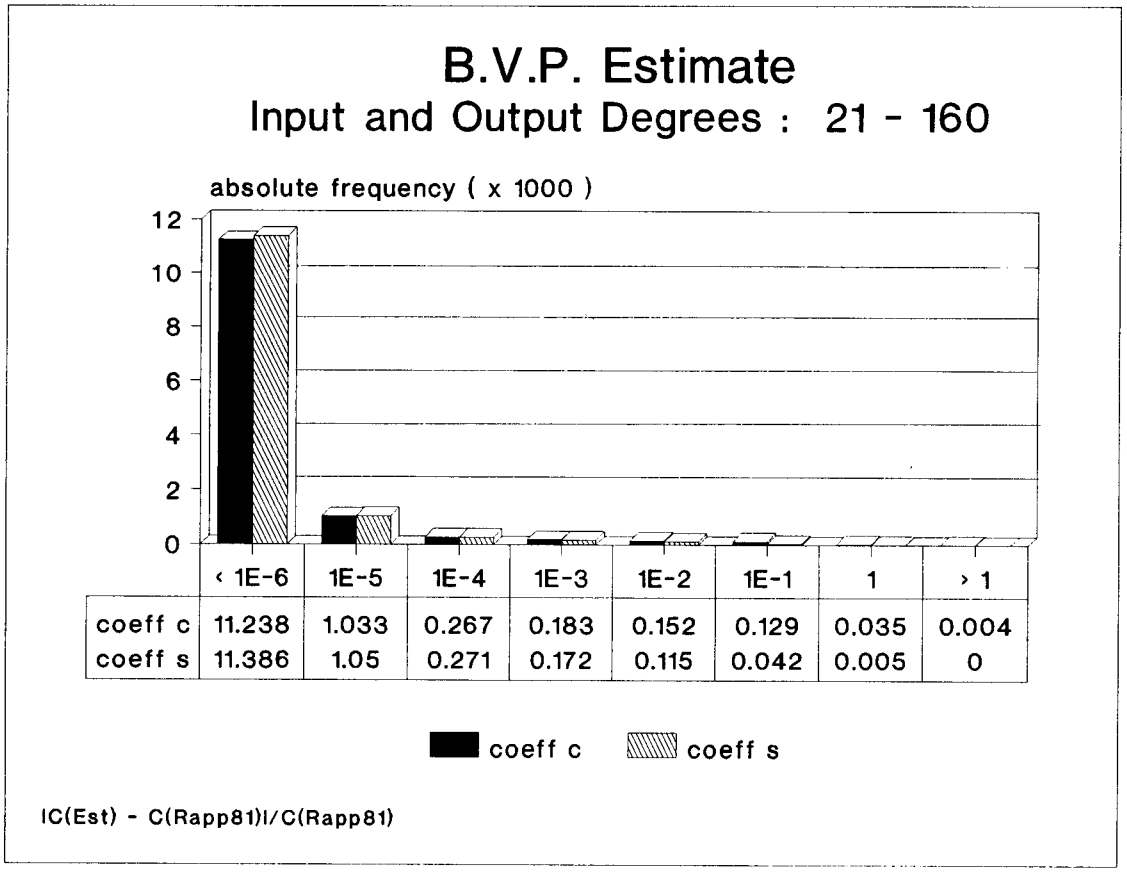

Figure 2.8: Histogram of discretization errors of quadratic formulas in terms of relative differences.

2.5. From b.v.p.'s to quadrature formulas.

The problem now is to see whether and how we will repeat the reasoning of § 2.4, if instead of $\bar{u}(P_{ij})$ we are rather given, always at the centers of the grid blocks, a functional relation defined through some boundary operator B

$$(Bu)(P_{ij}) = f_0(P_{ij}) \quad . \tag{2.79}$$

Since the operators of interest contain radial derivatives also (e.g. in Γ_{zz} as defined in (2.22)), formula (2.79) would not be meaningful if not complemented by the harmonicity condition in the exterior of the boundary sphere

$$\Delta u = 0 \quad , \quad (r > r_0) \quad ; \tag{2.80}$$

it is in fact the harmonicity condition that relates the values of u within the domain $(r > r_0)$ with the values of u on the boundary $(r = r_0)$.

Again we must transform (2.79) into an observation equation involving fields of measures on σ; whence we put

$$f_0(P_{ij})\Delta\sigma_{ij} \sim d\mu_0(P_{ij}) \qquad \text{(observation field)} \tag{2.81}$$

$$\nu_{ij}\Delta\sigma_{ij} \sim d\mu_w(P_{ij}) \qquad \text{(observation noise)} \tag{2.82}$$

and we write

$$d\mu_0(P) = (Bu)(P)d\sigma_P + d\mu_w(P) \quad . \tag{2.83}$$

We must give a precise meaning to (2.83). We then take any square integrable function g defined on σ, $(g \in L^2_\sigma)$, and set

$$\langle g, \mu \rangle = \frac{1}{4\pi} \int g(P)d\mu(P) \tag{2.84}$$

where the integral should be interpreted as an usual integral if μ has a regular L^2_σ density $(d\mu = \rho d\sigma, \ \rho \in L^2_\sigma)$, or as a Wiener integral if μ is a

Wiener measure. With this convention, we stipulate that (2.83) means

$$\langle g, \mu_0 \rangle = \langle g, Bu \rangle + \langle g, \mu_w \rangle \quad , \tag{2.85}$$

whatever is g in L^2_σ.

As we can see, in (2.85) it is written that if we compute the functional $\langle g, \mu_0 \rangle$, with the field of observations μ_0, we get a deterministic part and a stochastic part, $\langle g, \mu_w \rangle$, of zero mean, which has the characteristics of a noise. It follows that if it is our aim to find some functional h of u, namely if we want to estimate $\langle h, u \rangle$, with no bias, we must only find g such that

$$\langle g, Bu \rangle = \langle h, u \rangle \quad . \tag{2.86}$$

Any operator of interest to us is a polynomial in the differential operators $\frac{\partial}{\partial \varphi}$, $\frac{\partial}{\partial \lambda}$, $\frac{\partial}{\partial r}$ whose coefficients are smooth functions of φ, λ with the exception of isolated poles, like $\frac{1}{\cos \varphi}$ etc. Under these conditions it is easy to see that the domain of B in L^2_σ

$$D_B = \{u \in L^2_\sigma \quad ; \quad Bu \in L^2_\sigma\}$$

is dense in that space. Consequently it is possible to give, in a unique way, the definition of the adjoint of B, namely

$$\langle B^+ v, u \rangle = \langle v, Bu \rangle \quad . \tag{2.87}$$

If we extend, when necessary, the definition of B to make it equal to $(B^+)^+$, we find that both B and B^+ are closed operators, i.e. the graph $\{u, Bu\}$, considered as a manifold in the product space $L^2_\sigma \otimes L^2_\sigma$, is closed. For these operators a very useful theorem was stated by Banach, *the closed graph theorem* (cf. Yosida, 1978, chap. II, § 6) maintaining that if B (or B^+) is defined on the whole space, L^2_σ in our case, then it is continuous. Now assume that both B and B^+ are invertible, i.e. that

$$Bu = 0 \Rightarrow u = 0 \quad ; \quad B^+ v = 0 \Rightarrow v = 0 \tag{2.88}$$

and that the range of B, $R_B = \{Bu;\ u \in D_B\}$, is closed; then first of all R_B is dense in L^2_σ as if $v \perp R_B$ then, $\forall\ u \in D_B$ (which is by hypothesis dense in L^2_σ),

$$0 = \langle v, Bu\rangle = \langle B^+v, u\rangle \Rightarrow B^+v = 0 \Rightarrow v = 0 \quad ;$$

consequently R_B is the whole L^2_σ since it is a closed set, dense in such a space; therefore B^{-1} happens to be a closed operator defined on the whole space L^2_σ and then it is also continuous (i.e. bounded) by the closed graph theorem. The same holds true for B^+ by the symmetry of the adjunction operation. A very useful sufficient condition guaranteeing the applicability of the above theory is that

$$\langle u, Bu\rangle = \langle B^+u, u\rangle \geq c\|u\|^2 \qquad (2.89)$$

as mentioned in (Yosida, ibid (Chap. VII, § 5, corollary 2)).

Before returning to our specific problem, let us mention that even if for a certain operator B it is not true that

$$Bu = 0 \Rightarrow u = 0 \quad ,$$

but we can find a subspace of L^2_σ such that (2.89) holds in this subspace, then our theorem will be true on this subspace only and in particular both B^{-1} and $(B^+)^{-1}$ will exist as bounded operators in this subspace. Now we can go back to the problem (2.86) and assume that B is such that (2.89) is satisfied (at least for a subspace of L^2_σ); we observe that in (2.86) the unknown is g, while u is an arbitrary element in D_B, which is by hypothesis dense in L^2_σ; then (2.86) is equivalent to

$$B^+g = h \qquad (2.90)$$

and the solution of this equation, i.e.

$$g = (B^+)^{-1}h$$

exists and is unique for every $h \in L^2_\sigma$ by virtue of our assumptions. Let us take now

$$h = Y_{\ell m}$$

and we see that we can formulate the following theorem.

Theorem: If B has a dense domain in L^2_σ and if condition (2.89) is fulfilled, then there exists one and only one sequence of functions $Z_{\ell m}$ in L^2_σ, i.e.

$$Z_{\ell m} = (B^+)^{-1} Y_{\ell m} \quad , \tag{2.91}$$

such that $\{Z_{\ell m}, BY_{\ell m}\}$ form a complete bi-orthogonal system

$$\langle Z_{\ell m}, BY_{nk} \rangle = \delta_{\ell n} \delta_{\ell k} \quad . \tag{2.92}$$

and that the functionals

$$\hat{u}_{\ell m} = \langle Z_{\ell m}, \mu_0 \rangle \tag{2.93}$$

are unbiased estimates of $u_{\ell m}$, if μ_0 is related to u by the observation equation (2.85). The same holds true for any closed subspace of L^2_σ, spanned by a subsequence of $\{Y_{\ell_i m_i}\}$, if condition (2.89) is fulfilled in this subspace only; in this case $\{Z_{\ell_i m_i}\} = \{(B^+)^{-1} Y_{\ell_i m_i}\}$ is bi-orthogonal to all $\{BY_{\ell_i m_i}\}$ as well as orthogonal to all $\{Y_{\ell m}\}$ not belonging to the subsequence mentioned above. Some important remarks are in order when considering the possible applications of this theorem to our problems.

Remark 2.5.1: If B commutes with the rotation group, i.e. if we can state that for any rotation operator R defined by

$$Rf(\underline{x}) = f(R\underline{x})^7 \tag{2.94}$$

---

[7] On the right hand side R means only the 3-D rotation matrix to be applied to the vector $\underline{x}$, identified by a point on the unit sphere σ.

we have

$$RBu(\underline{x}) = BRu(\underline{x}) \quad , \tag{2.95}$$

then the operator B is diagonal in the spherical harmonics representation, and more particularly

$$BY_{\ell m} = b_\ell Y_{\ell m} \quad , \tag{2.96}$$

so that B is also self-adjoint and, if $b_\ell \neq 0$, we have

$$Z_{\ell m} = \frac{1}{b_\ell} Y_{\ell m} \quad . \tag{2.97}$$

In case $b_{\ell_i} = 0$ for a sequence of degrees $\{\ell_i\}$, we still have formula (2.97) for $n\{n_i\}$, and we also know that the coefficients $u_{\ell_{im}}$ are not estimable from our observation field μ_0. The same remark is valid for operators not commuting in general with rotations, but in any way diagonal with respect to the basis $\{Y_{\ell m}\}$, i.e. such that

$$BY_{\ell m} = b_{\ell m} Y_{\ell m} \quad . \tag{2.98}$$

Remark 2.5.2: Up to now we have not considered the action of block averaging our observations. As it was pointed out in chapter 2.2 this action can be approximately described by a moving average operator A defined by

$$Au(P) = \frac{1}{\overline{C}} \int_{C_P} u(Q) d\sigma_Q \tag{2.99}$$

where C_P is the spherical cap of center P and of radius ψ_0 such that its surface $\overline{C} = 2\pi(1-\cos\psi_0)$ has a pre-established value. The operator A commutes with rotations and it has the diagonal representation

$$AY_{\ell m} = \beta_\ell Y_{\ell m} \tag{2.100}$$

where β_ℓ are the Pellinen coefficients already mentioned in chapter 2.2 (cf. (2.33) there). For the block averaged field we must then substitute the observation equation (2.83) with

$$d\bar{\mu}_0 = (ABu)d\sigma + d\bar{\mu}_w \quad , \tag{2.101}$$

where $d\bar{\mu}_w$ is again a Wiener measure with the stochastic structure related to the individual error variance σ_ν^2, as in formula (2.36) of 2.2. Accordingly the sought sequence $Z_{\ell m}$ becomes in this case

$$\begin{aligned} \bar{Z}_{\ell m} &= (B^+A)^{-1}Y_{\ell m} = \\ &= A^{-1}(B^+)^{-1}Y_{\ell m} = \\ &= A^{-1}Z_{\ell m} \quad . \end{aligned} \tag{2.102}$$

When B is diagonal over the basis $\{Y_{\ell m}\}$, then (2.102) is very easily computed, since then

$$\bar{Z}_{\ell m} = A^{-1}\frac{Y_{\ell m}}{b_{\ell m}} = \frac{1}{\beta_\ell b_{\ell m}} Y_{\ell m} \quad ; \tag{2.103}$$

if B is not diagonal however, (2.102) can be easily computed only if the explicit form of the representation of $Z_{\ell m}$ in terms of $Y_{\ell k}$ is known.

2.6. The numerical solution of gradiometric b.v.p.'s: examples.

In this paragraph we shall apply the theory of chapter 2.5, to construct global models starting from the knowledge of the observables Γ_{zz} or Γ_{zy} or Γ_{yy} (cf. chapter 2.1), given as the average at the centers of the blocks of a $1^0 \times 1^0$ degree grid. Assuming that one has about 60 measurements per block with $\sigma_\nu = 10^{-2}$ E, one would expect for the average noise a σ_0 value

$$\sigma_0 \simeq 0.13\ 10^{-2}\ \text{E} \quad . \tag{2.104}$$

We have applied the same noise (2.104) to each of the components, although we know that Γ_{zy} is expected to be a more noisy observation.

To be more precise we have performed numerical experiments with Γ_{zz} and Γ_{zy}, for which the system $\{Z_{\ell m}\}$ is easily found. As for the Γ_{yy}, although we have a theoretical recipe to find approximately $Z_{\ell m}$, the corresponding numerical example is still a work for the future.

a. The Γ_{zz} component.

In this case the boundary operator is (cf. (2.22) in chapter 2.1)

$$B = \frac{\partial^2}{\partial r^2} \quad ; \tag{2.105}$$

this is naturally a rotationally invariant operator with eigenvalues

$$b_\ell = \frac{(\ell+1)(\ell+2)}{R^2} \left(\frac{R}{r}\right)^{\ell+3} \quad . \tag{2.106}$$

As we see b_ℓ are all positive so that the theory of chapter 2.5 applies and we can simply put

$$\hat{u}_{\ell m} = \frac{1}{b_\ell 4\pi} \langle Y_{\ell m}, \mu_0 \rangle =$$

$$\simeq \frac{1}{b_\ell 4\pi} \Sigma_{ij} \, Y_{\ell m}(P_{ij}) \Delta\mu_0(P_{ij})$$

$$(\Delta\mu_0(P_{ij}) = \Gamma_{zz0}(P_{ij}) \Delta\sigma_{ij}) \quad , \tag{2.107}$$

expressing our estimates in terms of the observables. What is interesting in formula (2.106) is not so much to prove its effectiveness in retrieving the potential coefficients, but rather to study how the noise is propagated through it. A first look at the ratio between input power per degree ($\sum_{-\ell}^{\ell} u_{\ell m}^2$) and estimated power per degree ($\sum_{-\ell}^{\ell} \hat{u}_{\ell m}^2$) as it is shown in Figure 2.9, confirms the quality of the estimate when no other noise but the numerical one is added in the experiment; the oscillation band, as one can realize, is smaller than ± 1%.

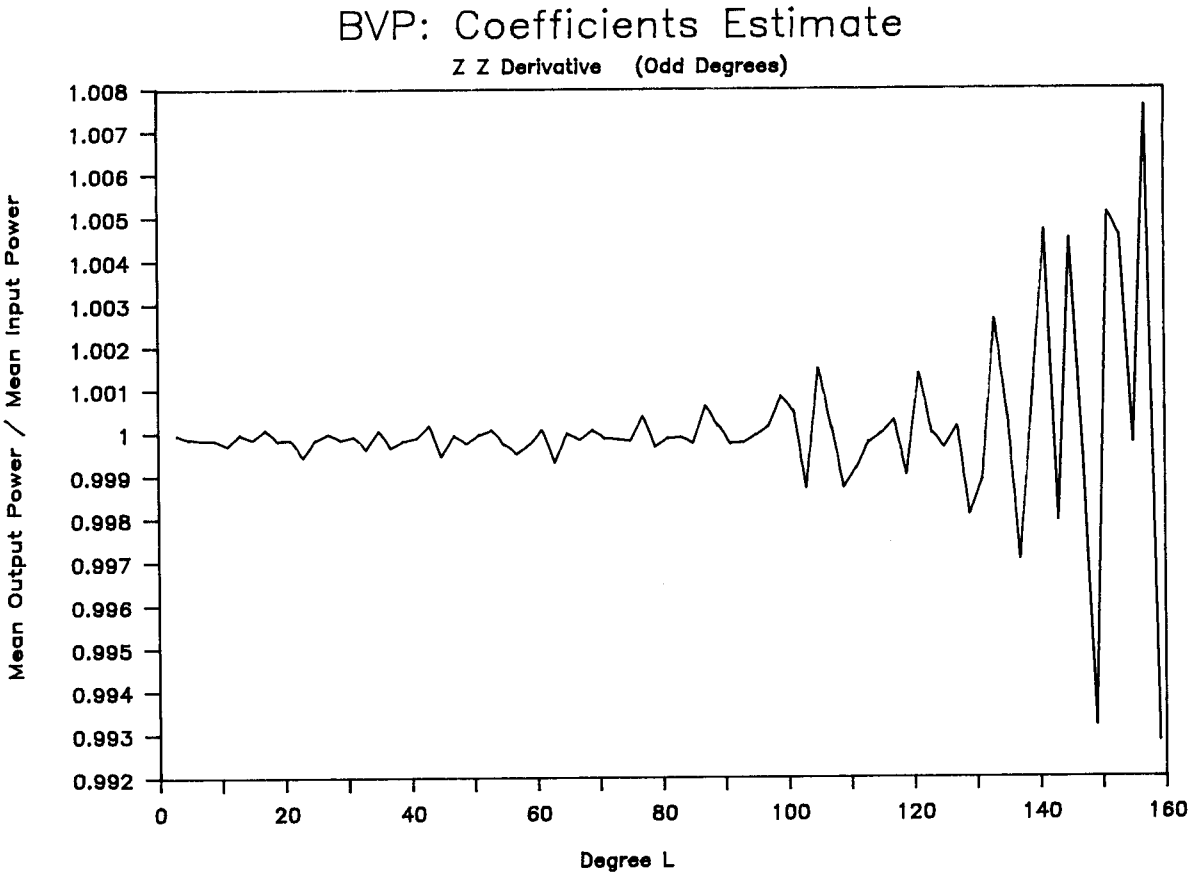

Figure 2.9: Ratio of estimated power over input (true) power per degree.

It should be noted that in this case no β_ℓ coefficients have been applied, because we have as a matter of fact used point values for Γ_{zz}. As for the error propagation, it can be derived theoretically from (2.107) and the Wiener rule; noting that μ_w is the random part of μ_0 we can write

$$\delta\hat{u}_{\ell m} = \frac{1}{b_\ell 4\pi} \int Y_{\ell m} \, d\mu_w \quad . \tag{2.108}$$

Following the same reasoning as in chapter 2.4, formulas (2.73), (2.74), (2.75), (2.77), (2.78), we find here

$$E_c^2 = \sum_{2\ell}^{N} \frac{\sigma_\nu^2 (2\ell+1)\pi^2}{8 N_0 b_\ell^2} \quad . \tag{2.109}$$

We can transform this into the commission error for geoid undulations by using the Bruns' relation so that a potential T is transformed into a height anomaly

$$\zeta = \frac{T}{\gamma} \quad .$$

In this way we find

$$E_c(\zeta) = \frac{E_c(T)}{\gamma} \tag{2.110}$$

and we can plot $E_c(\zeta)$ against the maximum degree N, obtaining a representation well visualizable in cm units: the curve is shown in Figure 2.10.

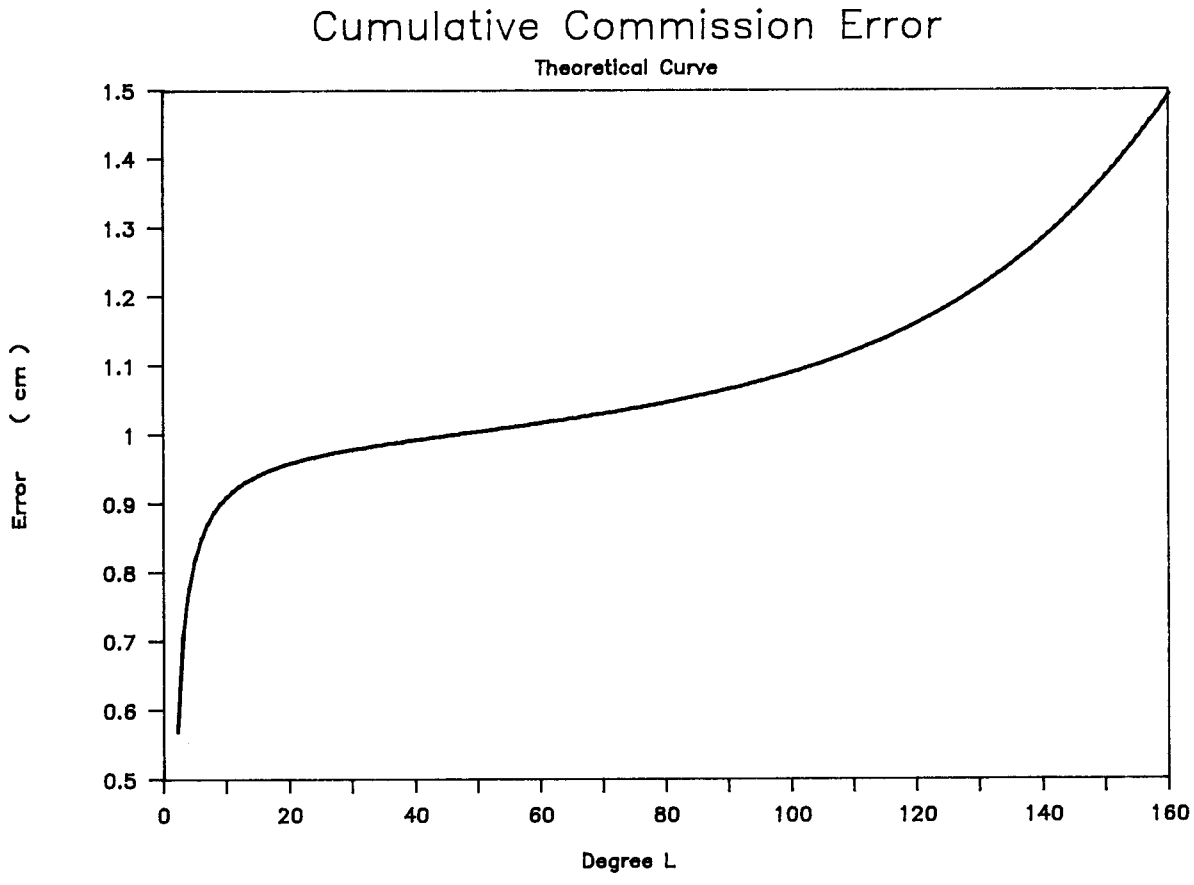

Figure 2.10: Theoretical cumulative commission error.

This curve has been tested against its empirical counterpart obtained from a discretized version of (2.107), i.e.

$$\delta\hat{u}_{\ell m} = \frac{1}{b_\ell 4\pi} \Sigma_{ij}\, Y_{\ell m}(P_{ij})\Delta\mu_w(P_{ij}) \qquad (2.111)$$

where $\Delta\mu_w(P_{ij})$ was generated from

$$\Delta\mu_w(P_{ij}) = \bar{\nu}_{ij}\, \Delta\sigma_{ij} \quad ,$$

by extracting a white noise $\bar{\nu}_{ij}$ with an r.m.s. $0.13 \cdot 10^{-2}$ E. The result can be seen in Figure 2.11 and despite the presence of a small systematic difference, we consider it as a confirmation of the theory.

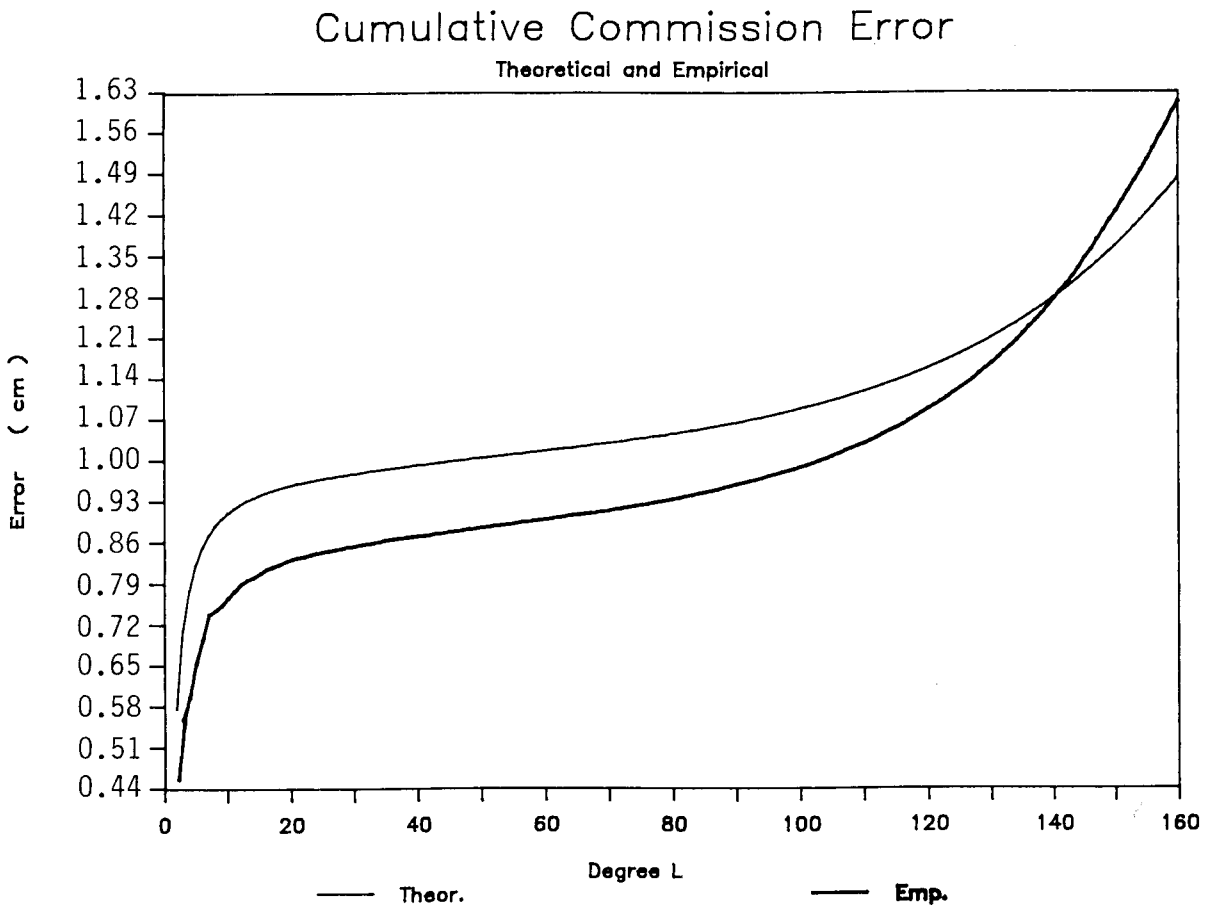

Figure 2.11: Comparison between theoretical and simulated cumulative commission error function.

Another important qualitative information we want to draw from this experiment is the ratio between the mean square power of the signal to be estimated and the mean square power of the noise affecting it, i.e. the index

$$\frac{S}{N} = \sqrt{\frac{\sum_{m=-\ell}^{\ell} \hat{u}_{\ell m}^2}{\sum_{m=-\ell}^{\ell} \delta u_{\ell m}^2}} \quad . \tag{2.112}$$

This is shown in Figure 2.12 and we see that in the range $2 \leq \ell \leq 160$ the signal to noise ratio is well above 1, in fact it ranges from 500 to 10.

Before passing to another example we want to solve the problem of defining the cut-off degree in this case. To this aim we must note that the commission error E_c^2 will increase degree by degree by the quantity $\frac{\sigma_\nu^2 (2\ell+1)\pi^2}{8N_0 b_\ell^2}$, while the omission error, if we assume a simple Kaula's rule, will decrease with $\left(\frac{\mu}{R}\right)^2 1.6 \frac{10^{-10}}{\ell^3}$: we must stop our estimation at that degree N where the former equals the latter since, from this point on we expect the oscillations caused by the propagated noise to be larger than the power of the corresponding degree. Equating the two terms and recalling formula (2.106) we find after some obvious simplifications

$$4.8 \cdot 10^6 \, q^{2\ell+6} = 1$$

$$\left(q = \frac{6,600}{6,400}\right)$$

which has the solution

$$\ell \simeq 250 \quad . \tag{2.113}$$

This value seems a little pessimistic but not too far from other results on the same problem (cf., O. Colombo, 1989a).

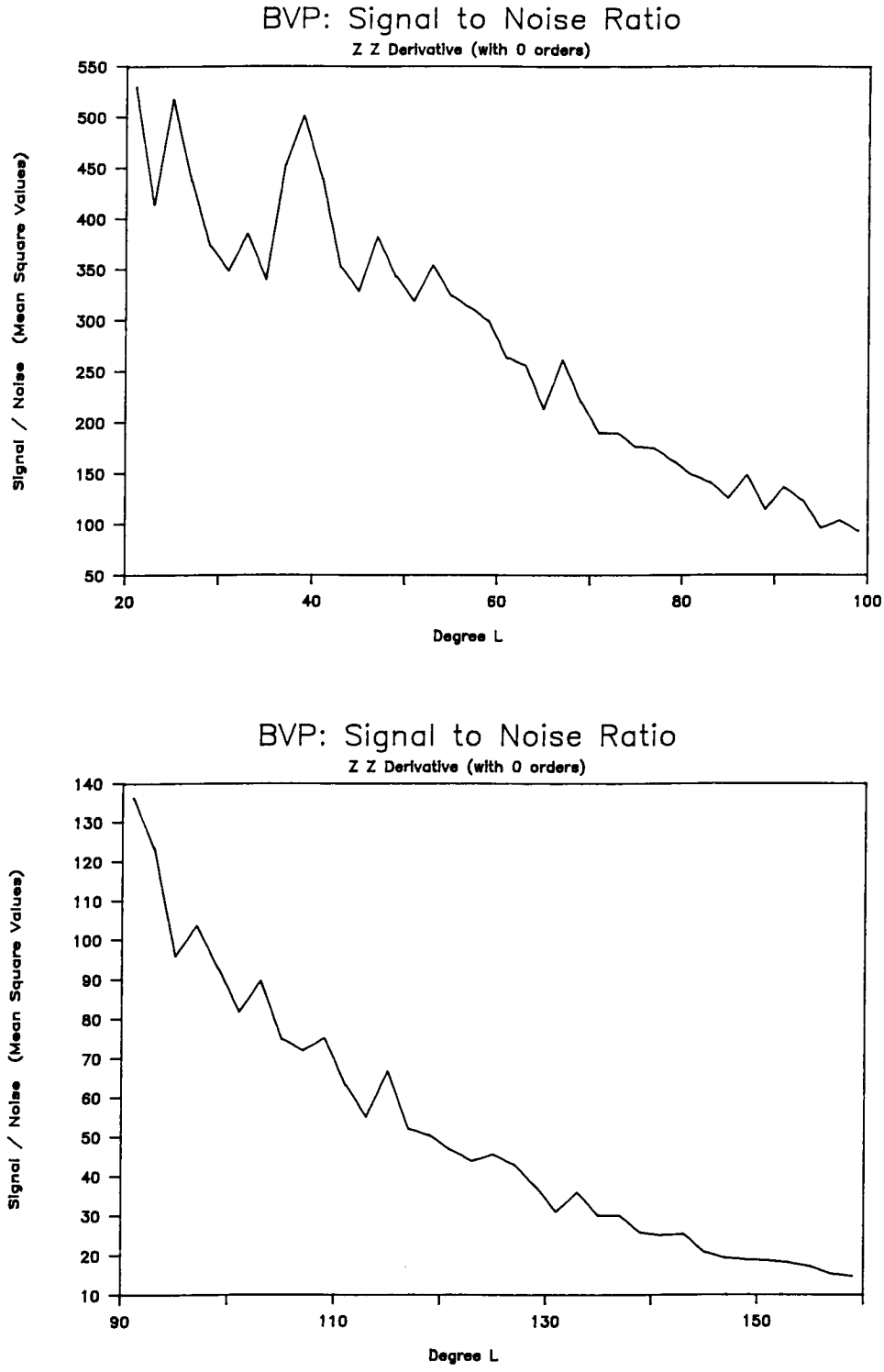

Figure 2.12: Signal to noise ratio degree by degree.

b. The Γ_{zy} component.

In this case the boundary operator is

$$B = \frac{1}{r \cos \varphi} \frac{\partial^2}{\partial r \partial \lambda} - \frac{1}{r^2 \cos \varphi} \frac{\partial}{\partial \lambda} \quad , \tag{2.114}$$

so that, observing that

$$\frac{\partial}{\partial \lambda} Y_{\ell m} = -m \, Y_{\ell, -m} \quad ,$$

we find

$$B \, Y_{\ell m} = \frac{m(\ell+2)}{\cos \varphi \, R^2} \left(\frac{R}{r}\right)^{\ell+3} Y_{\ell, -m} \quad . \tag{2.115}$$

Now we must observe that the operator $\{\cos \varphi B\}$ is such that its range is spanned by $\{Y_{\ell m}, \; m \neq 0\}$, i.e. it is a subspace of L^2_σ. In this subspace its eigenvalues $b_{\ell m}$ are all positive so that we can define a bi-orthogonal system $\{Z_{\ell m}\}$ by the formula

$$Z_{\ell m} = \cos \varphi \, \frac{Y_{\ell, -m}}{b_{\ell m}} \quad , \quad m \neq 0 \tag{2.116}$$

$$\left(b_{\ell m} = \frac{m(\ell+2)}{R^2} \left(\frac{R}{r}\right)^{\ell+3} \right) \quad .$$

The bi-orthogonality of $Z_{\ell m}$ with $BY_{\ell m}$ is obvious and thus we see that

$$\hat{u}_{\ell m} = \frac{1}{4\pi} \int Z_{\ell m} \, d\mu_0 =$$

$$= \frac{1}{b_{\ell m} \, 4\pi} \int Y_{\ell, -m} \cos \varphi \, d\mu_0 \quad , \quad m \neq 0 \tag{2.117}$$

is the proper unbiased estimation formula. The correctness of (2.117) can be verified for instance by a graph analogous to that in Figure 2.9, where the ratio between mean input power and mean output power is displayed degree per degree. The oscillation band is now smaller than $\pm$ 1 $^0/_{00}$ (cf. Figure 2.13).

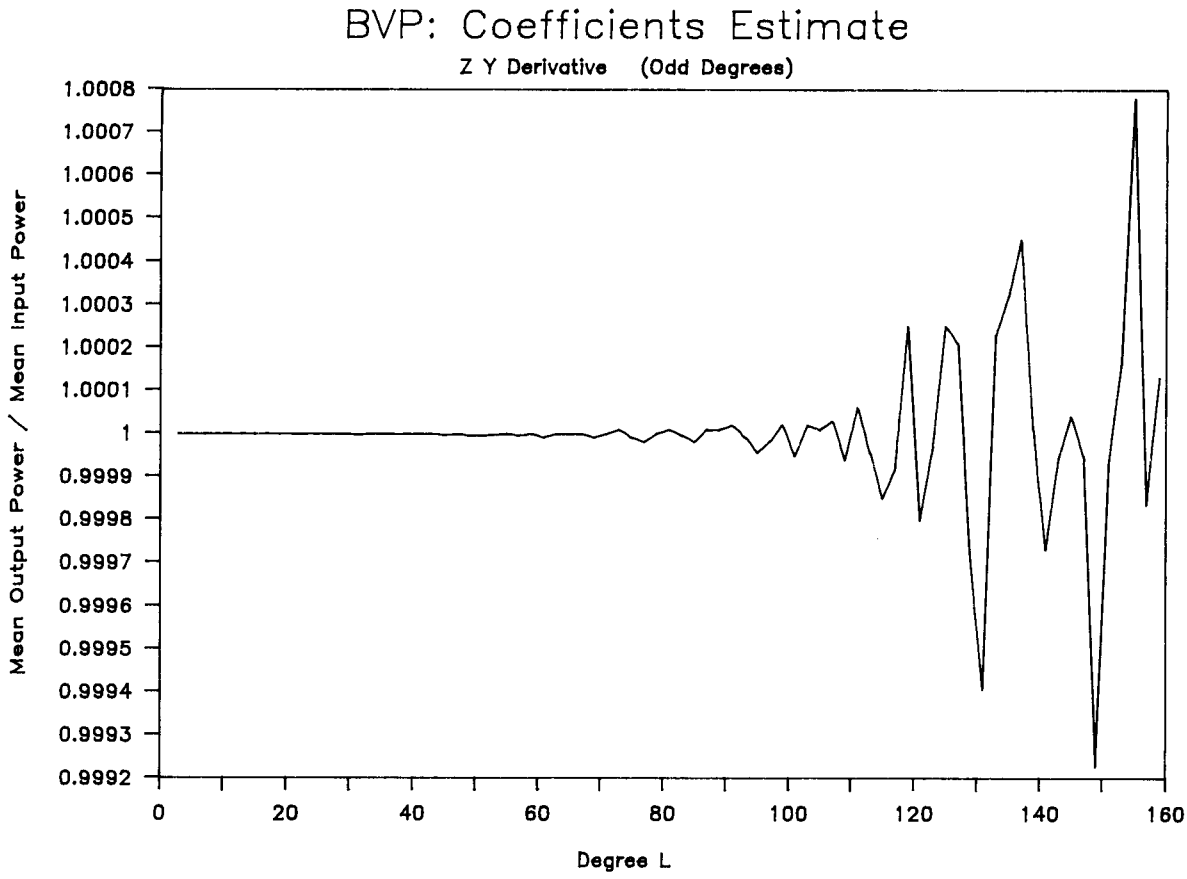

Figure 2.13: Input and output power ratio per degree.

In this case the propagated noise and the corresponding curve of the cumulative commission error in terms of geoid undulations is not easy to compute theoretically, however it can be computed for a numerical experiment from

$$E_c^2(\zeta) = \frac{1}{\gamma^2} \sum_{2}^{N} \sum_{-\ell}^{\ell} \delta\hat{u}_{\ell m}^2 \qquad (2.118)$$

where

$$\delta\hat{u}_{\ell m} = \frac{1}{b_{\ell m}} \frac{1}{4\pi} \int Y_{\ell,-m} \cos\varphi \, d\mu_w \quad . \qquad (2.119)$$

The result is shown in Figure 2.14, where we immediately see the inferior quality of the coefficients determined from Γ_{zy} as compared to those determined from Γ_{zz}.

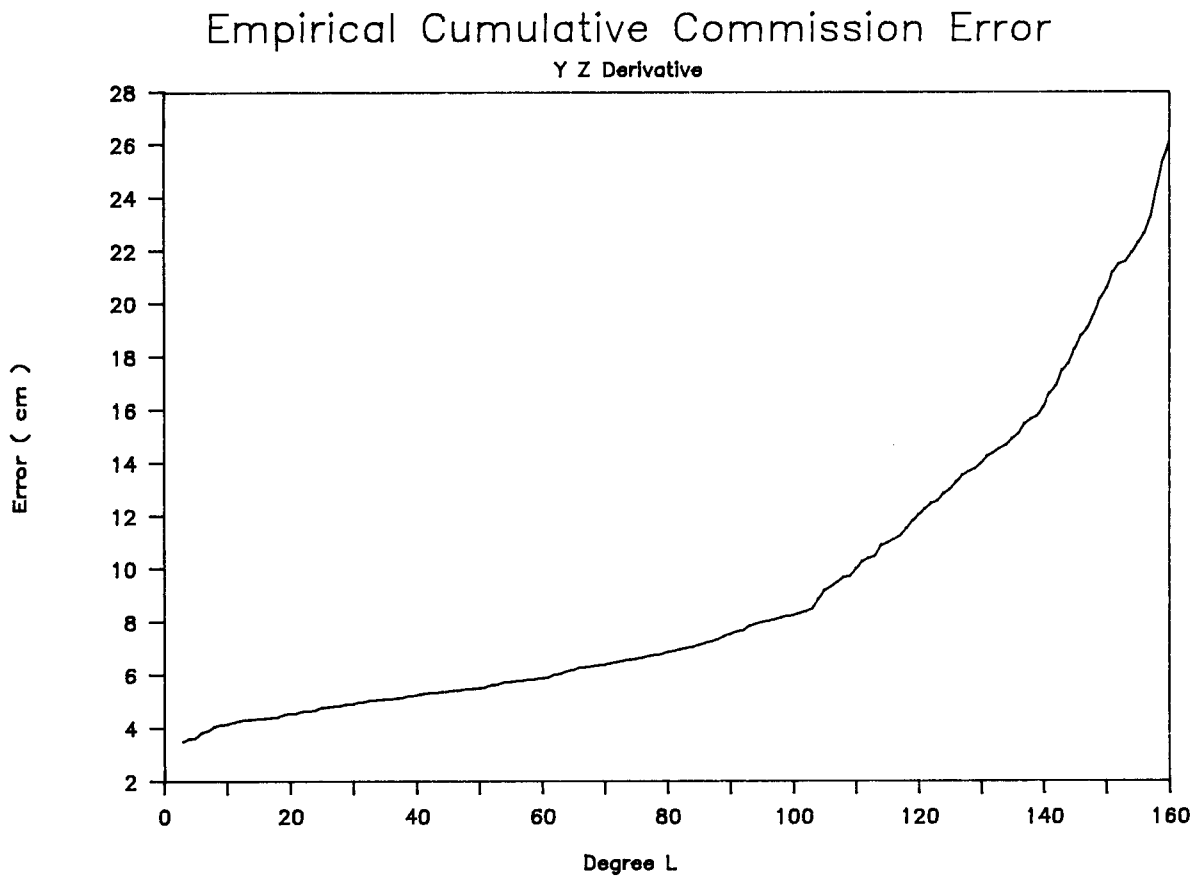

Figure 2.14: The cumulative commission error.

This fact is also reflected in a less favorable signal to noise ratio, which reaches the value 1 already at degree $\simeq$ 160: the corresponding curve is shown in Figure 2.15.

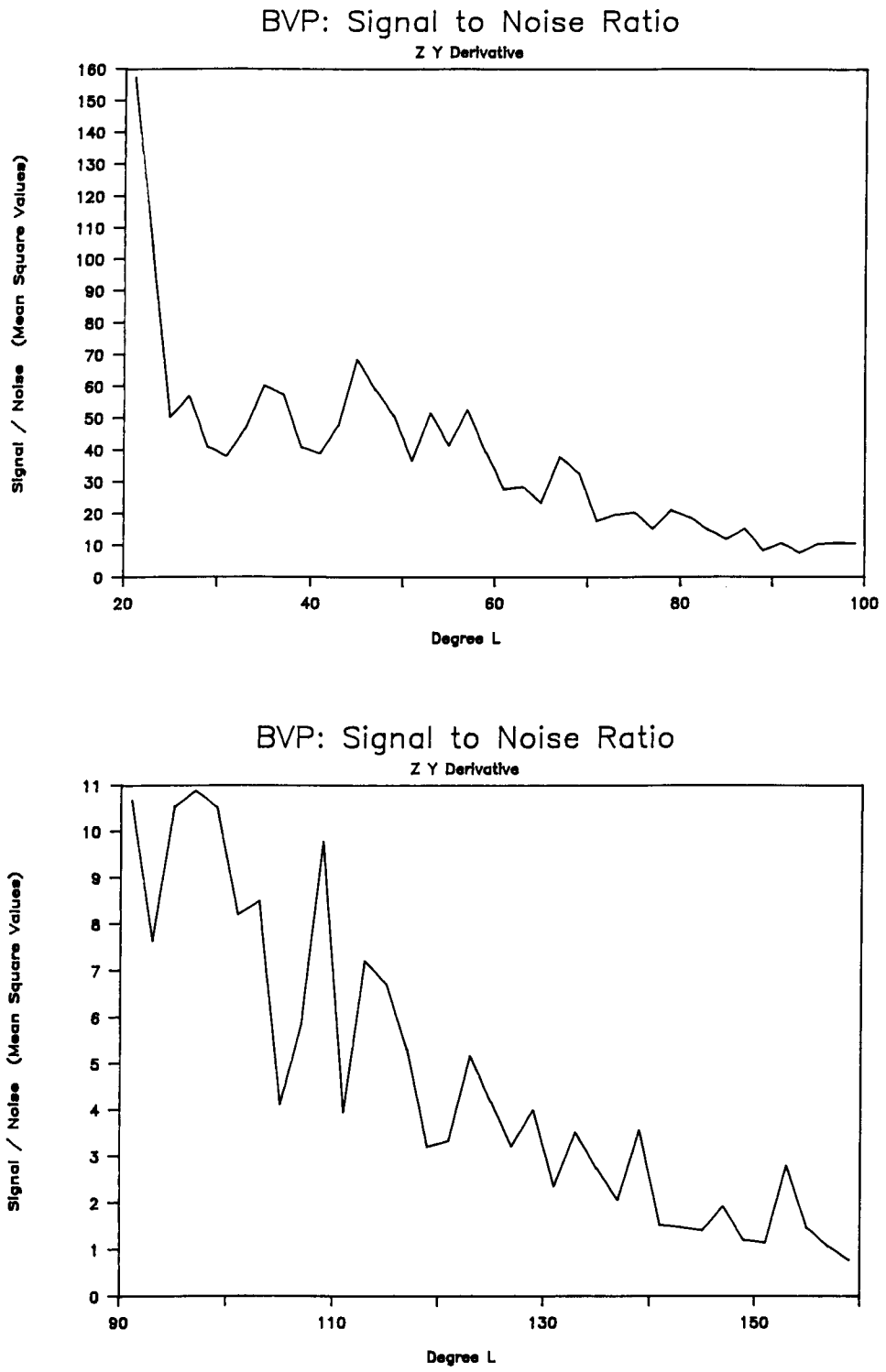

Figure 2.15: The signal to noise ratio for the Γ_{zy} observable.

c. The Γ_{yy} commponent.

This case is significantly more complicated than the others, because of the form of the boundary operator

$$B = \frac{1}{r^2 \cos^2 \varphi} \frac{\partial^2}{\partial \lambda^2} - \frac{\operatorname{tg} \varphi}{r^2} \frac{\partial}{\partial \varphi} + \frac{1}{r} \frac{\partial}{\partial r} \quad . \tag{2.120}$$

It is not obvious here how to visualize the set $\{Z_{\ell_m}\}$; so it becomes meaningful to check condition (2.89) of chapter 2.5, to be sure that such a sequence exists. As a matter of fact we see that

$$\begin{aligned} \frac{1}{4\pi} \langle T, BT \rangle = & - \frac{1}{4\pi} \int_\sigma \frac{1}{r^2 \cos^2 \varphi} \left(\frac{\partial T}{\partial \lambda}\right)^2 d\sigma \\ & - \frac{1}{4\pi r^2} \int d\lambda \int d\varphi \sin \varphi \, T \frac{\partial T}{\partial \varphi} + \\ & + \frac{1}{4\pi} \int T \left(\frac{1}{r} \frac{\partial T}{\partial r}\right) d\sigma \quad . \end{aligned} \tag{2.121}$$

The first integral in (2.121) is negative or zero; the second can be written as

$$\begin{aligned} & - \frac{1}{4\pi r^2} \int d\lambda \left[\sin \varphi \, \frac{1}{2} T^2\right]_{-\pi/2}^{\pi/2} + \frac{1}{4\pi} \cdot \frac{1}{2r^2} \int d\sigma \, T^2 \\ & = - \frac{1}{4r^2} \left[T^2(\varphi = \pi/2) + T^2(\varphi = -\pi/2)\right] + \frac{1}{2R^2} \Sigma_{\ell,m} u_{\ell_m}^2 \left(\frac{R}{r}\right)^{2\ell+4} \quad . \end{aligned}$$

The third integral is easy to compute in harmonic components, to give

$$\frac{1}{4\pi} \int d\sigma \, T \left(\frac{1}{r} \frac{\partial T}{\partial r}\right) = - \frac{1}{R^2} \Sigma (\ell+1) u_{\ell_m}^2 \left(\frac{R}{r}\right)^{2\ell+4} \quad .$$

By combining the three integrals we see that

$$\begin{aligned} \frac{1}{4\pi} \langle T, BT \rangle & \leqq - \frac{1}{R^2} \Sigma (\ell + \tfrac{1}{2}) u_{\ell_m}^2 \left(\frac{R}{r}\right)^{2\ell+4} \leqq \\ & \leqq - \frac{1}{2R^2} \Sigma \, u_{\ell_m}^2 \left(\frac{R}{r}\right)^{2\ell+4} \quad , \end{aligned} \tag{2.122}$$

so that -B satisfies the required condition and the theory of chapter 2.5 applies.

As for the determination of $Z_{\ell m}$, this can be devised only by an approximate algorithm, that we summarize in the sequel. The first step comes from the consideration that $BY_{\ell m}$ is proportional to cos $m\lambda$ or sin $m\lambda$, according to the sign of m. Accordingly it becomes natural to put

$$Z_{\ell m} = X_{\ell m}(\varphi)\cos\varphi \begin{cases} \cos m\lambda & m \geq 0 \\ -\sin m\lambda & m < 0 \end{cases} , \qquad (2.123)$$

$$(X_{\ell,-m} = X_{\ell,m})$$

where the choice of introducing a factor cos φ is just for convenience. By applying the orthonormality relation

$$\langle Z_{\ell m}, BY_{jk}\rangle = \delta_{\ell j}\delta_{mk} ,$$

after separating the dependence from λ, we arrive at the relation

$$\frac{1+\delta_{mo}}{4} \int_{-\pi/2}^{\pi/2} X_{\ell m}(\varphi) D_{jm} \bar{P}_{jm}(\varphi) d\varphi = \delta_{\ell j} , \qquad (2.124)$$

where

$$D_{jm} = [-m^2 - \frac{1}{2}\sin 2\varphi \frac{\partial}{\partial\varphi} - \frac{j+1}{2}(1 + \cos 2\varphi)] . \qquad (2.125)$$

On the other hand we can put

$$D_{jm}\bar{P}_{jm} = \sum_{0}^{[j/2]+1} D_{jk}^{m} \begin{cases} \cos 2k\varphi & \sin 2k\varphi \\ \sin(2k+1)\varphi & \cos(2k+1)\varphi \end{cases} \begin{matrix} (j \text{ even}) \\ (j \text{ odd}) \end{matrix} \qquad (2.126)$$

(m even) (m odd)

where the coefficients D_{jk}^{m} can be expressed explicitly in terms of Kaula's inclination functions (cf. (Brovelli & Sansò, 1990)). Accordingly it comes natural to put

$$X_{\ell m} = \sum_{0k}^{+\infty} X^{m}_{\ell k} \begin{Bmatrix} \cos 2k\varphi & \sin 2k\varphi \\ \sin(2k+1)\varphi & \cos(2k+1)\varphi \end{Bmatrix} , \qquad (2.127)$$

with the same ordering as in formula (2.126). Inserting (2.126) and (2.127) in (2.124) we get four infinite systems according to whether m is even or odd and both j and ℓ are even or odd; the cases j even and ℓ odd or vice versa are automatically accounted for by the simple fact that cosine and sine functions are orthogonal (over $[-\pi/2, \pi/2]$) because one is an even and the other an odd function. Naturally we are not able to solve numerically infinite systems, but we can always truncate the sum in (2.127) at a certain number L; one should be aware that in this way some aliasing is introduced, however we expect it to be very small if we take e.g. L = 300, because in this way all frequencies up to 600 are represented. An interesting remark is that once the coefficients $X^{m}_{\ell k}$ are computed, and this can be done once for all, it is possible to give an explicit formula for the estimate $\hat{u}_{\ell m}$ by combining them with the Fourier coefficients of the observational field Γ_{yy}.

2.7. How to deal with the overdetermined b.v.p.'s.

So far we have discussed how to determine the coefficients of the anomalous potential from one set of data; for instance we have treated separately the three types of observables Γ_{zz}, Γ_{zy}, Γ_{yy}. In this way we get three different estimates of the same set of coefficients with the exception of the coefficients of order zero, which cannot be estimated from Γ_{zy}; moreover it is to be noticed that in principle it is not reasonable to assume that from each of the three observables the coefficients are estimated up to the same maximum degree L.

Hence we can say that if we introduce a vector x defined as

$$x = \begin{bmatrix} u_{00} \\ u_{1-1} \\ u_{10} \\ u_{11} \\ u_{2-2} \\ \vdots \\ u_{LL} \end{bmatrix} \qquad (2.128)$$

and a projector P selecting which coefficients are estimated from one specific observable, we can write the observation equations

$$\hat{x} = P_j x + v_j \qquad (2.129)$$

and consider the problem of deriving one common estimate $\hat{x}$ from (2.129). We will do that by applying the least squares method, which is known to supply optimal estimates (among linear estimators), when the correct stochastic structure of the residuals v_j (i.e. $\hat{x}_j$ which enter into (2.129) as pseudo observables) is taken into account. Before doing that however an important remark is in order.

Remark 2.7.1: When we put the problem of combining the estimates $\hat{x}_j$ by equations (2.129), we have already abandoned the request of an optimal exploitation of the observations, even in the field of linear estimators.

In fact in principle no finite vector, like x, can draw completely the information contained in a continuous field, e.g. Γ_{zz}: only pushing the degree of estimation to infinity, in spite of the fact that each single coefficient can carry only very little signal as compared to the noise, can we have a complete extraction of the information from the observations. This purpose can be pursued and would lead to optimal estimates obtained as solutions of suitable integral equations (cf., Sansò, 1988); this approach however is more complicated and it is beyond the scope of this work.

Then we go back to the problem (2.129) and, for the moment, we assume to be able to compute the covariance matrices C_j of $\hat{x}_j$; it should be noted that

if we assume that each estimate $\hat{x}_j$ is derived from a different and independent observation, then we can assume that also $\hat{x}_j$ and $\hat{x}_k$ are independent for $j \neq k$.

With this specification the least squares estimate from (2.129) is obtained by the formula

$$\hat{x} = (\Sigma_j P_j^+ C_j^{-1} P_j)^{-1} \Sigma_j P_j^+ C_j^{-1} \hat{x}_j \quad . \tag{2.130}$$

We can observe that, should each observable supply an estimate for the same set of coefficients so that $P_j = I$, then formula (2.130) would assume the form of a single vector weighted average

$$\hat{x} = (\Sigma_j C_j^{-1})^{-1} \Sigma_j C_j^{-1} \hat{x}_j \quad . \tag{2.131}$$

Also, according to the least squares theory, we are in principle able to compute the covariance matrix of $\hat{x}$, namely

$$C_{\hat{x}\hat{x}} = (\Sigma_j P_j^+ C_j^{-1} P_j)^{-1} \tag{2.132}$$

and to test the hypothesis, implicit in our formulation, that the theoretical value of σ_0^2 is 1, based on the sample estimate

$$\hat{\sigma}_0^2 = \frac{\Sigma_j \hat{v}_j^+ C_j^{-1} v_j}{\Sigma n_j - (L+1)^2} \tag{2.133}$$

$$(n_j = \text{dimension of } P_j \hat{x}_j) \quad ,$$

and on the customary use of the χ^2 statistics. Noting that the dimension of the normal matrix, i.e. the dimension of x, is $(L+1)^2$, the computation of (2.130) would be a serious problem, was it not for the particular shape of C_j, which comes out to be block diagonal, at least for the cases of interest in gradiometry. In fact we can observe that for all three observables studied here, the bi-orthogonal system $\{Z_{\ell m}\}$ is such that it is proportional to simple trigonometric functions in λ, so that for any function ρ depending only on φ, we can state

$$<Z_{\ell m}, \rho Z_{nk}> = \frac{1}{4\pi} \int Z_{\ell m}(P) Z_{nk}(P) \rho(\varphi_P) d\sigma = 0 \qquad (2.134)$$

whenever $m \neq k$.

Subsequently let us start from estimates of the type

$$\hat{u}_{\ell m} = <Z_{\ell m}, \mu_o> \quad , \qquad (2.135)$$

where the observational field contains a noise (Wiener field) $d\mu_w$ with covariance structure

$$E\{d\mu_w(P) d\mu_w(Q)\} = \delta(P,Q) \rho(\varphi_P) d\sigma_P \quad , \qquad (2.136)$$

as it is for us (cf. formula (2.4) in paragraph 2.2). Then from formula (2.134) we see that

$$E\{(\hat{u}_{\ell m} - u_{\ell m})(\hat{u}_{nk} - u_{nk})\} = E\{<Z_{\ell m}, \mu_w><Z_{nk}, \mu_w>\} =$$

$$= <Z_{\ell m}, \rho(\varphi) Z_{nk}> = C_{\ell n, m} \delta_{mk} \quad . \qquad (2.137)$$

Formula (2.137) shows that when the components of x are reordered, first by order and then by degree, we find for the covariance matrices a block diagonal structure. In other words, formula (2.130) can be applied by splitting the computation order by order, so that at most we must solve systems of a few hundreds unknowns each time.

Remark 2.7.2: Although with the above discussion we see that our solution is now computable, one could be willing to produce a quick estimate of x at the expense of optimality, but without introducing biases. This can be done by simply taking a weighted average of the estimated coefficients.

3. TIMEWISE APPROACH.

The classical theory of global spherical harmonic analysis of the earth's gravitational field from tracking observations to artificial satellites has recently been described e.g. in (Marsh et al., 1988) or in (Reigber, 1989). In essence, in a linear least-squares adjustment the spherical harmonic coefficients are determined from a large number of tracking observations, such as range, range rate, or Doppler measurements. Now and in the sequel the coefficients shall be denoted $\Delta\bar{C}_{\ell m}$ and $\Delta\bar{S}_{\ell m}$ (the difference between the actual series coefficient and an approximate value, used for the computation of the reference orbit). The elements of the design matrix, connecting the observations with the unknown harmonic coefficients, are derived from the equations of motion. They are computed by numerical integration simultaneously with the integration of the reference orbit. In the early days of satellite geodesy considerable effort has been invested into the development of adequate analytical theories for their determination. The estimability of individual coefficients largely depends on the quality of the employed measurements and on the orbits of the involved satellites, in particular their resonance characteristics.

With the introduction of new satellite techniques, such as satellite-to-satellite tracking (SST) and gradiometry, the classical theory needed to be revisited. Typical for the new techniques is

- the orbit altitude is chosen extremely low (160 to 220 km);
- the inclination is close to 90^0 (polar orbit), and
- in principle a continuous stream of homogeneous measurements becomes available, independent of tracking from ground stations.

Thus the expectation is that the spherical harmonic coefficients can be determined complete up to high degree and order, from one satellite mission only. This implies, for example, for an expansion up to N = 200 or 300 an adjustment with 40 000 or 90 000, respectively, unknown coefficients. In principle even for problems of this dimension, with the use of modern vectorized computers, the classical approach can be followed and simulations in this direction have been successfully carried out by Balmino & Barriot (1990). However the effort is enormous and it is logical that more economic methods are investigated. The

computational burden but also the new situation of obtaining practically a continuous data stream suggested to look into semi-analytical methods that would produce block symmetries in the system of linear equations to be solved. Such an approach promises computational advantages so important that a slight loss in model precision would be acceptable, if the latter can be compensated by carrying out several iterations. This approach shall be denoted timewise in the sequel since the observations are considered functions of time.

The timewise approach was conceived for spherical harmonic analysis of SST data, see (Kaula, 1983), (Wagner, 1983), and (Colombo, 1984a). Thereby the observable range rates or the coefficients of their expansion into a Fourier series are connected with potential coefficients through the solution of Hill's or Lagrange planetary equations. More recently Colombo (1987 and 1989a) followed a similar approach for the components of the gradient tensor. In a certain way this case is easier than that of SST, because gradiometry and orbit improvement can be kept almost separately. It requires in a first step computation of the second derivatives of the disturbance potential expressed e.g. in Keplerian elements, (Kaula, 1966). This way a linear connection between gradients and potential coefficients is established. In a second step, the linear relation is used for error propagation so as to yield the a posteriori variance-covariance matrix of the potential coefficients. It becomes block diagonal since the expressions decouple according to order m and parity (n-m). Hence no orbit uncertainties are taken into account. Their inclusion would however be straightforward.

3.1. Principles of timewise method.

The principles of the timewise method for the error-analysis of gradiometer measurements have been developed by Colombo (1987 and 1989a). They shall be described and extended in this and following parts of chapter three. Thereby the notation shall be similar to that commonly employed in dynamic satellite geodesy and therefore quite different from that used in chapter 2.

From the solution of Laplace' equation outside the attracting masses the gravitational potential of the earth can be written as an infinite series of spherical harmonics:

$$V(P) = \frac{\mu}{R} \sum_{\substack{\ell=0 \\ \ell\neq 1}}^{\infty} \left(\frac{R}{r_P}\right)^{\ell+1} \sum_{m=0}^{\ell} [\bar{C}_{\ell m} \cos m\lambda_P + \bar{S}_{\ell m} \sin m\lambda_P]\bar{P}_{\ell m}(\cos \theta_P) \qquad (3.1)$$

with μ = GM the gravitational constant times the earth's mass, R the mean radius of the earth, $\{\theta_P, \lambda_P, r_P\}$ the spherical coordinates of the computation point P, $\{\bar{C}_{\ell m}, \bar{S}_{\ell m}\}$ the infinite set of fully-normalized spherical harmonic coefficients of degree ℓ and order m, and $\bar{P}_{\ell m}$ the fully-normalized associated spherical harmonics. In case a geo-centric coordinate system is chosen, the coefficients of degree one become zero by definition.

Introduction of a known set of approximate coefficients $\bar{c}_{\ell m}$ and $\bar{s}_{\ell m}$ leads to a corresponding expression of the disturbance potential T:

$$T(P) = \frac{\mu_0}{R} \sum_{\substack{\ell=0 \\ \ell\neq 1}}^{\infty} \left(\frac{R}{r_P}\right)^{\ell+1} \sum_{m=0}^{\ell} [\Delta\bar{C}_{\ell m} \cos m\lambda_P + \Delta\bar{S}_{\ell m} \sin m\lambda_P]\bar{P}_{\ell m}(\cos \theta_P) \quad (3.2)$$

where $\Delta\bar{C}_{\ell m} = \bar{C}_{\ell m} - \bar{c}_{\ell m}$ and $\Delta\bar{S}_{\ell m} = \bar{S}_{\ell m} - \bar{s}_{\ell m}$ are considered the unknowns of our problem.

For the timewise approach the problem has to be formulated along the orbit. Hence (3.2) is transformed from the earth-fixed $\{\theta, \lambda, r\}$-system to the orbit system, where the disturbance potential becomes a function of the Kepler orbit elements a, e, I, Ω, ω, and M (semi-major axis, eccentricity, inclination, right ascension of the node, argument of perigee, and mean anomaly). This transformation is described in (Kaula, 1966) and has been recently discussed in (Sneeuw, 1991). It leads to

$$T(P) = \frac{\mu_0}{R} \sum_{\ell=0}^{\infty} \left(\frac{R}{r_P}\right)^{\ell+1} \sum_{m=0}^{\ell} \sum_{p=0}^{\ell} \bar{F}_{\ell mp}(I)\{ \begin{bmatrix} \Delta\bar{C}_{\ell m} \\ -\Delta\bar{S}_{\ell m} \end{bmatrix}_{\ell-m:0}^{\ell-m:e} \cos \psi_{\ell mp} \qquad (3.3)$$

$$+ \begin{bmatrix} \Delta\bar{S}_{\ell m} \\ \Delta\bar{C}_{\ell m} \end{bmatrix}_{\ell-m:0}^{\ell-m:e} \sin \psi_{\ell mp} \}$$

where

$\bar{F}_{\ell mp}(I)$ ... normalized inclination functions

and

$$\psi_{\ell mp} = (\ell-2p)\omega_o + m\omega_e \qquad (3.4)$$

with

$\omega_o = \omega + M$ ("o" referring to "orbit")

and

$\omega_e = \Omega - \theta_G$ ("e" referring to "earth").

With $\psi_{\ell mp} = \dot{\psi}_{\ell mp}(t-t_0)$ the disturbance potential T is expressed as a function of time along the orbit.

In eq. (3.3) a number of assumptions is contained. The orbit is assumed to be circular (e = 0). Consequently e does not appear in (3.3) and no eccentricity functions need to be introduced, cf. (Kaula, 1966). Small eccentricities could be introduced quite easily, however. For the nominal or reference orbit it is assumed $\dot{a} = \dot{e} = \dot{I} = 0$ and constant $\dot{\Omega}$, $\dot{\omega}$, $\dot{M}$ and $\dot{\theta}_G$ (earth's angular velocity). Eq. (3.3) has the structure of a time series of T from which it should be possible to determine the unknown coefficients $\Delta\bar{C}_{\ell m}$ and $\Delta\bar{S}_{\ell m}$.

In gradiometry the second derivatives V_{ij} of the gravitational potential are measurable. Ideally they are measured in a local orthonormal cartesian triad, the instrument frame. After subtraction of the approximate gradients V'_{ij}, computed with the chosen normal field, we arrive at $\Gamma_{ij} = V_{ij} - V'_{ij}$. The Γ_{ij} can be built from the first and second derivatives of V in the orbit elements r, I, ω_0, and ω_e. Denoting

$$\alpha_{\ell m} = \begin{cases} \Delta\bar{C}_{\ell m} & \ell-m: \text{even} \\ -\Delta\bar{S}_{\ell m} & \ell-m: \text{odd} \end{cases}$$

and

$$\beta_{\ell m} = \begin{cases} \Delta\bar{S}_{\ell m} & \ell-m: \text{even} \\ \Delta\bar{C}_{\ell m} & \ell-m: \text{odd} \end{cases}$$

eq. (3.3) is written as

$$T = \frac{\mu_0}{R} \sum_{\ell=0}^{\infty} \left(\frac{R}{r}\right)^{\ell+1} \sum_{m=0}^{\ell} \sum_{p=0}^{\ell} \bar{F}_{\ell mp}(I)\{\alpha_{\ell m} \cos \psi_{\ell mp} + \beta_{\ell m} \sin \psi_{\ell mp}\} \quad . \quad (3.5)$$

Then we obtain, for example, for $T_{rr} = \partial^2 T/\partial r^2$

$$T_{rr} = \frac{\mu_0}{R} \sum_{\ell} \lambda_{\ell} \left(\frac{R}{r}\right)^{\ell+1} \sum_{m} \sum_{p} \bar{F}_{\ell mp}(I)\{\alpha_{\ell m} \cos \psi_{\ell mp} + \beta_{\ell m} \sin \psi_{\ell mp}\} \quad . \quad (3.6)$$

and

$$\lambda_{\ell} = (\ell+1)(\ell+2)/r^2 \quad .$$

For convenience the index range of the ℓ, m and p summations has been suppressed. Analogous expressions are found for all other derivatives in r, I, ω_o and ω_e. They are contained in Table A-1 of Appendix 1.

From Appendix 1 we take the expressions for the second derivatives T_{ij} in the local cartesian gradiometer triad. They are given in Table 3.1.

TABLE 3.1: T_{ij} components in local cartesian gradiometer triad.	
T_{xx}	$\frac{1}{r} T_r + \frac{1}{r^2} T_{\omega_0\omega_0}$
T_{xy}	$\frac{-1}{r^2 \sin I \cos \omega_0} [\tan \omega_0 T_{\omega_e} - \tan \omega_0 \cos I \, T_{\omega_0} + \cos I \, T_{\omega_0\omega_0} + T_{\omega_e\omega_0}]$ $\frac{1}{r^2 \sin \omega_0} [-\cot \omega_0 T_I + T_{I\omega_0}]$
T_{xz}	$\frac{1}{r} T_{r\omega_0} - \frac{1}{r^2} T_{\omega_0}$
T_{yy}	$-T_{xx} - T_{zz}$
T_{yz}	$\frac{1}{r \sin I \cos \omega_0} [\frac{1}{r} T_{\omega_e} - \frac{\cos I}{r} T_{\omega_0} - T_{\omega_e r} + \cos I \, T_{r\omega_0}]$ $\frac{1}{r \sin \omega_0} [\frac{-1}{r} T_I + T_{rI}]$
T_{zz}	T_{rr}

From Table 3.1 it is seen that the components T_{xy} and T_{yz} can be written in two ways depending on whether they are based on the curvilinear coordinates $\{r, I, \omega_o\}$ or $\{r, \omega_e, \omega_o\}$. The same holds true for T_{yy}, but we prefer to derive it indirectly from T_{xx} and T_{zz} via Laplace'equation. Furthermore we observe that T_{xy} and T_{yz} contain sin ω_o or cos ω_o in the denominator. They will cause singularities for certain arguments, but much worse, spoil the orthonormality properties of our "sine-cosine"-series to be used at a later stage. There exist two strategies to circumvent this problem. One is described in (Schrama, 1990; appendix B). Thereby the upper expressions of T_{xy} and T_{yz} are multiplied by $\cos^2 \omega_o$ and the lower ones by $\sin^2 \omega_o$. The sum yields e.g. for T_{yz}

$$2T_{yz} = \{\frac{1}{\sin I} [-\frac{1}{r} T_{r\omega_e} + \frac{1}{r^2} T_{\omega_e}] + \cot I \, [\frac{1}{r} T_{r\omega_0} - \frac{1}{r^2} T_{\omega_0}]\} \cos \omega_o +$$

$$+ [\frac{1}{r} T_{rI} - \frac{1}{r^2} T_I] \sin \omega_o \quad . \qquad (3.7)$$

The singularity is gone, the orthogonality of the "sine-cos"-series is maintained by manipulations described in (Schrama, ibid). The second approach, proposed in (Betti & Sansò, 1989) starts from the orbit system. The orbit plane defines the equator of a rotated coordinate system, with latitude $\varphi' = 0$. The derivative in cross-track direction can therefore be written as

$$T_y = \frac{1}{r} T_{\varphi'},$$

and

$$T_{xy} = \frac{1}{r^2 \cos \varphi'} T_{\varphi', \omega_0} + \frac{\sin \varphi'}{r^2 \cos^2 \varphi'} T_{\omega_0}$$

$$T_{yz} = \frac{1}{r} T_{r\varphi'} - \frac{1}{r^2} T_{\varphi'} .$$

The derivatives are evaluated along the orbit ($\varphi' = 0$). Thus $T_{xy} = \frac{1}{r^2} T_{\varphi', \omega_0}$. Hence all that is required, is the derivative of T, eq. (3.6), with respect to φ'. As shown in (Betti & Sansò, ibid) and discussed in (Sneeuw, 1991) it is

$$T_{\varphi'} = \frac{\mu_0}{R} \sum_{\ell=0}^{\infty} \left(\frac{R}{r}\right)^{\ell+1} \sum_{m=0}^{\ell} \sum_{p=0}^{\ell-1} \bar{F}^*_{\ell mp}(I)\{\alpha^*_{\ell m} \cos \psi_{\ell mp} + \beta^*_{\ell m} \sin \psi_{\ell mp}\} \qquad (3.8)$$

where

$$\alpha^*_{\ell m} = \begin{pmatrix} \Delta\bar{S}_{\ell m} \\ \Delta\bar{C}_{\ell m} \end{pmatrix}$$

$$\beta^*_{\ell m} = \begin{pmatrix} -\Delta\bar{C}_{\ell m} \\ \Delta\bar{S}_{\ell m} \end{pmatrix}$$

and $\bar{F}^*_{\ell mp}(I)$ is a new type of inclination function that incorporates the derivative with respect to φ'.

Actually it is more logical to introduce an index k = ℓ-2p, replacing p (cf. (Sneeuw, 1991)). For the range of k it holds

$[k|-\ell(2)+\ell]$ if the series contains $\bar{F}_{\ell mp} = \bar{F}^{k}_{\ell m}$ or its derivatives

or

$[k|-\ell+1(2)\ell-1]$ if it contains $\bar{F}^{*}_{\ell mp} = \bar{F}^{*k}_{\ell m}$.

Then the general expression of an arbitrary second derivative (i, j) becomes

$$T_{ij} = \frac{\mu_0}{R} \sum_{\ell} \left(\frac{R}{r}\right)^{\ell+1} \sum_{m} \sum_{k} \lambda^{(ij)}_{\ell k} \bar{F}^{(*)k}_{\ell m} [\alpha^{(*)}_{\ell m} \cos \psi_{km} + \beta^{(*)}_{\ell m} \sin \psi_{km}] \qquad (3.9)$$

with

$$\psi_{km} = k\omega_o + m\omega_e \quad . \qquad (3.10)$$

All $\lambda^{(ij)}_{\ell k}$ are listed in Table 3.2 together with a pointer * indicating the reference to $\bar{F}^{*k}_{\ell m}$, $\alpha^{*}_{\ell m}$ and $\beta^{*}_{\ell m}$, respectively, and a second one (+-) indicating that $-\alpha_{\ell m}/-\alpha^{*}_{\ell m}$ takes the place of $\beta_{\ell m}/\beta^{*}_{\ell m}$ and $\beta_{\ell m}/\beta^{*}_{\ell m}$ that of $\alpha_{\ell m}/\alpha^{*}_{\ell m}$.
Eq. (3.9) together with Table 3.2 provides the linear model connecting the tensor of the gravitational disturbance potential, T_{ij}, with the unknown coefficients $\Delta\bar{C}_{\ell m}$ and $\Delta\bar{S}_{\ell m}$.

Let us now assume a certain component T_{ij} is measurable and has been observed at N equidistant points along the orbit. The observed values are collected in the vector Γ of dimension (N x 1). Also the unknown coefficients form one vector $\underline{c}$. If the summation over degree ℓ is truncated at a maximum degree ℓmax and the three first degree terms are kept zero by definition its length is L = $(\ell max + 1)^2 - 3$. Then with (3.9) a linear adjustment model can be formulated:

$$\tilde{\Gamma} = Ac + \tilde{\epsilon} \qquad (3.11)$$

TABLE 3.2: $\lambda_{\ell k}^{(ij)}$ of the tensor components T_{ij} in the local cartesian gradiometer triad

component (ij)	$\lambda_{\ell k}$	pointers
xx	$-(\ell+1+k^2)/r^2$	
xy	$-k/r^2$	*
xz	$-(\ell+2)k/r^2$	(+ -)
yy	$-((\ell+1)^2-k^2)/r^2$	
yz	$-(\ell+2)/r^2$	* (+ -)
zz	$(\ell+1)(\ell+2)/r^2$	

with observation error vector $\tilde{\epsilon}$, where $E\{\epsilon\} = 0$ and the a priori variance covariance matrix be $E\{\tilde{\epsilon}\tilde{\epsilon}^T\} = Q_\Gamma = \sigma_0^2 I$ with I a N x N unit matrix and σ_0^2 the variance of the observed gradients. The coefficient matrix A is of dimension N x L. If $N \geq L$ and A of full rank the least-squares solution becomes

$$\hat{c} = (A^T Q_\Gamma^{-1} A)^{-1} A^T Q_\Gamma^{-1} \tilde{\Gamma} \qquad (3.12)$$

and the a posteriori variance-covariance matrix:

$$Q_c = (A^T Q_\Gamma^{-1} A)^{-1}$$

which becomes under the above assumption of constant variance

$$Q_c = \sigma_0^2 (A^T A)^{-1} \quad . \qquad (3.13)$$

Thus with A given the expected error propagation of a gradiometer mission can be tested for a variety of assumed a priori error variance levels without gradiometer data actually being available. It should be obvious that the main diagonal of Q_c contains the expected variance of the individual coefficients $\Delta\bar{C}_{\ell m}$ and $\Delta\bar{S}_{\ell m}$ and the off-diagonal terms their covariances. The feasibility of such an error propagation experiment depends on the complexity of solving the linear system (3.13). With A of dimension (N x L) the normal matrix A^TA is of dimension L x L. For ℓmax = 200 its size is of the order of 40 000 x 40 000. The solution of a system of this size would put extreme constraints on the accuracy, speed and size of even the most advanced supercomputers, cf. (Balmino & Barriot, 1990).

Colombo (1989b) could show that under a number of simplifying conditions A^TA attains a block diagonal structure with the maximum sub-block of size $(\frac{1}{2}\ \ell\text{max} + 1) \times (\frac{1}{2}\ \ell\text{max} + 1)$. Thus a situation comparable to the spacewise approach of chapter 2 can be achieved. The main line of the steps required to achieve the block-diagonality shall be discussed in the following.

Each element of the normal matrix A^TA consists of the inner product of two columns of A referring to two spherical harmonic coefficients (ℓ_1, m_1) and (ℓ_2, m_2). The inner product extends over all sampling points s, s = 1...N. Let one arbitrary element of the normal matrix, belonging to the gradient component (ij) and referring to the coefficients (ℓ_1, m_1) and (ℓ_2, m_2), be denoted $h^{(ij)}_{\ell_1 m_1 \ell_2 m_2}$. Then eq. (3.9) gives:

$$h^{(ij)}_{\ell_1 m_1 \ell_2 m_2} = \frac{\mu_0^2}{R^2} \left(\frac{R}{r}\right)^{\ell_1+1} \left(\frac{R}{r}\right)^{\ell_2+1} \sum_{s=1}^{N} \left(\sum_{k_1} \lambda^{(ij)}_{\ell_1 k_1} \bar{F}^{(*)k_1}_{\ell_1 m_1} \cos \psi_{k_1 m_1}(s) \right)$$

$$\times \left(\sum_{k_2} \lambda^{(ij)}_{\ell_2 k_2} \bar{F}^{(*)k_2}_{\ell_2 m_2} \cos \psi_{k_2 m_2}(s) \right) \qquad (3.14)$$

$$= \frac{\mu_0^2}{R^2} \left(\frac{R}{r}\right)^{\ell_1+\ell_2+2} \sum_{k_1} \sum_{k_2} \lambda^{(ij)}_{\ell_1 k_1} \lambda^{(ij)}_{\ell_2 k_2} \bar{F}^{(*)k_1}_{\ell_1 m_1} \bar{F}^{(*)k_2}_{\ell_2 m_2}$$

$$\left(\sum_{s=1}^{N} \cos \psi_{k_1 m_1}(s) \cos \psi_{k_2 m_2}(s) \right)$$

with analogous expressions for the products cos $\psi_{k_1m_1}(s)$ sin $\psi_{k_2m_2}(s)$ and sin $\psi_{k_1m_1}(s)$ sin $\psi_{k_2m_2}(s)$. Any block diagonality depends now on the applicability of the orthogonality relationships of trigonometric functions to the sum over s.

With (3.10) it is

$$\psi_{km} = \dot{\psi}_{km}(t-t_0) = \psi^0_{km} + \dot{\psi}_{km}t$$

and (3.15)

$$\dot{\psi}_{km} = k(\dot{\omega}+\dot{M}) + m(\dot{\Omega}-\dot{\theta}_G) = k\dot{\omega}_o + m\dot{\omega}_e \quad .$$

It is assumed that the total mission length T is exactly one repeat period (no repetition of groundtracks). With a sampling interval Δt this results in $N = \frac{T}{\Delta t}$. Then the mission period consists of the relative primes N_e nodal days and N_0 orbit revolutions, or $T = N_e \frac{2\pi}{\dot{\omega}_e} = N_0 \frac{2\pi}{\dot{\omega}_0}$. It follows (neglecting ψ^0_{km} which simply results in a constant phase shift)

$$\psi_{km} = (kN_0 + mN_e) \frac{2\pi}{T} j\Delta t = 2\pi(k + m \frac{N_e}{N_0}) N_0 \frac{j}{N}$$

$$= 2\pi\, b_{km}\, N_0 \frac{j}{N} \qquad j = 1,\ldots,N \quad . \qquad (3.16)$$

The conditions for b_{km} (and consequently each frequency) to be unique are derived in (Schrama, 1990). It can be shown that the number of revolutions

N_0 must be a prime number and $N_0 > 2\,\ell max$.	(3.17)

With these conditions fulfilled and the time series being uninterrupted the orthogonality relationships of trigonometric functions yield

$$
\begin{array}{lllll}
0 & \text{if} & m_1 \neq m_2 & \text{and/or} & k_1 \neq k_2 \\
\frac{N}{2} & \text{if} & m_1 = m_2 \neq 0 & \text{and} & k_1 = k_2 \\
 & \text{or} & m_1 = m_2 = 0 & \text{and} & (k_1 = k_2 \neq 0 \text{ or } k_1 = -k_2 \neq 0) \\
N & \text{if} & m_1 = m_2 = 0 & \text{and} & k_1 = k_2 = 0 \quad .
\end{array}
$$

If now the sequence of elements of c, i.e. of the coefficients $\Delta\bar{C}_{\ell m}$ and $\Delta\bar{S}_{\ell m}$ is chosen first according to m and then according to parity (ℓ even or odd) the desired block-diagonality is attained with the largest block of size ($\frac{1}{2}$ ℓmax +1) x ($\frac{1}{2}$ ℓmax + 1) for even ℓmax, even ℓ and m = 0. An individual non-zero element of the normal matrix A^TA is finally

$$
h^{(ij)}_{\ell_1 m \ell_2} = \frac{N}{2} \frac{\mu^2}{\bar{R}^2} \left(\frac{R}{\bar{r}}\right)^{\ell_1+\ell_2+2} \sum_k \lambda^{(ij)}_{\ell_1 k} \lambda^{(ij)}_{\ell_2 k} \bar{F}^{(*)k}_{\ell_1 m} \bar{F}^{(*)k}_{\ell_2 m} \quad \text{for } m \neq 0
$$

and (3.18)

$$
h^{(ij)}_{\ell_1 m \ell_2} = \frac{N}{2} \frac{\mu^2}{\bar{R}^2} \left(\frac{R}{\bar{r}}\right)^{\ell_1+\ell_2+2} \sum_k \lambda^{(ij)}_{\ell_1 k} \lambda^{(ij)}_{\ell_2 k} (\bar{F}^{(*)k}_{\ell_1 m} \bar{F}^{(*)k}_{\ell_2 m} + \bar{F}^{(*)-k}_{\ell_1 m} \bar{F}^{(*)k}_{\ell_2 m}) \text{ for } m = 0.
$$

with, in addition

$$
h^{(ij)}_{\ell_1 m \ell_2}[\Delta\bar{C}_{\ell_1 m}, \Delta\bar{C}_{\ell_2 m}] = h^{(ij)}_{\ell_1 m \ell_2}[\Delta\bar{S}_{\ell_1 m}, \Delta\bar{S}_{\ell_2 m}] \qquad \text{(except for m = 0)}
$$

$$
h^{(ij)}_{\ell_1 m \ell_2}[\Delta\bar{C}_{\ell_1 m}, \Delta\bar{S}_{\ell_2 m}] = h^{(ij)}_{\ell_1 m \ell_2}[\Delta\bar{S}_{\ell_1 m}, \Delta\bar{C}_{\ell_2 m}] = 0 \quad .
$$

The $\lambda^{(ij)}_{\ell k}$ together with the appropriate inclination functions for a certain component ij are taken from Table 3.2.

We are now in a position to compute for all gradiometer components or arbitrary combinations of the latter the elements of the normal matrix. After solving the L x L system of linear equations and introduction of the a priori measurement error variance of each component the posteriori variances of the

coefficients are derived. The solution procedure can be done individually for each sub-block. We shall return later to this method with some examples.

3.2. Lumped coefficient method.

The method just described could be classified as *timewise approach in the time domain*, because the observables are provided as a time series and solved as such. An important modification of this method, also from the practical point of view, is the *timewise approach in the frequency domain*. Thereby the original time series is transformed to the frequency or spectral domain. This means a DFT is computed. The Fourier coefficients serve as intermediary (pseudo-)observables from which the $\Delta\bar{C}_{\ell m}$ and $\Delta\bar{S}_{\ell m}$ are derived in a second step. Since these pseudo-observables represent linear combinations of a sequence of spherical harmonics they are comparable to lumped coefficients well-known from dynamic satellite geodesy (cf. (Wagner & Klosko, 1977)). The idea described here has been proposed for satellite-to-satellite tracking by Kaula (1983). It has been applied to satellite gradiometry in (Schrama, 1990 and 1991).

The practical advantage of this method is the following. It is reasonable to assume that a gradiometer measures with homogeneous precision throughout the entire mission, e.g. with the earlier quoted 0.01 $E/\sqrt{Hz}$. However it is not realistical to assume that the measurement errors represent perfectly white noise from the zero to the Nyquist frequency, defined by the sampling rate. We know, for example, that the measurement spectrum of the ARISTOTELES gradiometer will be white only in the band from $5 \cdot 10^{-3}$ Hz to 0.125 Hz, corresponding to a range from 27 to 675 cycles/revolution (cpr). We shall return to this aspect later. With the frequency domain approach an arbitrary type of noise model can conveniently be introduced.

Let us return to eq. (3.9), the series representation of the gradient disturbance T_{ij}. It is a summation over degree ℓ, order m and index k. If we carry out a summation over degree ℓ we find

$$T_{ij} = \sum_m \sum_k \left[A_{km}^{(ij)} \cos \psi_{km} + B_{km}^{(ij)} \sin \psi_{km} \right] \qquad (3.19)$$

with coefficients

$$A_{km}^{(ij)} = \frac{\mu_0}{R} \sum_{\ell} \left(\frac{R}{r}\right)^{\ell+1} \lambda_{\ell k}^{(ij)} \, \bar{F}_{\ell m}^{(*)k} \, \alpha_{\ell m}^{(*)}$$

and

$$B_{km}^{(ij)} = \frac{\mu_0}{R} \sum_{\ell} \left(\frac{R}{r}\right)^{\ell+1} \lambda_{\ell k}^{(ij)} \, \bar{F}_{\ell m}^{(*)k} \, \beta_{\ell m}^{(*)} \quad . \tag{3.20}$$

Eq. (3.19) is a Fourier series. Under the conditions described in the previous chapter, eq. (3.17), the (k,m)-combinations uniquely fill the entire spectrum. Hence it must be possible, with the observable T_{ij} given as a function of time, to derive the coefficients $A_{km}^{(ij)}$ and $B_{km}^{(ij)}$ by straightforward Fourier transformation and then consider them as pseudo-observations. Per order m the Fourier coefficients are a linear combination in ℓ of the potential coefficients $\Delta\bar{C}_{\ell m}$ and $\Delta\bar{S}_{\ell m}$. Hence the name lumped coefficients.

Collecting all $A_{km}^{(ij)}$ and $B_{km}^{(ij)}$ in the vector γ the linear system

$$\tilde{\gamma} = Bc + \tilde{v} \tag{3.21}$$

can be established with $E\{\tilde{v}\} = 0$ and $E\{\tilde{v}\tilde{v}^T\} = Q_\gamma$, where the elements of the coefficient matrix B follow from (3.20) and $\tilde{v}$ denotes the residual vector in the frequency domain. In this case the a posteriori variance-covariance matrix becomes

$$Q_c = (B^T Q_\gamma^{-1} B)^{-1} \quad . \tag{3.22}$$

Error modelling: In the case of a white noise error spectrum Q_Γ and Q_γ become diagonal, where $Q_\Gamma = \sigma_0^2 I$ and $Q_\gamma = \sigma_0^2 \frac{\Delta t}{T} I$. In the case of band-limited and/or coloured noise Q_γ still remains diagonal, with the diagonal containing the variance elements of the noise model, say σ_{km}^2. An example of the latter type is discussed in (Schrama, 1990). In that case Q_Γ is, as expected, a full-matrix, e.g. with Toeplitz structure (cf. (Levinson, 1947)). From (3.20)

and (3.22) the element of the normal matrix $B^T Q_\gamma^{-1} B$ - this time with the error model σ^2_{km} built in - becomes

$$h^{(ij)}_{\ell_1 m \ell_2} = \frac{1}{2} \frac{\mu^2}{R^2} \left(\frac{R}{r}\right)^{\ell_1+\ell_2+2} \sum_k \lambda^{(ij)}_{\ell_1 k} \lambda^{(ij)}_{\ell_2 k} \bar{F}^{(*)k}_{\ell_1 m} \bar{F}^{(*)k}_{\ell_2 m} \frac{1}{\sigma^2_{km}} \quad . \qquad (3.23)$$

For white noise it is $\sigma^2_{km} = \sigma^2_0 \frac{\Delta t}{T}$ and $\frac{T}{\Delta t} = N$. Thus we see that in this case the frequency domain method coincides with the time domain approach.
Or in other words: After a long derivation it turns out that the frequency domain method is more convenient. The time domain method only adds the DFT from time to frequency domain, which is carried out in (3.23) implicitely. The variance-covariance matrix of the observations in the frequency domain approach remain diagonal both in the white noise and the band-limited/coloured noise case, and block-diagonality can in all cases easily be proven. In the time domain approach the variance-covariance matrix is diagonal only under the assumption of white measurement noise. Although block-diagonality is maintained in the band-limited/coloured noise case too, this is much more difficult to show.

3.3. Error analysis of gradiometric mission scenarios.

The two timewise methods described in chapters 3.1 and 3.2 permit rather realistical analyses of mission outcomes prior to any satellite launch. Still, the solution of the block diagonal normal matrix for gravity field estimation simulations up to degree 200 or 300 requires a considerable effort and requires most of all for efficient computation algorithms for the inclination functions, see Appendix A-3. We shall now describe in short the main elements of an error propagation study. Then, with some examples, the effects of the measurement bandwidth limitation and of a non-polar orbit shall be shown.

Eqs. (3.13) and (3.22) yield the error variances of the estimated potential coefficients $\Delta\bar{C}_{\ell m}$ and $\Delta\bar{S}_{\ell m}$. Let us note the individual variance of a coefficient $\sigma^2_{\ell m}(\bar{C})$ or $\sigma^2_{\ell m}(\bar{S})$, respectively. The error degree variance is then

$$\sigma_\ell^2(\bar{C},\bar{S}) = \sum_{m=0}^{\ell} (\sigma_{\ell m}^2(\bar{C}) + \sigma_{\ell m}^2(\bar{S}))$$

and the expected average error variance of the individual coefficient:

$$\sigma_{\ell m}^2(\bar{C},\bar{S}) = \sigma_\ell^2(\bar{C},\bar{S})/(2\ell+1) \quad . \tag{3.24}$$

Both quantities are dimensionless. The corresponding error degree-order and degree variances of all those quantities related to the disturbance quantities by a linear, self-adjoint operator are determined by the eigenvalue of the latter. In general if the error degree variances or degree-order variances of a quantity q are to be computed it is

$$\sigma_\ell^2(q) = \lambda_\ell^2(q,T)\sigma_\ell^2(\bar{C},\bar{S}) \tag{3.25a}$$

and

$$\sigma_{\ell m}^2(q) = \lambda_\ell^2(q,T)\sigma_{\ell m}^2(\bar{C},\bar{S}) \quad . \tag{3.25b}$$

We are mostly interested in the expected error of geoid heights or gravity anomalies. Their eigenvalues are (with dimensions included)

$$\lambda\ (\Delta g,T) = \gamma(\ell-1) \qquad \text{gravity anomaly} \tag{3.26}$$

where γ is normal gravity and

$$\lambda_\ell(N,T) = R \quad . \qquad \text{geoid height} \tag{3.27}$$

A list of relevant eigenvalues is given in Table 3.3. Mean values, e.g. of size $1^0 \times 1^0$, can be incorporated in the same manner by the eigenvalues β_n of a smoothing operator, c.f. (Meissl, 1971; Pellinen, 1966).

TABLE 3.3: Dimensionless Eigenvalues $\lambda_\ell(T,\cdot)$.

$\lambda_\ell(T,N)$	1	geoid height
$\lambda_\ell(T,T_r)$	$-1/(\ell+1)$	gravity disturbance (Hotine)
$\lambda_\ell(T,\epsilon)$	$1/\sqrt{\ell(\ell+1)}$	surface gradient (vectorial deflection of the vertical)
$\lambda_\ell(T,\Delta g)$	$1/(\ell-1)$	gravity anomaly (Stokes)
$\lambda_\ell(T,T_{rr})$	$1/((\ell+1)(\ell+2))$	vertical gradient
$\lambda_\ell(T,\epsilon_z)$	$1/(\sqrt{\ell(\ell+1)}(\ell+2))$	horizontal gradients (T_{xz},T_{yz})
$\lambda_\ell(T,\Delta\Gamma_{zz})$	$4/((\ell-1)(\ell+4))$	gradient anomaly $\Delta\Gamma_{zz}$
$\lambda_\ell(T,(\Delta\Gamma_{xz},\Delta\Gamma_{yz}))$	$1/(\sqrt{\ell(\ell+1)}(\ell-1))$	vect. grad. anomalies $(\Delta\Gamma_{xz},\Delta\Gamma_{yz})$
$\lambda_\ell(T,\{2\Delta\Gamma_{xy},\ \Delta\Gamma_{xx}-\Delta\Gamma_{yy}\})$	$1/\sqrt{(\ell-1)\ell(\ell+1)(\ell+2)}$	grad. anomalies $\{2\Delta\Gamma_{xy},\Delta\Gamma_{xx}-\Delta\Gamma_{yy}\}$
$\lambda_\ell(T(r),T(R))$	$(R/r)^{\ell+1}$	upward continuation of T, T_r, T_{rr}
$\lambda_\ell(\bar{A},A)$	$\beta_\ell(\psi_0)$	operator from quantity A to its smoother version $\bar{A}$
$\lambda_\ell(\delta T,\Delta g)$	$Q_\ell(\psi_0)/2$	Stokes truncation operator

The error propagation of ch. 3.1 and 3.2 leads to estimates of the *commission error* in a function space of finite dimension. Actually one also needs to know the effect of the neglected high degree and order part, the *omission error*. It is usually modelled by a signal degree-variance model, e.g. of Tscherning & Rapp (1974) or Moritz (1980). A degree-variance model, with signal degree-variances c_ℓ, provides an estimate of the expected signal content per degree of the earth's gravity field. Since we have no reliable observational evidence of the high degree part - the part we want to determine by satellite gradiometry - these models could be off by orders of magnitude, as they represent purely an extrapolation to high degrees of the well-known lower ones.

With $\sigma_\ell^2(q)$ (or $\sigma_{\ell_m}^2(q)$) representing the commission error spectrum of a desired (smoothed) quantity q, and $c_\ell(q)$ (or $c_{\ell_m}(q)$) the omission part the two error variances become

$$\sigma^2_{CO}(q) = \sum_{\ell=2}^{\ell max} \sigma^2_\ell(q) = \sum_{\ell=2}^{\ell max} (2\ell+1)\sigma^2_{\ell_m}(q) \qquad \text{commission}$$

and (3.28a,b)

$$\sigma^2_{OM}(q) = \sum_{\ell=\ell max+1}^{\infty} c_\ell(q) = \sum_{\ell=\ell max+1}^{\infty} (2\ell+1)c_{\ell_m}(q) \quad . \qquad \text{omission}$$

The total error variance becomes

$$\sigma^2(q) = \sigma^2_{CM}(q) + \sigma^2_{OM}(q) \quad . \tag{3.29}$$

This procedure corresponds to ideal low pass filtering with cut-off degree ℓmax. A more optimal situation is attained with a Wiener-Kolmogorov type filter

$$h_\ell = \frac{c_\ell(q)}{c_\ell(q)+\sigma^2_\ell(q)} \tag{3.30}$$

which simulates a least-squares collocation situation. In that case it is

$$\sigma^2_{CO}(q) = \sum_{\ell=2}^{\infty} h^2_\ell \, \sigma^2_\ell(q) \qquad \text{commission}$$

and

$$\sigma^2_{OM}(q) = \sum_{\ell=2}^{\infty} (1 - h^2_\ell)c_\ell(q) \qquad \text{omission.}$$

Eq. (3.29) still holds. This concludes the description of all elements of our method of error propagation simulation.

It remains now to show what type of questions we can address with these methods. In ch. 3.1 all assumptions were described that apply to this model. The simplifications refer (1) to the orbit, (2) to the comensurability of N_0 and N_e, i.e. to a balance of the mission length and orbit choice, (3) to the maximum resolution ℓmax ($< \frac{N_0}{2}$) and (4) to the regular sampling without interruption. The orbit is assumed to be circular (e = 0). For the reference

orbit it is assumed $\dot{a} = \dot{e} = \dot{I} = 0$ and constant $\dot{\Omega}$, $\dot{\omega}$, $\dot{M}$, and $\dot{\theta}_G$. Actual deviations from these assumption can be taken into account by iteration. The mission length must be one (or several) full repeat cycle(s).

The following variables remain (see again (Colombo, 1987)) to be defined:

1. Each gradient component T_{ij} or a combination of components
2. Measurement noise level and noise spectrum (incl. bandwidth limitations) of each component.
3. Sample rate Δt.
4. Mission duration T ($N = T/\Delta t$).
5. Inclination I.
6. Mission altitude $h = r - R$.

Out of the six possibilities three can be varied without having to solve the large system of equations again, just by rescaling $(A^TA)^{-1}$. These are mission length T and sample rate Δt and in case of white noise, the a priori noise level σ_0. Slightly more effort is required for a change in h, as shown in (Colombo, ibid) and (Schrama, 1990). The downward continuation operators $\left(\frac{R}{r}\right)^{\ell+1} = \left(\frac{R}{R+h}\right)^{\ell+1}$ for each degree are not included in the normal matrix elements (3.18) or (3.23). Instead their reciprocal value is put into a diagonal matrix D. Then the solution for any desired h becomes

$$D^T(A^TA)^{-1}D \quad .$$

Finally changes in (1.) or (5.) require a full new computation.

3.4. Case studies of gradiometric error propagation.

With a few examples we try to demonstrate the use of this type of gradiometric error simulation. Two cases shall be considered: the consequences of a bandlimited error spectrum, and the effect of a non-polar orbit.

3.4.1. Bandwidth limitation.

In the course of the ARISTOTELES system studies it became clear that it would not be realistical to assume that the gradiometer noise is white over the entire measurement spectrum (0 Hz to 0.125 Hz) with a std.dev. of 0.01 E/$\sqrt{\text{Hz}}$. This specification can only be met over the band from $5 \cdot 10^{-3}$ Hz (= 27 cpr) to 0.125 Hz. What the exact noise characteristics will be below $5 \cdot 10^{-3}$ Hz is still uncertain. It is certain, however, that the zero frequency and the frequencies close to the zero frequency are not measurable at all. In other words the gradiometer is no absolute measurement and shall exhibit low frequency drift. Causes for these short-comings are e.g. thermal noise (no cryogenic cooling) or imperfections in the matching of the accelerometer components, that result in violations of the common-mode rejection principle.

It is therefore useful to look into the effect of any band-limitation of the instrument. To simulate this case the b_{km} frequency lines below a certain frequency are given a close to infinity variance value σ^2_{km}.

Let us assume conditions (3.17) of ch. 3.3 are met, which means no overlapping of frequencies b_{km} occurs. We test the effect of a white noise spectrum limited between β_1 and β_2. The upper limit β_2 is determined by the sample frequency, in our case 0.125 Hz, and therefore $\beta_2 = 665$. For β_1 three cases shall be tested: $\beta_1 = 27$ ($5 \cdot 10^{-3}$ Hz), $\beta_1 = 4$ ($8 \cdot 10^{-4}$ Hz) and $\beta_1 = 0$. With this information a list can be established of all (k,m) outside the frequency range. For the spectral lines (k,m) the weight $\frac{1}{\sigma^2_{km}}$ in (3.23) takes the value zero, i.e. the error variance goes to infinity.

Close inspection of eq. (3.23) reveals that these zero weights can have two consequences. Either the value of element $h^{(ij)}_{\ell_1 m \ell_2}$ of the normal matrix simply decreases without getting zero. This implies that the involved spherical harmonic coefficients are still estimable but will get a higher a

posteriori error variance. Or $h^{(ij)}_{\ell_1 m \ell_2}$ becomes zero, which leads to a singularity of the normal matrix, if $\ell_1 = \ell_2$ (diagonal element). One can, for example, easily see that all spherical harmonic degrees ℓ less than β_1 cause singularity. They are not estimable.

There are two ways to deal with the singularities. One can simply declare these coefficients not estimable and eliminate the corresponding rows and columns of the normal matrix. This corresponds to eliminating the coefficients from the original linear system. It is saying that no information about these coefficients is available, neither from gradiometry nor from elsewhere. This is the appropriate approach when analyzing the information content purely from the gradiometric experiment itself. In real world information about these coefficients is very likely to be available or comes from complementary sensors, such as on-board GPS, see (Schrama, 1991). This prior information can easiest be implemented by adding to each diagonal element of degree ℓ and order m the prior variance $\sigma^2_{\ell m}$ (prior):

$$h^{(ij)}_{\ell m \ell}\ (\text{new}) = h^{(ij)}_{\ell m \ell}\ (\text{old}) + \frac{1}{\sigma^2_{\ell m}(\text{prior})} \quad . \tag{3.31}$$

The procedure is called <u>regularization</u>. It can be applied to all diagonal elements and is interpreted as optimal weighting between prior and measured information. A very common choice for $\sigma^2_{\ell m}$ (prior) are the degree-order signal variances $c_{\ell m}$ as derived from one of the available signal degree-variance models such as Kaula's rule or the Tscherning-Rapp degree-variance model. More appropriate seems the use of the error variances of one of the geopotential models that came available recently, such as GEM-T1, GRIM-4, or TEG-1.

In Figure 3.1 the effect of bandwidth limitation on the degree-order error spectrum is demonstrated with an extreme example. It is assumed that either no bandwidth limitation exists at all (white noise over the full spectrum), or that no information is available either below $\beta_1 = \beta_{min} = 4$ ($8 \cdot 10^{-4}$ Hz) or below $\beta_1 = \beta_{min} = 27$ ($5 \cdot 10^{-3}$ Hz). The following mission scenario is assumed: measured gradiometer components (zz) and (yy); error std.dev. 0.01 E/$\sqrt{\text{Hz}}$, mission duration 6 months; sample rate 4 s; altitude 200

km; inclination 90^0. Regularization is applied with the Tscherning-Rapp degree-variance model. For comparison also a signal degree-order spectrum is included based on Kaula's rule of thumb. It can be seen that with $\beta_{min} = 27$ very little improvement of our current gravity field knowledge would be achieved.

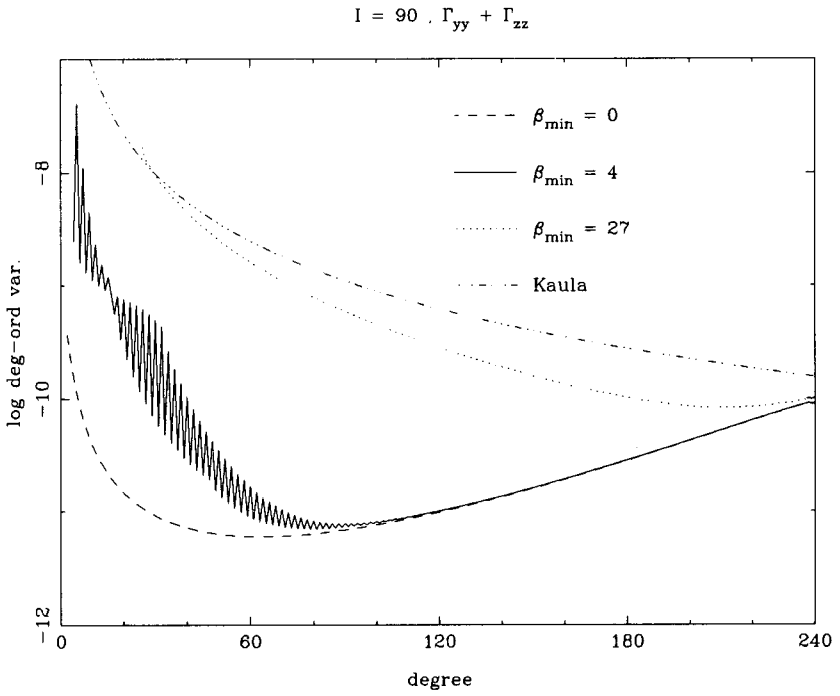

Figure 3.1: Effect of complete lower bandwidth limitation on error spectrum (per degree and order).

For comparison a more favorable situation is shown in Figure 3.2. It is based on the noise characteristics expected for the ARISTOTELES gradiometer. The gradiometer measures the components (zz) and (yy). The measurement band is limited between $\beta_{min} = 4$ and $\beta_2 = 665$. For the range between $\beta_{min} = 4$ and 27 $\frac{1}{f}$ coloured noise is assumed, for the range between $\beta = 27$ and β_2 white noise with 0.01 $E/\sqrt{Hz}$. All other parameters agree with those used for Figure 3.1. Regularization was carried out with the Tscherning-Rapp model.

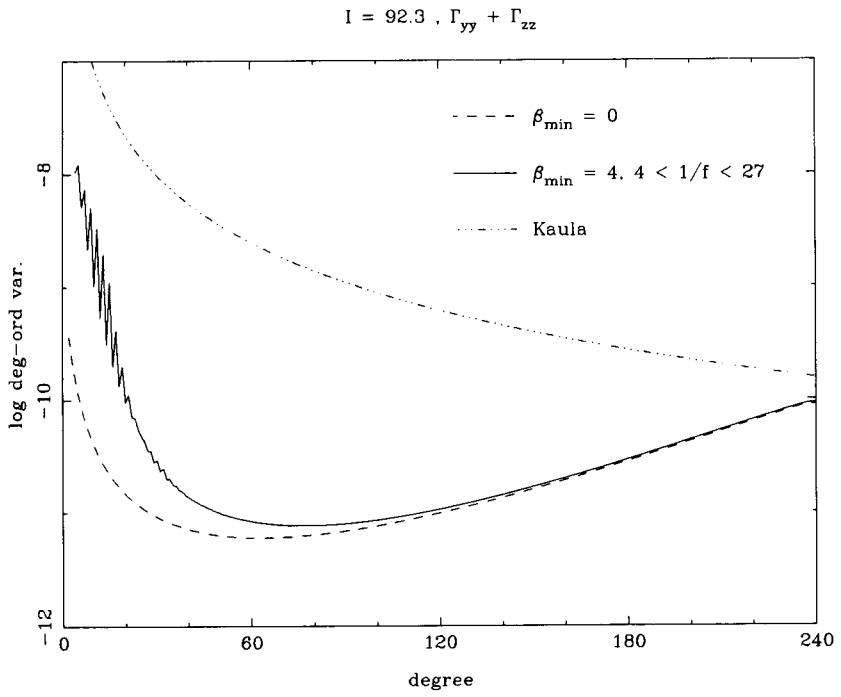

Figure 3.2: Error degree-order spectrum for a combined bandlimited ($< \beta_{min} = 4$), coloured noise ($4 < \frac{1}{f} < 27$), white noise 0.01 E/$\sqrt{Hz}$ model. For comparison ideal noise model of Figure 3.1 and the signal spectrum are included too.

Figure 3.3 shows the scenario expected for the ARISTOTELES mission. The mission parameters are altitude 200 km, duration 6 months and inclination $92^0.3$. The gravity field is determined from a combination of gradiometry ((zz) + (yy)) and GPS carrier phase measurements. For GPS the assumptions are std.dev. 3 cm white noise in x,y,z and sample rate 30 s; for gradiometry 1/f coloured noise between β = 4 and 27 and white noise 0.01 E/$\sqrt{Hz}$ above 27; sample rate 4 s.

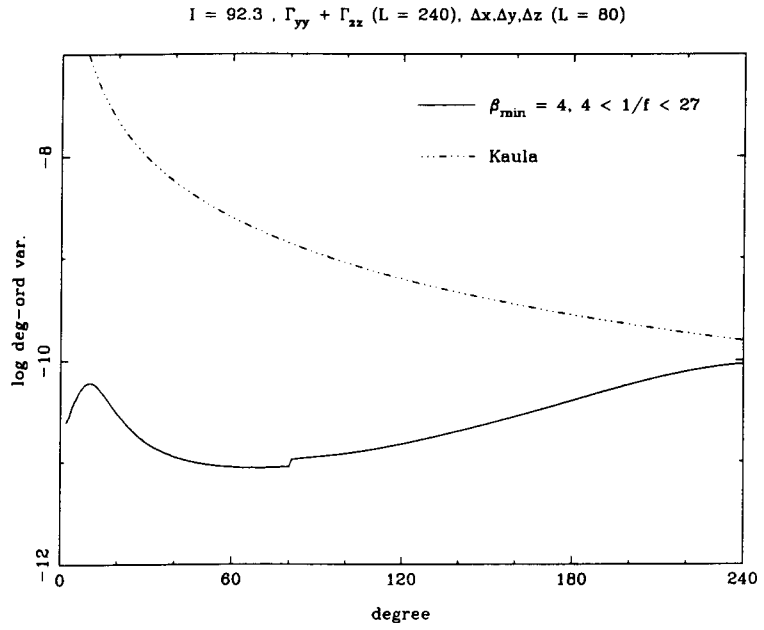

Figure 3.3: Combination of spaceborne GPS (3 cm) and gradiometry ((zz) and (yy)): the ARISTOTELES scenario.

3.4.2. Non-polar orbit.

A second aspect of special interest is the effect of a non-polar orbit. The polar orbit, usually assumed in the spacewise approach, would lead to a complete coverage of the sphere with data. It is, however, not a very realistic assumption, as it is not possible to keep a spacecraft in a "perfect" polar orbit. Usually one will have to do with a slightly non-polar orbit, say I = 92^0 or e.g. a sun-synchronous orbit with I = 96.33^0. It is then the question what the effect of this non-ideal situation is. So far we did not study this question in depth.

It is obvious that with an inclination I ≠ 90^0 the two polar regions with half angle (90^0 - I) are not covered with data. This should affect the estimation of spherical harmonics, as they depend on global support. If regularization is applied the polar gaps get so-to-say covered with data (value zero) but of inferior quality. Singularity is avoided in this case. With the mission duration unchanged the total data rate remains unchanged as well. Hence non-polar inclination results in denser data coverage of all covered

regions. Finally the outcome shall depend on the type of observed gradient component. At maximum latitude (φ = I) the out-of-plane gradient components are looking towards the poles. All these aspects together are of influence.

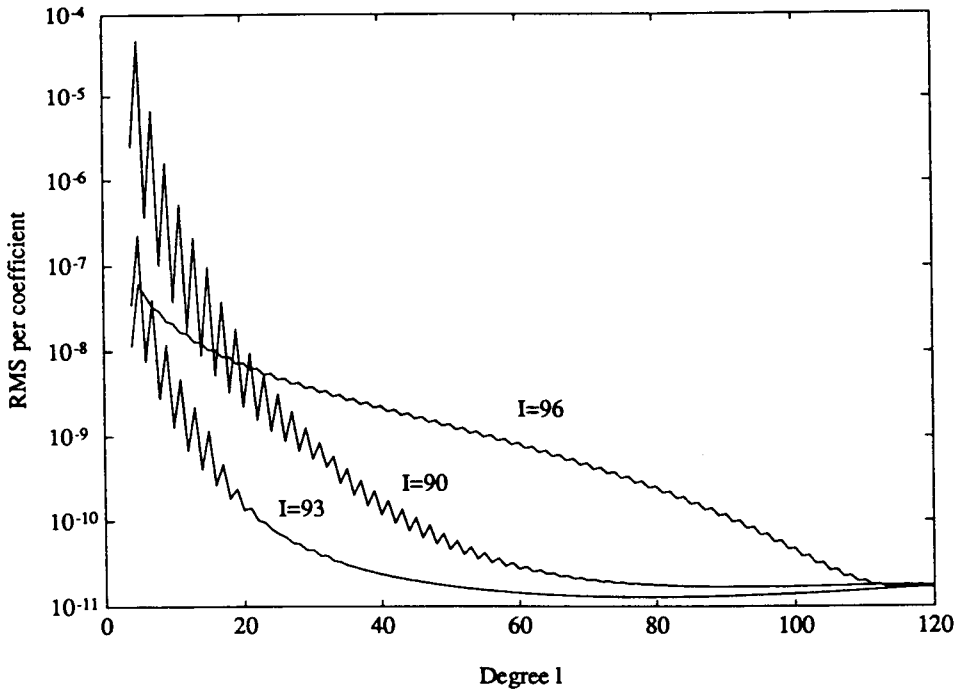

Figure 3.4: The r.m.s. per coefficient per degree derived from T_{zz} for I = 90_0, 93^0 and 96^0 at h = 200 km. The mean r.m.s. per coefficient per degree is computed using a least squares approach for T_{zz} assuming $4 < \beta < \infty$, a $1/\beta$ behavior below β_{min} = 27 cpr, a sampling time of 4 s and mission duration of 6 months.

Figure 3.4 shows the effect of non-polar data coverage with the Γ_{zz} component. The effective measurement band used for this case is that of Figure 3.2. Moreover we assumed a 4 s sampling rate and 6 months of data. It must be pointed out that the choice for ℓmax dominates the outcome of these computations. Here we have chosen ℓmax = 120 which corresponds to latitude steps of 1.5^0 on the sphere. Yet is remarkable that the I = 93^0 case results in an optimum for ℓmax = 120 whereas I = 90^0 and I = 96^0 are suboptimal. A reason could be an

improved coverage for a 1.5^0 equivalent grid near the poles at $I \neq 93^0$; namely for the most northern and southern parallels.

4. SPACEWISE VERSUS TIMEWISE - A COMPARISON.

In the previous two chapters the main characteristics of the spacewise and timewise analysis were described. We shall conclude with a short comparison.

In chapter 2 two versions of the spacewise approach were discussed, the least-squares method (ch. 2.3) and the quadrature method (ch. 2.4). It was demonstrated that, although the quadrature approach is not optimal, it possesses a number of advantages, such as the avoidance of aliasing and most of all simplicity. Both spacewise approaches are intimately connected to the solution of the geodetic boundary value problem (g.b.v.p.). Satellite gradiometry becomes one data source in the geodetic arsenal and various overdetermined or mixed b.v.p. can be addressed. An immediate practical advantage of the spacewise approach is that it does not depend on a continous data stream. Data gaps, interruptions, jumps e.g. as a result of manoeuvres do not pose a problem as long as the sphere is covered sufficiently dense. Even larger data gaps after completion of a mission can be corrected for by interpolation or insertion of a priori information. On the other hand the spacewise approach lacks any connection to the peculiarities of the orbit, its variation in heights, its resonance behaviour or its uncertainty. In addition, it is not obvious how to implement coloured measurement noise models.

Also the timewise approach was divided into two categories, the timewise approach in the time domain (ch. 3.1) and that in the frequency domain or lumped coefficient approach (ch. 3.2). However we could show that under the assumption of an uninterrupted data stream the time domain approach can be reduced to the lumped coefficient method. The timewise methods are closer related to the physics of a space experiment. All orbit features are naturally built in, orbit errors can easily be added, combination with tracking measurements in one model is possible, and sample and measurement noise characteristics are part of the model. The block diagonality of the normal matrix can be maintained, however, only under the very stringent condition of the availability of a full number of repeat cycles. Hence there exists no easy way to test for example the effect of orbit manoeuvres or data gaps.

Thus we see that from the theoretical and practical point of view timewise and spacewise approach are complementary, the former closer related to the g.b.v.p. and therefore to physical geodesy and the latter to orbit dynamics

and consequently to satellite geodesy. For a polar, spherical orbit and denser data both methods should approach towards the same limit. This limit must be the solution of the fixed (classical) boundary value problem with one, several or all second derivatives of the gravitational potential as boundary functions. The boundary surface is a sphere at satellite altitude and generated by the total set of observations. In the case of the spacewise method this limit is understood in the sense described in chapter 2, in that of the timewise method it is attained as an infinite set of consecutive revolutions that densely cover the sphere in the limit. However this proposition needs to be proven. See in particular (Migliaccio & Sansò, 1989) and (Brovelli & Sansò, 1990).

After this being said the equivalence of the four methods (IA = spacelike quadrature, IB = spacelike least-squares, IIA = timelike time domain, II B = timelike lumped coefficient) is shown experimentally. For this purpose the propagated error spectrum is determined for the observed component T_{zz}. It is assumed measurement noise std.dev. $\sigma = 10^{-2}\ E/\sqrt{Hz}$, altitude h = 200 km, eccentricity e = 0, inclination I = 90^0, sample rate Δt = 4 s, mission length T = 4 months. For method IA the degree-order variance is computed according to eq. (2.78) with

$$\sigma^2_{\ell_m} = \frac{\pi^2}{8}\frac{\Delta t}{T}\sigma^2 \quad .$$

For method IB it is assumed that first $1^0 \times 1^0$ block equal angular averages are computed from the point measurements. This yields 60 samples per block. The std.dev. of each block is determined as

$$\bar{\sigma}^2_{1x1} = \frac{\sigma^2}{\sqrt{60}} \quad .$$

In the case of method IIA and IIB formulas (3.13) and (3.14) and (3.23), respectively, are applied. Error propagations showed that the four methods are in complete agreement.

APPENDICES.

A-1: Coordinate systems.

The gravitational potential is usually expressed as a series of spherical harmonics using the spherical coordinates r, λ, θ (see fig. A-1.1) ($\theta = 90^0 - \varphi$).

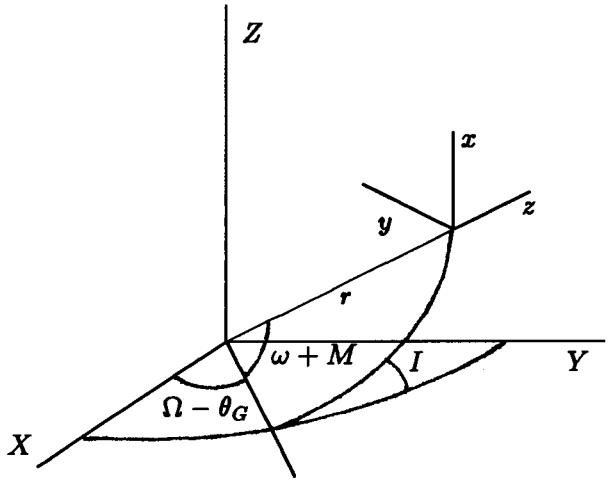

FIGURE A-1.1.

When dealing with satellite methods an expression of the geopotential as function of the orbital elements a, e, I, Ω, ω, M (respectively the semi-major axis, eccentricity, inclination, right ascension of node, argument of perigee and mean anomaly) is more convenient. Here we shall deal with circular orbits (hence e = 0) and consider a to be constant throughout a mission, leaving us with four orbital elements, which may be considered variables to locate a point on the orbit. For convenience we furthermore introduce the variables ω_o and ω_e defined as:

$$\omega_o = \omega + M$$

$$\omega_e = \Omega - \theta_G \qquad \text{(A-1.1)}$$

where θ_G is the right ascension of the Greenwich meridian. In the case of a circular orbit ω is not defined. The subscript "o" refers to orbit and the subscript "e" to earth (see Schrama, 1989).

Points along a satellite orbit are not arbitrarily located in space but are related to each other due to the satellite motion. Consider a satellite orbit with constant ω_e. Letting the three parameters r, I, ω_o vary all points in 3-dimensional space can be located. Hence r, I, ω_o may be considered as coordinates. However, this is not the case if we consider an orbit with constant I and varying ω_e. Then all the points in 3-dimensional space with $\theta < 90^0 - I$ can not be located using r, ω_e, ω_o as coordinates. But since we are only interested in the points along orbits, this possibility (constant I, varying r, ω_e, ω_o) is also of use to us. It will appear later that both cases may be used to describe the potential derivatives.

The angles λ, θ, ω_e, ω_o are in fact taken with respect to a geocentric cartesian coordinate system (X,Y,Z), connected to the earth in such a way that the X-axis points in the direction of the Greenwich meridian and the Z-axis coincides with the rotation axis of the earth (see Figure A-1.1).

The last coordinate system we have to consider is the local, right-handed Cartesian coordinate system (x,y,z) in which the actual gradiometric measurements are taken. The z-axis of this system points radially outwards, the x-axis points along-track and the y-axis cross-track.

Whenever convenient, the four coordinate systems mentioned above will be denoted by:

$\{x_i,\ i = 1,2,3\}$	(x,y,z)	local cartesian coordinates
$\{x_I,\ I = 1,2,3\}$	(X,Y,Z)	geocentric cartesian coordinates
$\{x_a,\ a = 1,2,3\}$	(r,I,ω_o) or (r,ω_e,ω_o)	orbit coordinates
$\{x_A,\ A = 1,2,3\}$	(r,λ,θ)	spherical coordinates

In the following the relationship between these different coordinate systems will be treated as far as necessary for the gradiometry analysis. We need these relations since we want to express the measurements done in the local cartesian coordinate system in terms of potential coefficients as they appear

in a series expansion of the gravitational potential, either in spherical coordinates (spherical harmonic expansion) or in orbit coordinates (expansion in inclination functions).

Potential expansion.

The expression for the earth's gravitational disturbance potential in a series of spherical harmonics using the spherical coordinates $x_A = (r, \lambda, \theta)$ is:

$$T = \frac{\mu_0}{R} \sum_{\substack{\ell=0 \\ \ell \neq 1}}^{\infty} \left(\frac{R}{r}\right)^{\ell+1} \sum_{m=0}^{\ell} [\Delta\bar{C}_{\ell m} \cos m\lambda + \Delta\bar{S}_{\ell m} \sin m\lambda] \bar{P}_{\ell m}(\cos \theta) \quad \text{(A-1.2)}$$

where μ_0 : gravitational constant times mass of the earth
R : mean equatorial radius
$\Delta\bar{C}_{\ell m}, \Delta\bar{S}_{\ell m}$: normalized potential coefficients
$\bar{P}_{\ell m}(\cos \theta)$: normalized Legendre functions
ℓ, m : degree and order.

This expression may be transformed to a series expansion in the orbital parameters $(r, I, \omega_e, \omega_o)$ (see Appendix A-3 or Kaula, 1966) which yields for a circular orbit:

$$T = \frac{\mu_0}{R} \sum_{\ell=0}^{\infty} \left(\frac{R}{r}\right)^{\ell+1} \sum_{m=0}^{\ell} \sum_{p=0}^{\ell} \bar{F}_{\ell mp}(I) \left\{ \begin{bmatrix} \Delta\bar{C}_{\ell m} \\ -\Delta\bar{S}_{\ell m} \end{bmatrix} \cos \psi_{\ell mp} + \begin{bmatrix} \Delta\bar{S}_{\ell m} \\ \Delta\bar{C}_{\ell m} \end{bmatrix} \sin \psi_{\ell mp} \right\}_o^e \quad \text{(A-1.3)}$$

where "e" refers to the case where ℓ-m is even and "o" refers to ℓ-m is odd and

$\bar{F}_{\ell mp}$: normalized inclination functions
$\psi_{\ell mp}$: $(\ell - 2p)\omega_o + m\omega_e$.

Potential derivatives.

From eq. (A-1.2) and (A-1.3) all the first and second order derivatives of the potential with respect to r, λ, θ and r, I, ω_e, ω_o can be derived.

The derivatives with respect to the spherical coordinates from eq. (A-1.2) are well known and easy to derive. Since they are not really needed in this context they are not explicitly given here. We need the partial derivatives with respect to r, I, ω_o, ω_e from eq. (A-1.3). Since, as explained earlier, either the orbit parameters (r, I, ω_o) or (r, ω_e, ω_o) are considered as coordinates we do not need the mixed second order partial derivatives with respect to I and ω_e.

All the partial derivatives can be written in the following manner:

$$T_a = \frac{\mu_0}{R} \sum_{\ell} \lambda_{\ell}^{(a)} \left(\frac{R}{r}\right)^{\ell+1} \sum_{m} \sum_{p} \bar{F}_{\ell mp}^{(a)}(I) \left(\alpha_{\ell m}^{(a)} \cos \psi_{\ell mp} + \beta_{\ell m}^{(a)} \sin \psi_{\ell mp}\right) \quad \text{(A-1.4)}$$

where the "a" is not an index but a symbolic notation for expressing one of the partial derivatives. So a can take the values:

$$r, I, \omega_o, \omega_e$$

or as (ab) for the second derivatives

$$rr, II, \omega_o\omega_o, \omega_e\omega_e$$

$$rI, r\omega_o, r\omega_e, I\omega_o, \omega_o\omega_e \quad .$$

With this convention, for example when ab = rI, the notation T_{ab} means $\frac{\partial^2 T}{\partial r \partial I}$. Now let us introduce the following notation:

$$\alpha_{\ell m} = \begin{bmatrix} \Delta\bar{C}_{\ell m} \\ -\Delta\bar{S}_{\ell m} \end{bmatrix}_{\ell-m:\,\text{odd}}^{\ell-m:\,\text{even}} \qquad \bar{F}'_{\ell mp} = \frac{\partial}{\partial I}\,\bar{F}_{\ell mp}$$

$$\beta_{\ell m} = \begin{bmatrix} \Delta\bar{S}_{\ell m} \\ \Delta\bar{C}_{\ell m} \end{bmatrix}_{\ell-m:\,\text{odd}}^{\ell-m:\,\text{even}} \qquad \bar{F}''_{\ell mp} = \frac{\partial^2}{\partial I^2}\,\bar{F}_{\ell mp}$$

Then we find for the factor $\lambda_{\ell}^{(ab)}$ and the products $\bar{F}_{\ell mp}^{(ab)}(I)\ \alpha_{\ell m}^{(ab)}$ and $\bar{F}_{\ell mp}^{(ab)}\ \beta_{\ell m}^{(ab)}$ the values listed in Table A-1.1 below.

TABLE A-1.1.

ab	$\lambda_{\ell}^{(ab)}$	$\overline{F}_{\ell mp}^{(ab)}\ \alpha_{\ell m}^{(ab)}$	$\overline{F}_{\ell mp}^{(ab)}\ \beta_{\ell m}^{(ab)}$
r	$-\frac{(\ell+1)}{r}$	$\alpha_{\ell m}\ \overline{F}_{\ell mp}$	$\beta_{\ell m}\ \overline{F}_{\ell mp}$
I	1	$\alpha_{\ell m}\ \overline{F}'_{\ell mp}$	$\beta_{\ell m}\ \overline{F}'_{\ell mp}$
ω_o	1	$(\ell-2p)\beta_{\ell m}\overline{F}_{\ell mp}$	$-(\ell-2p)\alpha_{\ell m}\overline{F}_{\ell mp}$
ω_e	1	$m\beta_{\ell m}\overline{F}_{\ell mp}$	$-m\alpha_{\ell m}\overline{F}_{\ell mp}$
rr	$\frac{(\ell+1)(\ell+2)}{r^2}$	$\alpha_{\ell m}\overline{F}_{\ell mp}$	$\beta_{\ell m}\overline{F}_{\ell mp}$
II	1	$\alpha_{\ell m}\overline{F}''_{\ell mp}$	$\beta_{\ell m}\overline{F}''_{\ell mp}$
$\omega_o\omega_o$	-1	$(\ell-2p)^2\alpha_{\ell m}\overline{F}_{\ell mp}$	$(\ell-2p)^2\beta_{\ell m}\overline{F}_{\ell mp}$
$\omega_e\omega_e$	-1	$m^2\alpha_{\ell m}\overline{F}_{\ell mp}$	$m^2\beta_{\ell m}\overline{F}_{\ell mp}$
rI	$-\frac{(\ell+1)}{r}$	$\alpha_{\ell m}\overline{F}'_{\ell mp}$	$\beta_{\ell m}\overline{F}'_{\ell mp}$
$r\omega_o$	$-\frac{(\ell+1)}{r}$	$(\ell-2p)\beta_{\ell m}\overline{F}_{\ell mp}$	$-(\ell-2p)\alpha_{\ell m}\overline{F}_{\ell mp}$
$r\omega_e$	$-\frac{(\ell+1)}{r}$	$m\beta_{\ell m}\overline{F}_{\ell mp}$	$-m\alpha_{\ell m}\overline{F}_{\ell mp}$
$\omega_o\omega_e$	-1	$m(\ell-2p)\alpha_{\ell m}\overline{F}_{\ell m\ p}$	$m(\ell-2p)\beta_{\ell m}\overline{F}_{\ell mp}$
$I\omega_o$	1	$(\ell-2p)\beta_{\ell m}\overline{F}'_{\ell mp}$	$-(\ell-2p)\alpha_{\ell m}\overline{F}'_{\ell mp}$

Coordinate transformation.

We assume that the gradiometer delivers the second order potential derivatives (or after linearization those of the disturbance potential T) with respect to the local cartesian coordinates x_i: $V_{ij} \equiv \frac{\partial^2 V}{\partial x_i \partial x_j}$. So we want to express these V_{ij} in a series expansion in terms of potential coefficients. Since we can easily obtain the derivatives of V with respect to x_a (eq. A-1.4) we need the transformation from x_a to x_i.

Differentiating the potential once and using the chain rule of differentation gives

$$V_i \equiv \frac{\partial V}{\partial x_i} = \frac{\partial V}{\partial x_a} \frac{\partial x_a}{\partial x_i} \equiv A_i^a V_a \qquad \text{(summation over a)} \quad . \tag{A-1.5}$$

Differentiating again yields:

$$V_{ij} = \frac{\partial^2 V}{\partial x_i \partial x_j} = \frac{\partial}{\partial x_j} (A_i^a V_a) = \frac{\partial}{\partial x_j} (\frac{\partial x_a}{\partial x_i} \frac{\partial V}{\partial x_a}) =$$

$$= \frac{\partial^2 x_a}{\partial x_i \partial x_j} \frac{\partial V}{\partial x_a} + \frac{\partial x_a}{\partial x_i} \frac{\partial}{\partial x_b} (\frac{\partial V}{\partial x_a}) \frac{\partial x_b}{\partial x_j} =$$

$$\equiv A_{ij}^a V_a + A_i^a A_j^b V_{ab} \quad . \tag{A-1.6}$$

We have the V_a and V_{ab} from eq. (A-1.4) and Table A-1.1. What we still need in order to carry out the transformation are the partial derivatives between the two coordinate sets: A_i^a and A_{ij}^a. These can be obtained in the following way. Consider a point P' in the neighbourhood of P (P is the origin of the local system). The geocentric cartesian coordinates of P', $x_I(P')$, can be written as

$$x_I(P') = x_I^0 + B_I^i(P) x_i(P') \tag{A-1.7}$$

in which

$$x_I^o = B_I^J(P)h_J(P)$$

$$h_I(P) = \begin{pmatrix} 0 \\ 0 \\ r(P) \end{pmatrix}$$

and B is the transformation matrix derived through successive rotations over $-\omega_o$, $-I$, $-\omega_e$, or

$$B = R_3(-\omega_e)R_1(-I)R_3(-\omega_o) \quad .$$

Eq. (A-1.7) states that the geocentric cartesian coordinates of P' are the sum of the geocentric coordinates of P (first term on the right hand side) and the rotated local coordinates of P' (second term). For all points P' defined in this way the elements of x_I^o and $B_I^i(P)$ are functions of the (constant) orbit coordinates x_a of point P. Thus eq. (A-1.7) gives the geocentric Cartesian coordinates of P' as a function of its local Cartesian coordinates.

Assuming P' lies on a (nearby) orbit we may also write the geocentric cartesian coordinates of P' as

$$x_I(P') = B_I^J(P')h_J(P') \qquad \text{(A-1.8)}$$

where the elements of B_I^J and h_I are now functions of the orbit coordinates of P'. From eq. (A-1.7) the partial derivatives become

$$\frac{\partial x_I}{\partial x_i} \equiv A_i^I \qquad \frac{\partial^2 x_I}{\partial x_i \partial x_j} \equiv A_{ij}^I$$

and from eq. (A-1.8)

$$\frac{\partial x_I}{\partial x_a} \equiv A_a^I \qquad \frac{\partial^2 x_I}{\partial x_a \partial x_b} \equiv A_{ab}^I \quad .$$

Using the chain rule of differentiation the desired partial derivatives A_i^a are obtained since

$$A_i^I = A_a^I A_i^a \qquad \Rightarrow \qquad A_i^a = (A_a^I)^{-1} A_i^I \quad .$$

The second partial derivatives A_{ij}^a are obtained in a similar manner by again differentiating the chain rule above.

As mentioned above, we can take as x_a-coordinates either (r, I, ω_o) or (r, ω_e, ω_o). In the former case, we find for the partial derivatives:

$$\frac{\partial r}{\partial z} = 1 \qquad \frac{\partial^2 r}{\partial x^2} = \frac{1}{r} \qquad \frac{\partial^2 r}{\partial y^2} = \frac{1}{r}$$

$$\frac{\partial I}{\partial y} = \frac{1}{r \sin \omega_o} \qquad \frac{\partial^2 I}{\partial y \partial z} = \frac{-1}{r^2 \sin \omega_o} \qquad \frac{\partial^2 I}{\partial x \partial y} = \frac{-\cos \omega_o}{r^2 \sin^2 \omega_o}$$

$$\frac{\partial \omega_o}{\partial x} = \frac{1}{r} \qquad \frac{\partial^2 \omega_o}{\partial y^2} = \frac{\cos \omega_o}{r^2 \sin \omega_o} \qquad \frac{\partial^2 \omega_o}{\partial x \partial z} = -\frac{1}{r^2} \quad .$$

All the other partial derivatives are zero. In the latter case we have:

$$\frac{\partial r}{\partial z} = 1 \qquad \frac{\partial^2 r}{\partial x^2} = \frac{1}{r} \qquad \frac{\partial^2 r}{\partial y^2} = \frac{1}{r}$$

$$\frac{\partial \omega_e}{\partial y} = \frac{-1}{r \sin I \cos \omega_o} \qquad \frac{\partial \omega_e}{\partial y^2} = \frac{-\cos I \sin \omega_o}{r^2 \sin^2 I \cos^3 \omega_o}$$

$$\frac{\partial^2 \omega_e}{\partial y \partial z} = \frac{1}{r^2 \sin I \cos \omega_o} \qquad \frac{\partial^2 \omega_e}{\partial x \partial y} = \frac{-\sin \omega_o}{r^2 \sin I \cos^2 \omega_o}$$

$$\frac{\partial \omega_o}{\partial x} = \frac{1}{r} \qquad \frac{\partial^2 \omega_o}{\partial x \partial z} = \frac{-1}{r^2} \qquad \frac{\partial\, \omega_o}{\partial x \partial y} = \frac{\sin \omega_o \cos I}{r^2 \cos^2 \omega_o \sin I}$$

$$\frac{\partial \omega_o}{\partial y} = \frac{\cos I}{r \sin I \cos \omega_o} \qquad \frac{\partial^2 \omega_o}{\partial y \partial z} = \frac{-\cos I}{r^2 \sin I \cos \omega_o}$$

$$\frac{\partial^2 \omega_o}{\partial y^2} = \frac{\sin \omega_o (\sin^2 I \sin^2 \omega_o - 2\sin^2 I + 1)}{r^2 \sin^2 I \cos^3 \omega_o}$$

and all the others being zero.

Note that the derivatives of ω_o are not the same in both cases. Now we may compute from eq. (A-1.6) the local gradients V_{ij} and find in the case of (r, I, ω_o):

$$V_{xx} = \frac{1}{r} V_r + \frac{1}{r^2} V_{\omega_o \omega_o}$$

$$V_{xy} = \frac{-\cos \omega_o}{r^2 \sin^2 \omega_o} V_I + \frac{1}{r^2 \sin \omega_o} V_{I\omega_o}$$

$$V_{xz} = -\frac{1}{r^2} V_{\omega_o} + \frac{1}{r} V_{r\omega_o} \qquad \text{(A-1.9)}$$

$$V_{yy} = \frac{\cos \omega_o}{r^2 \sin \omega_o} V_{\omega_o} + \frac{1}{r} V_r + \frac{1}{r^2 \sin^2 \omega_o} V_{II}$$

$$V_{yz} = \frac{-1}{r^2 \sin \omega_o} V_I + \frac{1}{r \sin \omega_o} V_{rI}$$

$$V_{zz} = V_{rr} \quad .$$

In the case of the parameter set (r, ω_e, ω_o) we find

$$V_{xx} = \frac{1}{r} V_r + \frac{1}{r^2} V_{\omega_o \omega_o}$$

$$V_{xy} = \frac{-1}{r^2 \sin I \cos \omega_o} [\tan \omega_o V_{\omega_e} - \tan \omega_o \cos I V_{\omega_o} + V_{\omega_e \omega_o} + \cos I V_{\omega_o \omega_o}]$$

$$V_{xz} = \frac{1}{r} V_{\omega_o} - \frac{1}{r^2} V_{\omega_o}$$

$$V_{yy} = \frac{1}{r} V_r + \frac{1}{r^2 \sin^2 I \cos^2 \omega_o} [-\tan \omega_o \cos I \, V_{\omega_e} + V_{\omega_e\omega_e} +$$

$$+ \tan \omega_o(\sin^2 I \sin^2 \omega_o - 2\sin^2 I + 1)V_{\omega_o} -$$

$$- 2\cos I \, V_{\omega_e\omega_o} + \cos^2 I \, V_{\omega_o\omega_o}]$$

$$V_{yz} = \frac{1}{r \sin I \cos \omega_o} [\frac{1}{r} V_{\omega_e} - \frac{\cos I}{r} V_{\omega_o} - V_{\omega_e r} + \cos I \, V_{\omega_o r}]$$

$$V_{zz} = V_{rr}$$

which simplify in the case of $I = \frac{\pi}{2}$ to:

$$V_{xx} = \frac{1}{r} V_r + \frac{1}{r^2} V_{\omega_o\omega_o}$$

$$V_{xy} = \frac{-1}{r^2 \cos \omega_o} V_{\omega_e\omega_o} - \frac{\sin \omega_o}{r^2 \cos^2 \omega_o} V_{\omega_e}$$

$$V_{xz} = \frac{1}{r} V_{\omega_o r} - \frac{1}{r^2} V_{\omega_o}$$

$$V_{yy} = \frac{1}{r} V_r + \frac{1}{r^2 \cos^2 \omega_o} V_{\omega_e\omega_e} + \frac{-\sin \omega_o}{r^2 \cos \omega_o} V_{\omega_o}$$

$$V_{yz} = \frac{1}{r^2 \cos \omega_o} V_{\omega_e} - \frac{1}{r \cos \omega_o} V_{\omega_e r}$$

$$V_{zz} = V_{rr} \quad .$$

Note that some gradients expressed in the parameters (r, I, ω_o) have a singularity at the points $\omega_o = 0$ and $\omega_o = \pi$ and those expressed in (r, ω_e, ω_o) in the points $\omega_o = \pm \frac{\pi}{2}$ due to the respective sine and cosine terms in the denominators. This is nothing to be surprised about since also the well-known

expressions for the gradients in spherical coordinates (see e.g. Rummel, 1986 or Tscherning, 1976) have the same kind of singularities for the points $\varphi = \pm \frac{\pi}{2}$ (poles). Of course these singularities have no physical meaning but are caused by the choice of the coordinate system.

A-2: Legendre recursions.

A numerical evaluation of Legendre polynomials and functions up to high degree and order is most easily done using recursive relationships. Starting from the recursive formulas for the Legendre functions the equivalent recursive formulas for the first and second order derivatives are obtained by simple differentiation with respect to the argument θ. We find for the recursive relationships:

1. Diagonal recursion ($n \geq 2$):

$$\bar{P}_{\ell,\ell} = f_1 \sin\theta \, \bar{P}_{\ell-1,n-1}$$

$$\bar{P}_{\ell,\ell} = f_1(\cos\theta \, \bar{P}_{\ell-1,\ell-1} + \sin\theta \, \bar{P}_{\ell-1,\ell-1})$$

$$\bar{P}''_{\ell,\ell} = f_1(-\sin\theta \, \bar{P}_{\ell-1,\ell-1} + 2\cos\theta \, \bar{P}_{\ell-1,\ell-1} + \sin\theta \, \bar{P}''_{\ell-1,\ell-1}) \quad .$$

2. Horizontal recursion - first step ($n \geq 1$):

$$\bar{P}_{\ell,\ell-1} = f_2 \cos\theta \, \bar{P}_{\ell-1,\ell-1}$$

$$\bar{P}'_{\ell,\ell-1} = f_2(-\sin\theta \, \bar{P}_{\ell-1,\ell-1} + \cos\theta \, \bar{P}'_{\ell-1,\ell-1})$$

$$\bar{P}''_{\ell,\ell-1} = f_2(-\cos\theta \, \bar{P}_{\ell-1,\ell-1} + 2\sin\theta \, \bar{P}'_{\ell-1,\ell-1} + \cos\theta \, \bar{P}''_{\ell-1,\ell-1}) \quad .$$

3. Horizontal recursion - next steps:

$$\bar{P}_{\ell,m} = f_3(f_4 \cos\theta \, \bar{P}_{\ell-1,m} - f_5 \, \bar{P}_{\ell-1,m})$$

$$\bar{P}'_{\ell,m} = f_3(-f_4 \sin\theta \, \bar{P}_{\ell-1,m} + f_4 \cos\theta \, \bar{P}'_{\ell-1,m} - f_5 \, \bar{P}'_{\ell-2,m})$$

$$\bar{P}''_{\ell,m} = f_3(-f_4 \cos\theta \, \bar{P}_{\ell-1,m} - 2f_4 \sin\theta \, \bar{P}'_{\ell-1,m} + f_4 \cos\theta \, \bar{P}''_{\ell-2,m}$$

$$- f_5 \, \bar{P}''_{\ell-2,m}) \quad .$$

where

$$f_1 = \sqrt{\frac{2\ell+1}{2\ell}}$$

$$f_2 = \sqrt{2\ell+1}$$

$$f_3 = \sqrt{\frac{2\ell+1}{(\ell-m)(\ell+m)}}$$

$$f_4 = \sqrt{2\ell-1}$$

$$f_5 = \sqrt{\frac{(\ell-m-1)(\ell+m-1)}{2\ell-3}} \quad .$$

As starting values we use:

$$\bar{P}_{00} = 1 \qquad \bar{P}_{11} = \sqrt{3}\sin\theta$$
$$\bar{P}'_{00} = 0 \qquad \bar{P}'_{11} = \sqrt{3}\cos\theta$$
$$\bar{P}''_{00} = 0 \qquad \bar{P}''_{11} = -\sqrt{3}\sin\theta \quad .$$

All the above relationships are valid for normalized Legendre functions. Vertical (downwards) recursions are also possible, but they have the disadvantage that a factor $\sin^{-1}\theta$ appears in the formulas. For small θ this factor can lead to numerical singularities. Another disadvantage of downwards recursions is that possible numerical errors or underflows will distort a much greater part of the ℓ,m-scheme (see Koop and Stelpstra, 1989).

A-3. Inclination functions.

A-3.1. An explicit expression for inclination functions.

Inclination functions appear in the transformation of the potential function $V(r,\phi,\lambda)$ to a function $V(r,\omega_0,\omega_e,I)$. Here r, ϕ and λ represent the spherical coordinates, radius, latitude and longitude respectively whereas r, ω_0, ω_e and I are related to orbital elements, compare figure A-3.1.

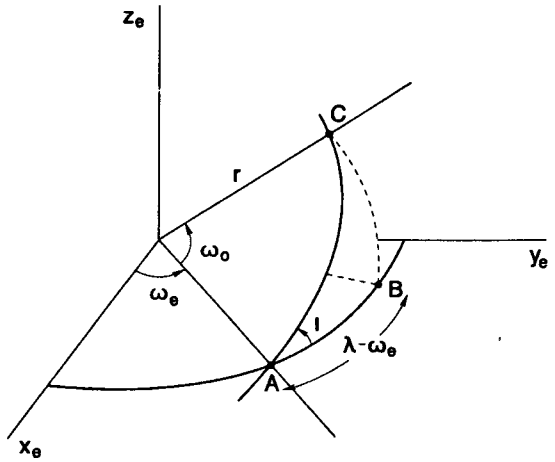

Figure A-3.1: Orbital elements r, ω_0, ω_e, and I.

The relation between (r,ϕ,λ) and (r,ω_0,ω_e,I) is

$$\begin{bmatrix} x \\ y \\ z \end{bmatrix} = R_3(-\omega_e)R_1(-I) \begin{bmatrix} r\cos\omega_0 \\ r\sin\omega_0 \\ 0 \end{bmatrix} = r \begin{bmatrix} \cos\lambda\cos\phi \\ \sin\lambda\cos\phi \\ \sin\phi \end{bmatrix}$$

where R denotes a rotation matrix. This results in:

$$\begin{aligned} \cos\omega_e\cos\omega_0 - \sin\omega_e\sin\omega_0\cos I &= \cos\phi\cos\lambda \\ \sin\omega_e\cos\omega_0 + \cos\omega_e\sin\omega_0\cos I &= \cos\phi\sin\lambda \\ \sin\omega_0\sin I &= \sin\phi \end{aligned} \qquad \text{(A-3.1a-c)}$$

compare also (Schrama, 1989; p. 16 and 71). In order to derive the inclination functions eq. (A-3.1a-c) are substituted in the expression:

$$V_{\ell m}(r,\phi,\lambda) = \frac{\mu}{R}\left(\frac{R}{r}\right)^{\ell+1}[C_{\ell m}\cos m\lambda + S_{\ell m}\sin m\lambda]P_{\ell m}(\sin\phi) \quad . \qquad (A\text{-}3.2)$$

First we will derive binominal expansions for cos mλ and sin mλ. Using the formula of De Moivre we find that

$$e^{jm\lambda} = (\cos\lambda + j\sin\lambda)^m = \cos m\lambda + j\sin m\lambda$$

where $j = \sqrt{-1}$. Accordingly

$$\cos m\lambda = \frac{1}{2}[e^{jm\lambda} + e^{-jm\lambda}] \quad ,$$

$$\sin m\lambda = \frac{-j}{2}[e^{jm\lambda} - e^{-jm\lambda}] \quad . \qquad (A\text{-}3.3a,b)$$

Furthermore we know that

$$e^{jm\lambda} = e^{jm(\lambda-\omega_e)}\, e^{jm\omega_e}$$

$$e^{-jm\lambda} = e^{-jm(\lambda-\omega_e)}\, e^{-jm\omega_e} \quad . \qquad (A\text{-}3.4a,b)$$

Additionally the terms $\cos(\lambda-\omega_e)$ and $\sin(\lambda-\omega_e)$ are related, in the spherical triangle A, B, C in figure A-3.1, to ω_0, I and ϕ:

$$\cos(\lambda-\omega_e) = \frac{\cos\omega_0}{\cos\phi} \quad , \qquad \sin(\lambda-\omega_e) = \frac{\sin\omega_0\cos I}{\cos\phi} \quad . \qquad (A\text{-}3.5a\text{-}b)$$

A substitution of (A-3.5a-b) in (A-3.4a-b) results in:

$$e^{jm(\lambda-\omega_e)}\, e^{jm\omega_e} =$$

$$= \frac{1}{\cos^m\phi}[\cos\omega_0 + j\cos I\sin\omega_0]^m[\cos m\omega_e + j\sin m\omega_e]$$

$$= \sum_{s=0}^{m}\binom{m}{s} j^s \frac{\cos^s I\sin^s\omega_0\cos^{m-s}\omega_0}{\cos^m\phi}[\cos m\omega_e + j\sin m\omega_e] \qquad (A\text{-}3.6a)$$

and

$$e^{-jm(\lambda-\omega_e)}\, e^{-jm\omega_e} =$$

$$= \sum_{s=0}^{m} \binom{m}{s} (-j)^s \frac{\cos^s I \sin^s \omega_0 \cos^{m-s} \omega_0}{\cos^m \phi} [\cos m\omega_e - j \sin m\omega_e] \quad . \quad \text{(A-3.6b)}$$

From eq. (A-3.6a-b) substituted in (A-3.3a-b) it follows that:

$$\cos m\lambda = \mathrm{Re} \sum_{s=0}^{m} \binom{m}{s} j^s \frac{\cos^s I \sin^s \omega_0 \cos^{m-s} \omega_0}{\cos^m \phi} [\cos m\omega_e + j \sin m\omega_e]$$

$$\sin m\lambda = \mathrm{Re} \sum_{s=0}^{m} \binom{m}{s} j^s \frac{\cos^s I \sin^s \omega_0 \cos^{m-s} \omega_0}{\cos^m \phi} [\sin m\omega_e - j \cos m\omega_e] \quad \text{(A-3.7a-b)}$$

compare also (Kaula, 1966). Secondly we multiply (A-3.7a-b) with the Legendre functions:

$$P_{\ell m}(\sin \phi) = \cos^m \phi \sum_{t=0}^{k} T_{\ell m t} \sin^{\ell-m-2t} \phi \quad ,$$

$$T_{\ell m t} = \frac{(-1)^t (2\ell-2t)!}{2^\ell t!\,(\ell-t)!\,(\ell-m-2t)!} \quad \text{(A-3.8)}$$

$$(k = \text{integer part of } (\ell-m)/2)$$

which can be found in (Kaula, ibid) or (Heiskanen and Moritz, 1967). Substitution of (A-3.7a-b) and (A-3.8) in (A-3.2) results in:

$$v_{\ell m} = \frac{\mu}{R} \left(\frac{R}{r}\right)^{\ell+1} \{(C_{\ell m} \cos m\omega_e + S_{\ell m} \sin m\omega_e)$$

$$+ j(C_{\ell m} \sin m\omega_e - S_{\ell m} \cos m\omega_e)\} \times \sum_{t=0}^{k} T_{\ell m t} \sin^{\ell-m-2t} (I)$$

$$\times \sum_{s=0}^{m} \binom{m}{s} j^s [\cos^s I \cos^{m-s} \omega_0 \sin^{\ell-m-2t+s} \omega_0] \quad \text{(A-3.9)}$$

where we replaced sin ϕ by sin $\omega_0 \cdot$ sin I.

Let a = ℓ - m -2t + s and b = m - s, then $\cos^b \omega_0 \sin^a \omega_0$ is expressed in a binomial expansion:

$$\sin^a \omega_0 \cos^b \omega_0 = [-\frac{j}{2}(e^{j\omega_0} - e^{-j\omega_0})]^a [\frac{1}{2}(e^{j\omega_0} + e^{-j\omega_0})]^b$$

$$= \frac{(-1)^a j^a}{2^{a+b}} \sum_{c=0}^{a} \sum_{d=0}^{b} \binom{a}{c}\binom{b}{d} (-1)^c e^{j(a+b-2c-2d)\omega_0} \qquad \text{(A-3.10)}$$

Eq. (A-3.10) substituted in (A-3.9) results in:

$$v_{\ell m} = \frac{\mu}{R}\left(\frac{R}{r}\right)^{\ell+1} \sum_{t=0}^{k} T_{\ell mt} \sin^{\ell-m-2t}(I) \sum_{s=0}^{m} \binom{m}{s} j^s \cos^s I \times$$

$$(-j)^{\ell-m-2t+s} 2^{2t-\ell} \sum_{c=0}^{\ell-m-2t+s} \sum_{d=0}^{m-s} \binom{\ell-m-2t+s}{c}\binom{m-s}{a}$$

$$(-1)^c e^{j[(\ell-2(t+c+d))\omega_0+m\omega_e]} (C_{\ell m} - j S_{\ell m}) \quad . \qquad \text{(A-3.11)}$$

Note that

$$(j)^s (-j)^{\ell-m-2t+s} = (-1)^{\ell-m-2t+s} (j)^{\ell-m-2t+2s} \quad .$$

Remember that

$j^i = (-1)^{i/2}$ for even i and

$j^i = j \cdot j^{i-1} = j(-1)^{(i-1)/2}$ for odd i.

For ℓ-m: even one gets

$$j^{\ell-m+2(s-t)} = (-1)^{(\ell-m)/2 + s-t} = (-1)^{k+s-t}$$

$$(-1)^{\ell-m+2t-s} = (-1)^s$$

so that

$$(-1)^{s} \cdot (-1)^{k+s-t} = (-1)^{k+t} \quad .$$

For ℓ-m: odd one gets

$$j^{\ell-m+2(s-t)} = j(-1)^{(\ell-m-1)/2 \,+s-t}$$

$$(-1)^{\ell-m-2t+s} = (-1)(-1)^{s}$$

so that

$$(-1)(-1)^{s} \cdot j(-1)^{(\ell-m-1)/2 \,+s-t} = -j(-1)^{2s}(-1)^{k-t} = -j(-1)^{k+t} \quad .$$

In eq. (A-3.11) for ℓ - m: even:

$$(C_{\ell m} - j\, S_{\ell m})e^{jx} = (C_{\ell m} - j\, S_{\ell m})(\cos x + j \sin x)$$

$$= (C_{\ell m} \cos x + S_{\ell m} \sin x) + j(-S_{\ell m} \cos x + C_{\ell m} \sin x)$$

and for ℓ - m: odd:

$$-j(C_{\ell m} - j\, S_{\ell m})e^{jx} = -j(C_{\ell m} \cos x + S_{\ell m} \sin x)$$

$$+ (-S_{\ell m} \cos x + C_{\ell m} \sin x) \quad .$$

Keeping only the real part of eq. (A-3.11):

$$V_{\ell m} = \frac{\mu}{R}\left(\frac{R}{r}\right)^{\ell+1} \sum_{t=0}^{k} T_{\ell m t} \sin^{\ell-m-2t}(I)\,(-1)^{k+t} \sum_{s=0}^{m}\binom{m}{s}\cos^{s} I \times$$

$$2^{2t-\ell} \sum_{c=0}^{\ell-m-2t+s} \sum_{d=0}^{m-s} \binom{\ell-m-2t+s}{c}\binom{m-s}{d}(-1)^{c} \times$$

$$\left\{\begin{bmatrix} C_{\ell m} \\ -S_{\ell m} \end{bmatrix} \cos(x) + \begin{bmatrix} S_{\ell m} \\ C_{\ell m} \end{bmatrix} \sin(x)\right\}_{\ell-m:\,\text{odd}}^{\ell-m:\,\text{even}}$$

where $(x) = (\ell-2(t+c+d))\omega_0 + m\omega_e$. The next step is a rearrangement of the indices. We substitute $p = t + c + d$. The ranges of p are as follows:

$$p_{min} = 0 \quad \text{for} \quad t = 0, \quad c = 0 \quad \text{and} \quad d = 0 \quad .$$

Taking into account that c_{max} is decreased when d_{max} is increased, c_{max} is optimal when

$$d = 0\ ; \quad s = m \quad \Rightarrow \quad c_{max} = \ell-2t$$

and as a result $p = t + \ell - 2t + 0 = \ell - t$ from which we conclude that $0 \le p \le \ell$ and $t \le p$. With this we find:

$$V_{\ell m} = \frac{\mu}{R}\left(\frac{R}{r}\right)^{\ell+1} \sum_{p=0}^{\ell} F_{\ell m p}(I) \left\{\begin{bmatrix} C_{\ell m} \\ -S_{\ell m} \end{bmatrix} \cos\psi_{\ell m p} + \begin{bmatrix} S_{\ell m} \\ C_{\ell m} \end{bmatrix} \sin\psi_{\ell m p}\right\}_{\ell-m:\,\text{odd}}^{\ell-m:\,\text{even}}$$

$$\psi_{\ell m p} = (\ell-2p)\omega_0 + m\omega_e$$

$$F_{\ell m p}(I) = \sum_{t=0}^{t_{max}} T_{\ell m t} \sin^{\ell-m-2t}(I)\,(-1)^{k+t}\,2^{2t-\ell}$$

$$\times \sum_{s=0}^{m}\binom{m}{s}\cos^{s} I \sum_{c=C_{min}}^{C_{max}} \binom{\ell-m-2t+s}{c}\binom{m-s}{p-t-c}(-1)^{c}$$

with $\quad k \le (\ell-m)/2, \qquad t_{max} = \min(k,p),$

$\quad c_{min} = \max(0,p-t), \quad c_{max} = \min(\ell-m-2t+s, m-s).$

As a result the explicit expression for the inclination function $F_{\ell mp}(I)$ becomes:

$$F_{\ell mp}(I) = \sum_{t=0}^{t_{max}} \sum_{s=0}^{m} \sum_{c=c_{min}}^{c_{max}} \frac{(2\ell-2t)!\,(-1)^{k+2t+c}}{2^{2\ell-2t}\,t!\,(\ell-t)!\,(\ell-m-2t)!}$$

$$\times \sin^{\ell-m-2t}(I) \binom{m}{s} \cos^{s}(I) \binom{\ell-m-2t+s}{c} \binom{m-s}{p-t-c} \quad .$$

Note that $(-1)^{k+2t+c} = (-1)^{k-c}$ as is found in (Kaula, 1966).

A.3.2. Related inclination functions.

In appendix A.1 we computed the potential derivatives with respect to local cartesian coordinates (x,y,z). We found, for example, for the derivative in y-direction (cross-track):

$$V_y = \frac{1}{r \sin \omega_o} V_I \quad . \qquad \text{(A-3.2.1)}$$

In order to compute V_I we need the derivatives of the inclination functions with respect to I: $F'_{\ell mp}(I) = \frac{\partial F_{\ell mp}}{\partial I}$. These derivatives can be easily computed as will be shown in the next section. However, when trying to integrate eq. (A-3.2.1) over the whole sphere, orthogonality properties are lost due to the factor $\sin \omega_0$ in the denominator. Furthermore, the point for which $\omega_0 = 0$ appears to be a singularity. Following (Betti & Sansò, 1989) the idea is now to write the cross-track derivative as

$$V_y = \frac{1}{r} V_{\varphi'}, \qquad \text{(A-3.2.2)}$$

where φ' is the angle perpendicular to the orbital plane (see figure A-3.2).

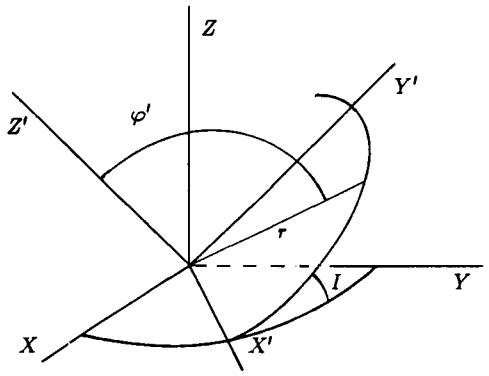

Figure A-3.2: Orbit plane and cross-track angle φ'.

In that case both problems mentioned above will not occur. When comparing eq. (A-3.2.1) and (A-3.2.2) we see that

$$\frac{1}{\sin \omega_0} V_I = V_{\varphi'},$$

so that a series expansion for $V_{\varphi'}$ has to exist in which the term $\sin^{-1} \omega_0$ is already incorporated. This expansion can be found in an analogous manner as in the foregoing section A-3.1, where we derived the inclination functions. Taking the derivative of eq. (A-3.1.9) with respect to I and deviding by $\sin \omega_0$ we find

$$\frac{1}{\sin \omega_0} \frac{\partial V_{\ell m}}{\partial I} = \frac{\mu}{R} \left(\frac{R}{r}\right)^{\ell+1} \mathrm{Re}\left[\sum_{t=0}^{k} T_{\ell mt} \sum_{s=0}^{m} \binom{m}{s} j^s f(I) g(\omega_e) h(\omega_0)\right]$$

where

$$f(I) = \sin^{\ell-m-2t-1} I \cos^{s-1} I[(\ell-m-2t)\cos^2 I - s \sin^2 I]$$

$$g(\omega_e) = (C_{\ell m} - jS_{\ell m}) e^{jm\omega_e} \qquad \text{(A-3.2.3)}$$

$$h(\omega_0) = \sin^{\ell-m-2t+s-1} \omega_0 \cos^{m-s} \omega_0 \quad .$$

Proceeding now in an equivalent way as in the foregoing section we arrive at

$$\frac{1}{\sin \omega_0} \frac{\partial V_{\ell m}}{\partial I} = \frac{\mu}{R} \left(\frac{R}{r}\right)^{\ell+1} \sum_{p=0}^{\ell-1} F^*_{\ell mp}(I) \left\{ \begin{bmatrix} S_{\ell m} \\ C_{\ell m} \end{bmatrix}_0^e \cos \psi^*_{\ell mp} + \begin{bmatrix} -C_{\ell m} \\ S_{\ell m} \end{bmatrix}_0^e \sin \psi^*_{\ell mp} \right\}$$

where

$$\psi^*_{\ell mp} = (\ell-2p-1)\omega_0 + m\omega_e \qquad \text{(A-3.2.4)}$$

$$F^*_{\ell mp}(I) = \sum_{t=0}^{t_{max}} T_{\ell mt} \sum_{s=0}^{m} \binom{m}{s} f(I) 2^{2t-\ell+1} (-1)^{k+1} \times$$

$$\times \sum_{c=C_{min}}^{C_{max}} \binom{\ell-m-2t+s-1}{c} \binom{m-s}{p-t-c} (-1)^c$$

$f(I)$ as in eq. (A-3.2.3)

k = integer part of $(\ell-m)/2$

$t_{max} = \min(k, p)$

$C_{max} = \min(\ell-m-2t+s-1, m-s)$

$C_{min} = \max(0, p-t)$.

Computation of the related inclination functions $F^*_{\ell mp}(I)$ is done in an equivalent manner as the inclination functions and their derivatives w.r.t I as will be shown in the next section.

A-3.3. Computation of inclination functions.

Inclination functions may be computed using recurrent relations as we did in the former section for the Legendre functions. Another possibility is to formulate the problem in terms of an unit potential function developed along a great circle with inclination I as described in Wagner (1983) and Schrama (1989). The related inclination functions $F^*_{\ell mp}$ can be computed in the same way, as well as the derivatives of the inclination functions with respect to I.

Since the procedure for computation of $F_{\ell mp}$ (or the normalized inclination functions $\bar{F}_{\ell mp}$) is clearly described in Schrama (ibid), we will show here only

the analogous method for the $\bar{F}^{*}_{\ell mp}$.

Along a circular unit orbit (defined by $\Omega = \theta_G = e = 0$, $a = 1$ and $M + \omega = u$) we evaluate the function $\frac{\partial V_{\ell m}}{\partial \varphi'}$, which can be obtained by applying the chain rule

$$\frac{\partial V_{\ell m}}{\partial \varphi'} = \frac{\partial V_{\ell m}}{\partial \varphi}\frac{\partial \varphi}{\partial \varphi'} + \frac{\partial V_{\ell m}}{\partial \lambda}\frac{\partial \lambda}{\partial \varphi'}$$

$$\frac{\partial V_{\ell m}}{\partial \varphi} = \bar{P}'_{\ell m} \quad (\cos m\lambda + \sin m\lambda) \qquad \text{(A-3.3.1)}$$

$$\frac{\partial V_{\ell m}}{\partial \lambda} = m\bar{P}_{\ell m} \quad (\cos m\lambda - \sin m\lambda)$$

where we used the unit potential function $V_{\ell m}$ defined by $\mu = R = r = \bar{C}_{\ell m} = \bar{S}_{\ell m} = 1$.

Now we have to find the partical derivatives $\frac{\partial \varphi}{\partial \varphi'}$, $\frac{\partial \lambda}{\partial \varphi'}$. From Figure A-3.2 we have

$$\begin{aligned} X &= \cos\varphi \cos\lambda & X' &= \cos\varphi' \cos\omega_0 \\ Y &= \cos\varphi \sin\lambda & Y' &= \cos\varphi' \sin\omega_0 \\ Z &= \sin\varphi & Z' &= \sin\varphi' \end{aligned} \qquad \text{(A-3.3.2)}$$

Between the two systems x_I and x_I, only a rotation about the X-axis by an angle I exists:

$$\begin{bmatrix} X \\ Y \\ Z \end{bmatrix} = \begin{bmatrix} 1 & 0 & 0 \\ 0 & \cos I & -\sin I \\ 0 & \sin I & \cos I \end{bmatrix} \begin{bmatrix} X' \\ Y' \\ Z' \end{bmatrix} . \qquad \text{(A-3.3.3)}$$

Using (A-3.3.3) in (A-3.3.2) leads to:

$$\begin{aligned} \cos\varphi \cos\lambda &= \cos\varphi' \cos\omega_0 \\ \cos\varphi \sin\lambda &= \cos\varphi' \sin\omega_0 \cos I - \sin\varphi' \sin I \\ \sin\varphi &= \cos\varphi' \sin\omega_0 \sin I + \sin\varphi' \cos I \end{aligned} \qquad \text{(A-3.3.4a,b,c)}$$

Differentiating (A-3.3.4c) yields for $\varphi' = 0$:

$$\frac{\partial \varphi}{\partial \varphi'} = \frac{\cos I}{\cos \varphi}$$

and differentiating the quotient of (A-3.3.4b) and (A-3.3.4a)

$$\frac{\partial \lambda}{\partial \varphi'} = - \frac{\sin I \cos \lambda}{\cos \varphi} \quad .$$

Now we have from eq. (A-3.2.4) for the unit potential

$$V_{\ell m}^{\varphi'} = \sum_{p=0}^{\ell-1} \bar{F}^*_{\ell mp} \{\cos(\ell-2p-1)u + \begin{bmatrix} -1 \\ \\ 1 \end{bmatrix}_0^e \sin(\ell-2p-1)u\}$$

which in fact is a Fourier series.
Introducing $k^* = \ell-2p-1$ this yields

$$V_{\ell m}^{\varphi'} = \sum_{k^*=0/1,2}^{\ell-1} \{(\bar{F}^*_{\ell m(\ell-1+k^*)/2} + \bar{F}^*_{\ell m(\ell-1-k^*)/2}) \cos k^* u +$$

$$+ (\bar{F}^*_{\ell m(\ell-1-k^*)/2} - \bar{F}^*_{\ell m(\ell-1+k^*)/2}) \begin{bmatrix} -1 \\ \\ 1 \end{bmatrix}_0^e \sin ku\}$$

where $k^* = 0, 2, 4, \ldots, \ell-1$ for odd ℓ
$k^* = 1, 3, 5, \ldots, \ell-1$ for even ℓ .

Comparison with an ordinary Fourier series

$$V_{\ell m}^{\varphi'} = \sum_{i=0}^{\ell-1} C_i^{\varphi'} \cos iu + S_i^{\varphi'} \sin iu$$

yields

$$\bar{F}^{*}_{\ell m(\ell-1)/2} = C_0^{\varphi'} \qquad \text{for odd } \ell$$

$$\bar{F}^{*}_{\ell m(\ell-1+k^*)/2} = (C_{k^*}^{\varphi'} + S_{k^*}^{\varphi'})/2 \qquad \text{for } \ell\text{-m: even}$$

$$\bar{F}^{*}_{\ell m(\ell-1-k^*)/2} = (C_{k^*}^{\varphi'} - S_{k^*}^{\varphi'})/2 \qquad \text{for } \ell\text{-m: even}$$

$$\bar{F}^{*}_{\ell m(\ell-1+k^*)/2} = (C_{k^*}^{\varphi'} - S_{k^*}^{\varphi'})/2 \qquad \text{for } \ell\text{-m: odd}$$

$$\bar{F}^{*}_{\ell m(\ell-1-k^*)/2} = (C_{k^*}^{\varphi'} + S_{k^*}^{\varphi'})/2 \qquad \text{for } \ell\text{-m: odd} \quad .$$

The coefficients C_{k^*} and S_{k^*} are derived by computing the unit potential at discrete points along a great circle and performing a FFT.

REFERENCES.

Balmino, G., J.P. Barriot: Methods of global recovery of harmonic coefficients from SGG in the general case, in: Study on precise gravity field determination methods and mission requirements (phase 2), ESA contract 81553/88/F/FL, 1990.

Betti, B. and F. Sansò: The integrated approach to satellite geodesy, in: Theory of satellite geodesy and gravity field determination (eds.: F. Sansò, R. Rummel), 373-416, Springer, Berlin, 1989.

Brovelli, M. and F. Sansò: Gradiometry: the study of the V_{yy} component in the BVP approach, Manuscripta Geodaetica, vol. 15, no. 4, 240-248, 1990.

Colombo, O.L.: Numerical methods for harmonic analysis on the sphere, OSU report no. 310, 1981.

Colombo, O.L.: The global mapping of gravity with two satellites, Netherlands Geodetic Commission, Publications on Geodesy, New Series, vol. 7, no. 3, Delft, 1984a.

Colombo, O.L.: Altimetry, orbits and tides, Report EG&G Washington Analytical Services Inc., NASA TM 86180, 1984b.

Colombo, O.L.: The global mapping of the gravity field with an orbiting full-tensor gradiometer: an error analysis, presented at XIX assembly of IUGG, Vancouver, 1987.

Colombo, O.L., Advanced techniques for high resolution mapping of the gravitational field, in: Theory of satellite geodesy and gravity field determination (eds.: F. Sansò, R. Rummel), 335-368, Springer, Berlin, 1989a.

Colombo, O.L., Mapping the earth's gravity field with orbiting GPS receivers, IAG General Meeting, Edinburgh, 1989b.

Glaser, R.J., E.J. Sherry: Relationships of gravity gradients to spherical harmonics, JPL, C.I.T., Pasadena, 1971.

Heiskanen, W.A., H. Moritz: Physical geodesy, Freeman, San Francisco, 1967.

Jekeli, C., R.H. Rapp: Accuracy of the determination of mean anomalies and mean geoid undulations from a satellite gravity field mapping mission, Dept. Geodetic Science, 307, Ohio State University, Columbus, 1980.

Kaula, W.M.: Theory of satellite geodesy, Blaisdell, Waltheim, 1966.

Kaula, W.M., Inference of variations in the gravity field from satellite to satellite tracking, J.Geoph.Res., 88, B10, 8345-8349, 1983.

Köhnlein, W.: On the gravity gradient at satellite altitudes, Special report 246, Smithonian Astrophysical Observatory, Cambridge, Mass., 1967.

Koop, R. and D. Stelpstra, On the computation of the gravitational potential and its first and second order derivatives, Manuscripta Geodaetica, 14, 373-382, 1989.

Levinson, N.: The Wiener RMS (Root Means Square) error criterion in filter design and prediction, Journ. Math. Physics, 25, 4, 261-278, 1947.

Marsh, J.G., F.J. Lerch, B.H. Putney, D.C. Christodoulidis, D.E. Smith, T.L. Felsentreger and B.V. Sanchez: A new gravitational model for the earth from satellite tracking, Data: GEM-T1, Journ. Geophys. Res., 93, B6, 6169-6215, 1988.

Meissl, P.: A study of covariance functions related to the Earth's disturbing potential, Dept. Geodetic Science, 151, Ohio State University, Columbus, 1971.

Migliaccio, F., F. Sansò: Data processing for the Aristoteles mission, in: proc. Italian workshop on the European solid-earth mission Aristoteles, 92-123, Trevi, 1989.

Misner, C.W., K.S. Thorne, J.A. Wheeler: Gravitation, Freeman and Comp., San Francisco, 1971.

Moritz, H.: Integral formulas and collocation, Manuscripta Geodaetica, 1, 1-40, 1976.

Moritz, H.: Advanced physical geodesy, Herbert Wichmann Verlag, Karlsruhe, 1980.

Paik, H.J., J-P. Richard: Development of a sensitive superconducting gravity gradiometer, NASA Contract Report 4011, 1986.

Pavlis, N.K.: Modelling and estimation of a low degree geopotential model from terrestrial gravity data, Dept. Geodetic Science, 386, Ohio State University, Columbus, 1988.

Pellinen, L.P.: A method for expanding the gravity potential of the earth in spherical harmonic functions, translated from Russian ACIC-TC-1282, NTIS: AD-661810, Publ. Nedra, Moscow, 1966.

Rapp, R.H., C.C. Tscherning: Closed covariance expression for gravity anomalies, geoid undulation and deflections of the vertical, Dept. Geodetic Science, 208, Ohio State University, Columbus, 1974.

Rapp, R.H., J.Y. Cruz: Spherical harmonic expansions of the earth's gravitational potential to degree 360 using 30' mean anomalies, Dept. Geodetic Science, 376, Ohio State University, Columbus, 1986.

Rapp, R.H.: Combination of satellite, altimetric and terrestial gravity data, in: Theory of satellite geodesy and gravity field determination (eds.: F. Sansò, R. Rummel), 261-283, Springer, Berlin, 1989.

Reed, G.B.: Application of kinematic geodesy for determining the short wave length components of the gravity field by satellite gradiometry, Dept. Geodetic Science, 201, Ohio State University, Columbus, 1973.

Reigber, C.: Gravity field recovery from satellite tracking data, in: Theory of satellite geodesy and gravity field determination (eds.: F. Sansò, R. Rummel), 197-234, Springer, Berlin, 1989.

Reinhardt, V.S., F.O. Vonbun, J.P. Turneaure: A supersensitive accelerometer for spacecraft gradiometry, in: Proc. IEEE position location and navigation symposium, Atlantic City, 1982 .

Rummel, R.: Determination of short-wavelength components of gravity field from SST or satellite gradiometry - an attempt to an identification of problem areas, Manuscripta Geodaetica, 4, 107-148, 1978.

Rummel, R., Colombo O.L.: Gravity field determination from satellite gradiometry, Bulletin Geodésique, 59, 3, 233-246, 1985.

Rummel, R.: Satellite gradiometry, in: Meth. and numerical techniques in physical geodesy, (ed. H. Sünkel), 317-364, Springer, Berlin, 1986.

Rummel, R., P.J.G. Teunissen, M. van Gelderen: Uniquely and overdetermined geodetic boundary value problems by least squares, Bulletin Geodésique, 63, 1, 1-33, 1989.

Sansò, F.: The Wiener integral and the overdetermined b.v.p.'s of physical geodesy, Manuscripta Geodaetica, 13, 2, 75-98, 1988.

Sansò, F.: On the aliasing problem in the spherical harmonic analysis, Bulletin Geodésique, 64, 4, 313-330, 1990.

Schneider, M.: Observation equations based on expansions into eigenfunctions, Manuscripta Geodaetica, 9, 3, 169-208, 1984.

Schrama, E.J.O.: The role of orbit errors in processing of satellite altimeter data, Netherlands Geodetic Commission, New Series, no. 33, 1989.

Schrama, E.J.O.: Gravity field error analysis: applications of GPS receivers and gradiometers on low orbiting platforms, NASA TM 100769, 1990.

Schrama, E.J.O.: Gravity field error analysis: Applications of GPS receivers and gradiometers on low orbiting platforms, Journal of Geophysical Research, vol. 96, no. B12, 20041-20051, 1991.

Sneeuw. N.: Inclination functions, TU Delft, fac. of geodesy, FMR internal report 91.2, 1991.

Tscherning, C.C., R.H. Rapp: Closed covariance expressions for gravity anomalies, geoid undulations, and deflections of the vertical implied by anomaly degree variance models, Dept. Geodetic Science, 208, Ohio State University, Columbus, 1974.

Tscherning, C.C.: Comparison of second-order derivatives of the normal potential based on the representation by Legendre series, Manuscripta Geodaetica, 1, 71-92, 1976.

Wagner, C.A., S.M. Klosko: Gravitational harmonics from shallow resonant orbits, Cel. Mech., vol 16, 143-163, 1977.

Wagner, C.A.: Direct determination of gravitational harmonics from Low-Low gravsat data, Journal of Geophysical Research, vol. 88, no. B12, 10,309-10,321, 1983.

Wells, W.C. (ed.): Spaceborne gravity gradiometers, NASA conference publication 2305, 1983.

Yosida, K.: Functional analysis, Springer Verlag, Heidelberg, 1978.